



INSTITUTE FOR DEFENSE ANALYSES

## UXO Burial Prediction Fidelity

Jeremy A. Teichman  
Jenya Macheret  
Shelley M. Cazares

July 2017

Approved for public release;  
distribution is unlimited.

IDA Document NS D-8616

Log: H 17-000412

INSTITUTE FOR DEFENSE ANALYSES 4850  
Mark Center Drive  
Alexandria, Virginia 22311-1882



*The Institute for Defense Analyses is a non-profit corporation that operates three federally funded research and development centers to provide objective analyses of national security issues, particularly those requiring scientific and technical expertise, and conduct related research on other national challenges.*

#### About This Publication

This work was conducted by the Institute for Defense Analyses (IDA) under contract HQ0034-14-D-0001, Project AM-2-1528, "Assessment of Traditional and Emerging Approaches to the Detection and Classification of Surface and Buried Unexploded Ordnance (UXO)," for the Director, Environmental Security Technology Certification Program (ESTCP) and Strategic Environmental Research and Development Program (SERDP), under the Deputy Under Secretary of Defense, Installations and Environment. The views, opinions, and findings should not be construed as representing the official position of either the Department of Defense or the sponsoring organization.

#### For More Information

Shelley M. Cazares, Project Leader  
scazares@ida.org, 703-845-6792

Leonard J. Buckley, Director, Science and Technology Division  
lbuckley@ida.org, 703-578-2800

#### Copyright Notice

© 2017 Institute for Defense Analyses  
4850 Mark Center Drive, Alexandria, Virginia 22311-1882 • (703) 845-2000.

This material may be reproduced by or for the U.S. Government pursuant to the copyright license under the clause at DFARS 252.227-7013 (a)(16) [Jun 2013].

# Executive Summary

---

## Background

IDA recently performed a numerical analysis for the Strategic Environmental Research and Development Program (SERDP) to explore the fidelity of computational models for predicting the initial penetration depth of unexploded ordnance (UXO) in underwater sites. This briefing describes the details of our analysis.

SERDP has funded the development of many computational models to predict how underwater UXO migrates and becomes exposed over time. A munition's initial penetration depth into the sediment is an input into these models. Other computational models have already been developed to predict the initial penetration depth of underwater mines. SERDP would like to know if and how these existing mine models could be repurposed for UXO. This issue was the focus on our analysis.

## Recommendations

1. Improve sandy sediment-penetration models.
2. Develop mobility models for silt.
3. Develop mobility models for partly buried objects.
4. Develop scour burial models for silt.
5. Improve models of consolidation and creep.
6. Exercise caution in improving hydrodynamic models to support initial sediment-penetration estimates—the effect of better hydrodynamics may be dwarfed by stochasticity due to unknown precise initial conditions at the waterline.
7. Existing sediment-penetration models (other than STRIKE35) are designed for near-cylindrical mines—for munitions, however, projectile-specific drag, lift, and moment coefficients are needed for estimating hydrodynamic stability and gross velocity.

8. Modules of existing depth penetration models are nearly independent and could and should be mixed and matched with little effort to choose best-of-breed for each phase (aero/hydrodynamic/sediment).
9. Use simplified models within the sensitivity analytical framework to understand when and how initial sediment-penetration predictions can be improved.
10. Use burial regime map to evaluate whether proposed improvements in model fidelity will have operational utility.

# Contents

---

Background.....	4
Overview.....	6
Useful Fidelity of Initial Burial Depth.....	8
A Notional Map.....	15
Mobility .....	21
Scour.....	27
Erosion.....	33
Combining Effects of Mobility, Scour, and Erosion.....	39
Map Assumptions.....	43
Implications .....	45
Risk Buckets .....	47
A Quantitative Example of the Burial Regime Map .....	49
Achievable Fidelity of Initial Burial Depth .....	52
Hydrodynamic Phase.....	91
Sediment Phase.....	99
Combine Hydrodynamic and Sediment Phases.....	103
Where Would Additional Fidelity Help?.....	112
Findings and Recommendations .....	124
Backups.....	129
References.....	A-1

# **UXO Burial Prediction Fidelity**

Jeremy Teichman, Jenya Macheret,  
Shelley Cazares

Institute for Defense Analyses  
Science & Technology Division

6 July 2017

The Institute for Defense Analyses (IDA) is a not-for-profit company that operates three Federally Funded Research and Development Centers (FFRDCs). We perform scientific and technical analyses for the U.S. Government on issues related to national security.

Recently, we performed a numerical analysis for the Strategic Environmental Research and Development Program (SERDP) to explore the fidelity of computational models for predicting the initial penetration depth of unexploded ordnance (UXO) in underwater sites. This briefing describes the details of our analysis. A separate briefing provides a shorter summary. Please contact Shelley Cazares, [scazares@ida.org](mailto:scazares@ida.org), 703 845 6792, for the summary briefing.

## **IDA | Background**

- Models are being built to understand how underwater unexploded ordnance (UXO) migrates and becomes exposed over time in response to water and sediment motion.
- Such models need initial sediment penetration estimates as inputs.
- Other models have been built to estimate these initial conditions for mines dropped into water.
- Can these mine models be useful for underwater UXO remediation?
- What else, if anything, needs to be modified, built, or measured to estimate initial penetration of a munition into the seabed floor?



SERDP has funded the development of many computational models to predict how underwater UXO migrates and becomes exposed over time. A munition's initial penetration depth into the sediment is an input into these models.

Other computational models have already been developed to predict the initial penetration depth of underwater mines.

SERDP would like to know if and how these existing mine models could be repurposed for UXO. This issue was the focus on our analysis.

## **IDA | Overview**

- What fidelity (accuracy and precision) in initial sediment penetration is **useful** for underwater UXO remediation?
  - Must feed models of mobility and exposure
    - Erosion/accretion, scour, currents, etc.
- What fidelity is **achievable**?
  - Sediment penetration model fidelity
  - Sediment property uncertainty
  - Initial conditions for sediment impact
    - Aerodynamic/ballistic model
    - Hydrodynamic model
- Where would **additional** fidelity help?

IDA set out to answer the following questions regarding estimates of UXO initial penetration depth in an underwater environment:

- What fidelity (i.e., accuracy and precision) is useful for underwater UXO remediation projects when estimating a munition's initial penetration depth into the sediment?
- What fidelity is already achievable via existing penetration models that have already been developed for underwater mines?
- Where (and when) would additional fidelity be helpful for underwater UXO remediation projects?

# **USEFUL FIDELITY OF INITIAL BURIAL DEPTH**

We begin with our first question: What fidelity (i.e., accuracy and precision) is *useful* for underwater UXO remediation projects when estimating a munition's initial penetration depth into the sediment?

- **Important questions:**
  - Will a munition be exposed at a given time?
  - Will a munition be mobile during a given time interval?
- **Important factors:**
  - Initial penetration depth
    - $d_0$  (e.g., 1–50 cm)
  - Bottom water velocity (scour burial and mobility)
    - $v_b$  (e.g., 0.5–1 m/s)
  - Erosion/accretion (burial/unburial)
    - $\delta_h$  (e.g.,  $\pm 20$  cm)

When determining if an underwater site must be remediated of UXO, some of the questions that the site manager may ask are:

- Will a munition be exposed at any given time?
- Will a munition become mobile during a given time interval?

To answer these questions, one must consider several different quantities, such as:

- the munition's initial penetration depth into the sediment,
- the velocity of water at the water-sediment boundary (i.e., the bottom water velocity), and
- the erosion and accretion of the sediment over time.

This analysis primarily focuses on the model's ability to predict the munition's initial penetration depth into the sediment. To fully consider this quantity, however, we must also explore other quantities, such as the bottom water velocity and the sediment erosion/accretion.

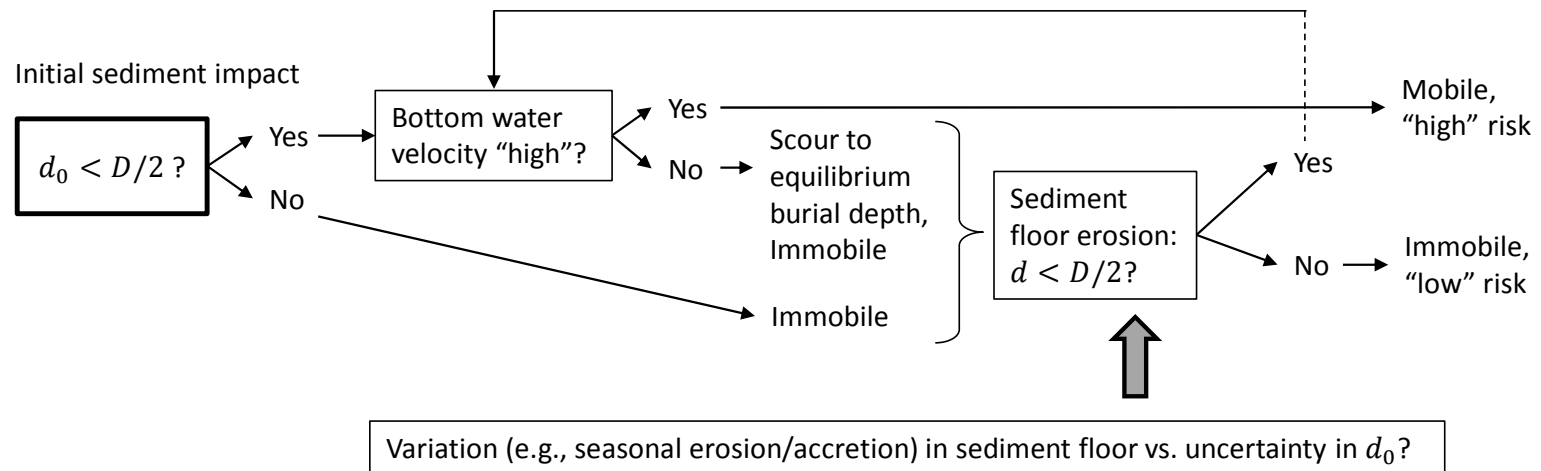
# IDA | Understanding the fate of a given munition

## Munition Burial Depth Analysis

Initial Stage: munition in sediment at depth  $d_0$



Mobility condition:  $d_0 < D/2$





The fate of the munition after its initial penetration into the sediment is determined by the process shown in this figure. Roughly speaking:

- If the initial penetration depth is deeper than the munition's half diameter, then the munition is immobile (Rennie and Brandt 2015) and, therefore, it is stable and presents low risk.
- Otherwise, the munition's mobility will depend on the magnitude of the bottom water velocity:
  - If the bottom water velocity is sufficiently high, then the munition is mobile and deemed to be high risk.
  - If, on the other hand, the bottom water velocity is low, then the munition remains stationary, and the water flow around it leads to the scour process that gradually brings the munition down to the scour equilibrium depth.
    - The buried munition will remain at this equilibrium scour depth if variations in sediment floor depth (i.e., erosion) take place on a much longer timescale than those of the scour process.
    - If, on the other hand, the variations in sediment floor depth (i.e., erosion) take place quickly, on the timescale equal to or shorter than that of scour (e.g., due to sudden events), then the munition may become exposed and potentially mobile, with its mobility determined by the magnitude of the bottom water velocity, as discussed previously.

## **IDA** | Initial burial regime map: Notional sketch

Deeper initial  
penetration

Initial penetration depth,  $d_0$

### **Map is specific to:**

- Location
  - Depth
  - Sediment properties
  - Sea-bed evolution
- Munition type
- Time period

Faster currents

Bottom water velocity,  $v_b$

## A Notional Map

A two-dimensional map helps us consider what fidelity in initial sediment-penetration estimates would be useful for any given underwater UXO remediation project. In the next several slides, we discuss how we could construct this map for any given site, taking into consideration mobility, scour, and erosion:

Initial sediment-penetration conditions (position, orientation, sediment disturbance, etc.) are determined by many factors:

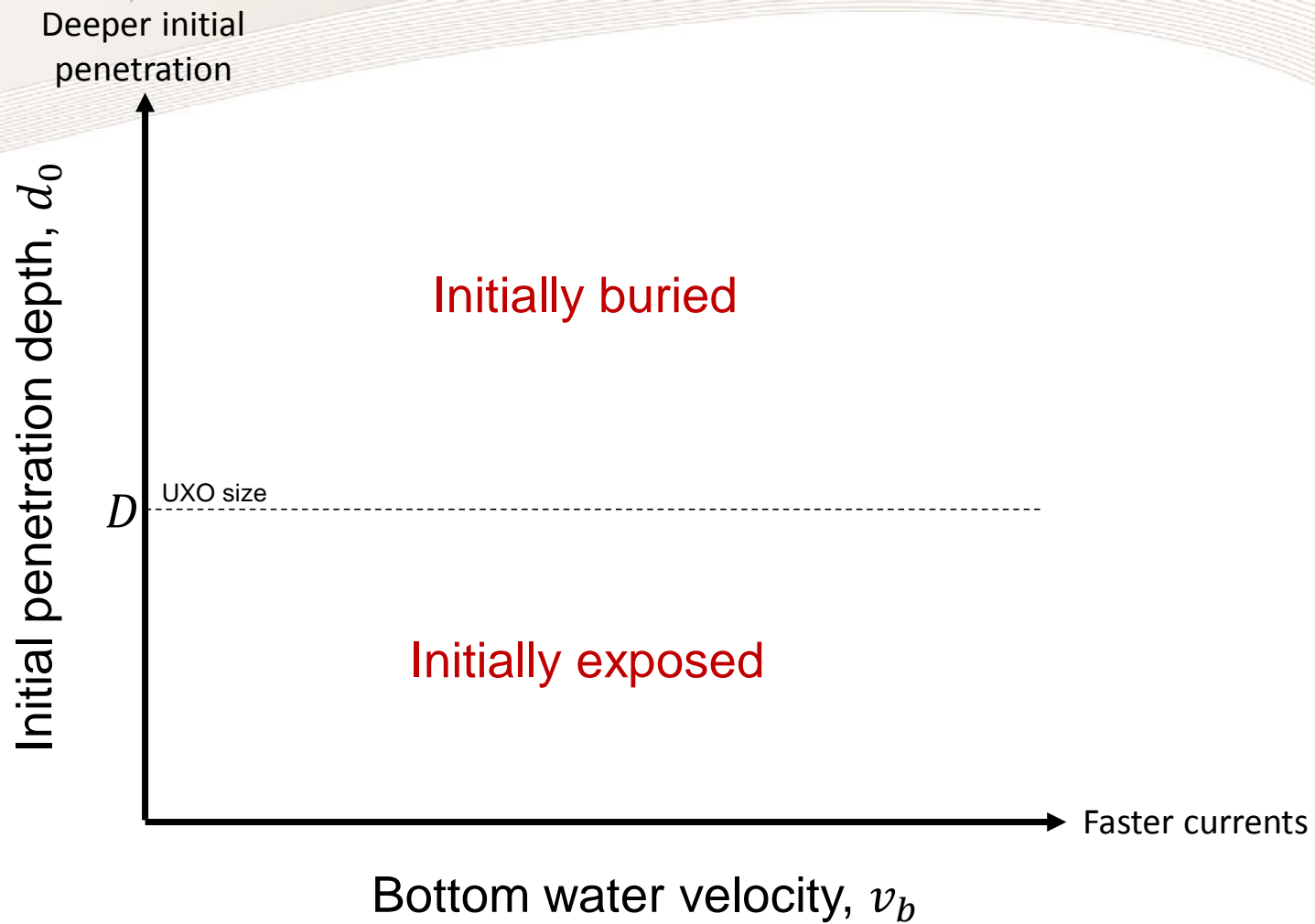
- Local conditions (such as water depth, current, and sediment characteristics),
- Conditions of impact (such as trajectory, speed, and angle of attack), and
- Munition characteristics (including drag coefficient, density, shape, and size).

Currents, sediment conditions and evolution, and munition characteristics then determine the later fate of the munition.

To illuminate the relationship of initial sediment-penetration conditions to the later fate of the munition, we categorize each case by the initial penetration depth on the vertical axis and the bottom water velocity (i.e., the velocity of the water current near the water-sediment interface) on the horizontal axis. The principal fates we want to explore are exposure and mobility, both of which are driven by water currents. On this parametric landscape we then build up a series of distinguishable regions of interest. These regions of interest will help us explore what fidelity (i.e., accuracy and precision) in initial penetration models will be useful for underwater UXO remediation projects.

Note that upward along the vertical axis corresponds to deeper initial penetration into the sediment. Similarly, rightward along the horizontal axis corresponds to faster currents.

## IDA | Initial burial regime map: Notional sketch



## **A Notional Map**

$D$  is the munition dimension in the vertical direction. For typical broadside impact, this is the munition diameter. Munitions buried deeper than  $D$  are fully buried ( $d_0 > D$ ). Values of  $0 < d_0 < D$  correspond to partly exposed munitions.

## IDA Initial burial regime map: Notional sketch

Deeper initial  
penetration

Initial penetration depth,  $d_0$

Initially buried

$D$

UXO size

Initially exposed

### Recommendation #1:

- Existing sediment penetration models are focused on silty sediment.
- Sandy sediment penetration models need further work.

Faster currents

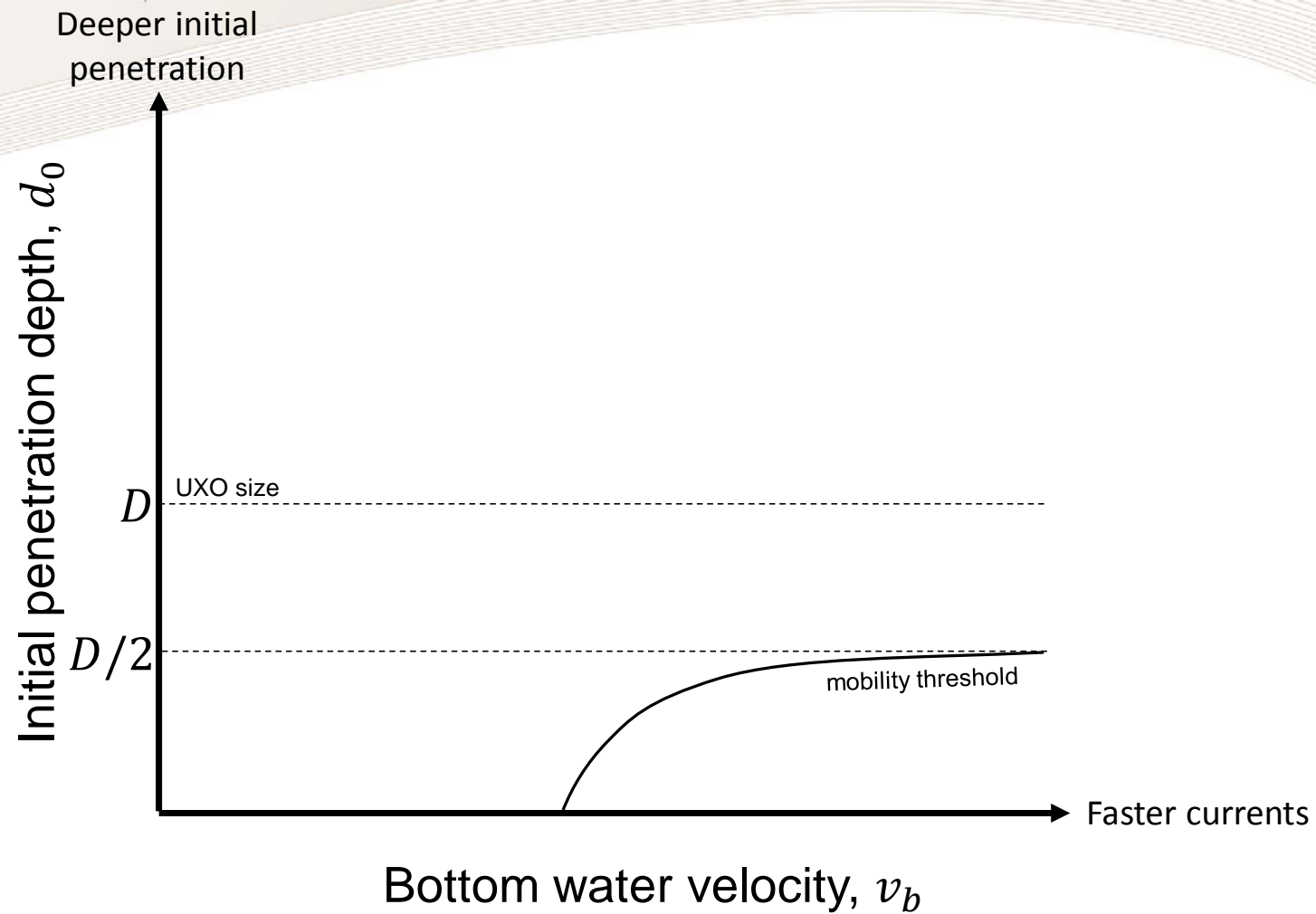
Bottom water velocity,  $v_b$

## A Notional Map

Note that existing penetration models (developed for mines) are focused on sediments such as loose clay, silt, or mud. Because of the greater bearing strength of sandy sediments, sinking mines typically do not self-bury in sand (Rennie and Brandt 2015), and so mine-in-sand penetration models were not needed for underwater *mine* remediation projects.

However, when fired, munition projectiles travel through the water with velocities sometimes much higher than terminal descent velocity. Therefore, sand-penetration models *would* be useful for underwater *UXO* remediation projects. Further development is needed to accurately predict penetration into sandy sediments.

## **IDA** | Initial burial regime map: Notional sketch





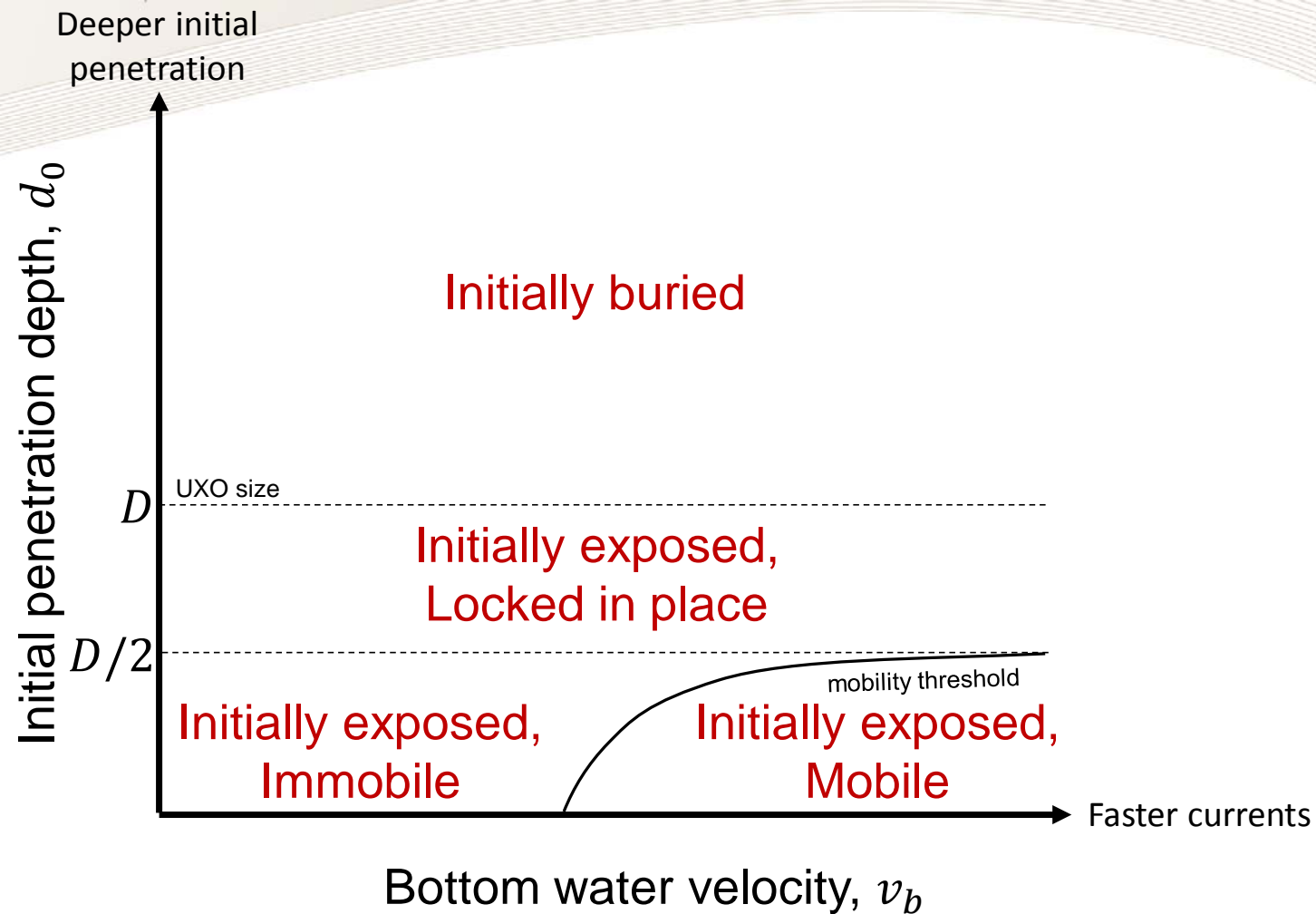
## **Mobility**

The water current can dislodge munitions and carry them away from their initial impact location. Munitions buried to more than half their diameter are generally considered to be locked-down and immobile (Rennie and Brandt 2015). Existing mobility models characterize a mobility threshold for a cylindrical object sitting upon the sediment surface (i.e., proud) in terms of parameters such as the Shields number and the surface roughness of the sediment bed (Rennie and Brandt 2015).

IDA developed its own model for predicting mobility thresholds, consistent with the phenomenological model quoted in section 4.2 of Rennie and Brandt 2015 for fully unburied munitions but extending to partly buried munitions via physics first principles. See backup slide “Mobility Model: Balance of Moments about Contact Point” for more details.

A munition’s mobility threshold is particularly important because it affects the location of the munition. In addition, once a partly buried munition is mobilized, all details of its initial impact become irrelevant, and its future fate and computation of associated risk become insensitive to its initial penetration depth.

## IDA Initial burial regime map: Notional sketch

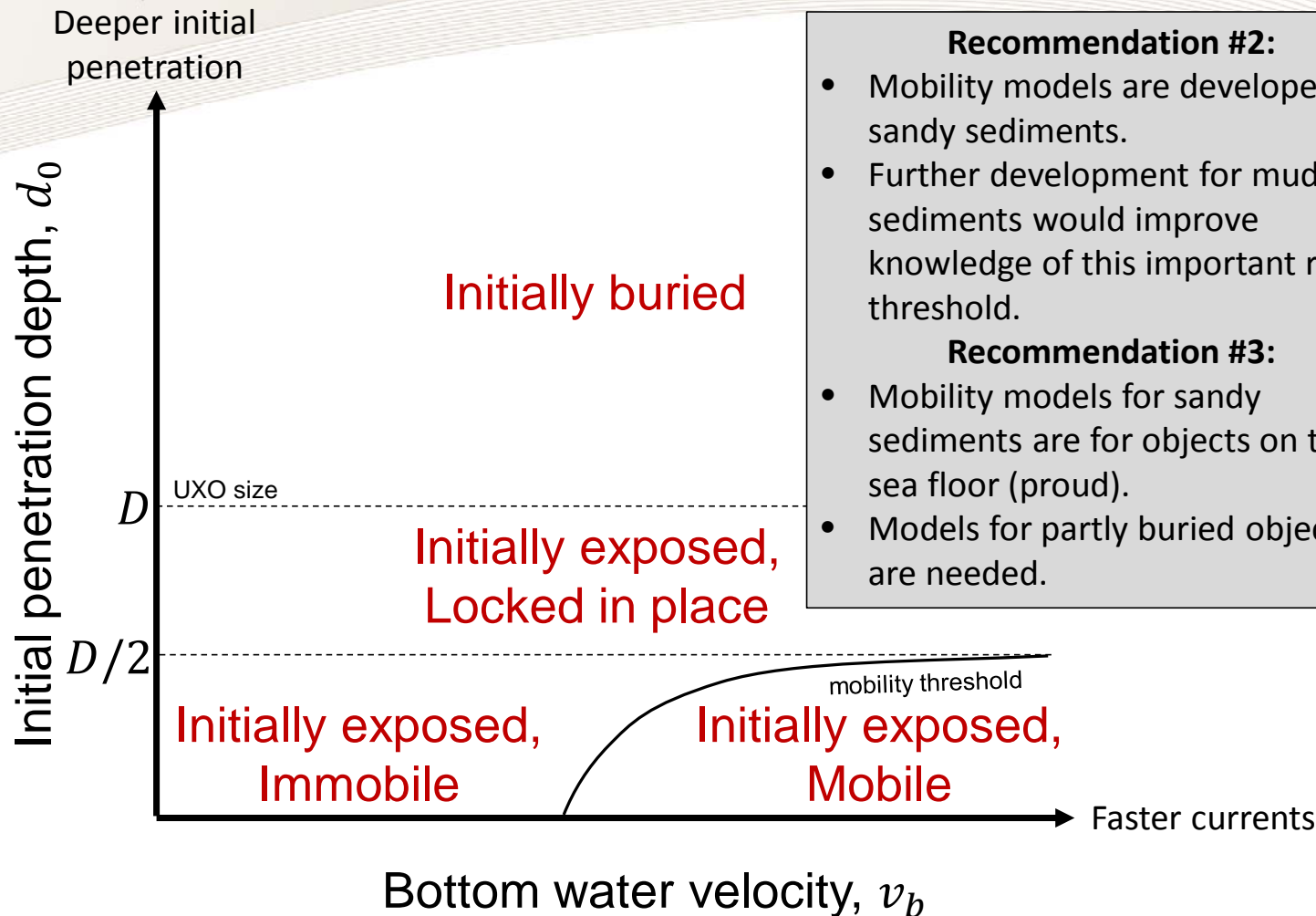


## Mobility

Thus, once it is known that a munition is mobile, additional accuracy in estimating its initial penetration depth does not add value to an underwater site manager. That is, if a munition lies *anywhere* under the mobility threshold curve (i.e., in the red “Initially exposed, Mobile” region of this map), it is not important to know exactly *where* in this region it falls. No further fidelity is needed for initial penetration models.

It is important to note the following: a time frame has now been implicitly added to this map. Water currents change with time. The water current velocity (i.e., bottom water velocity) associated with a munition on the map (i.e., its location on the horizontal axis) is the water current velocity over the time frame for initial munition mobility before anything occurs (i.e., erosion due to a sudden event) to change the state of the munition’s burial.

## **IDA** | Initial burial regime map: Notional sketch



### **Recommendation #2:**

- Mobility models are developed for sandy sediments.
- Further development for mud-like sediments would improve knowledge of this important risk threshold.

### **Recommendation #3:**

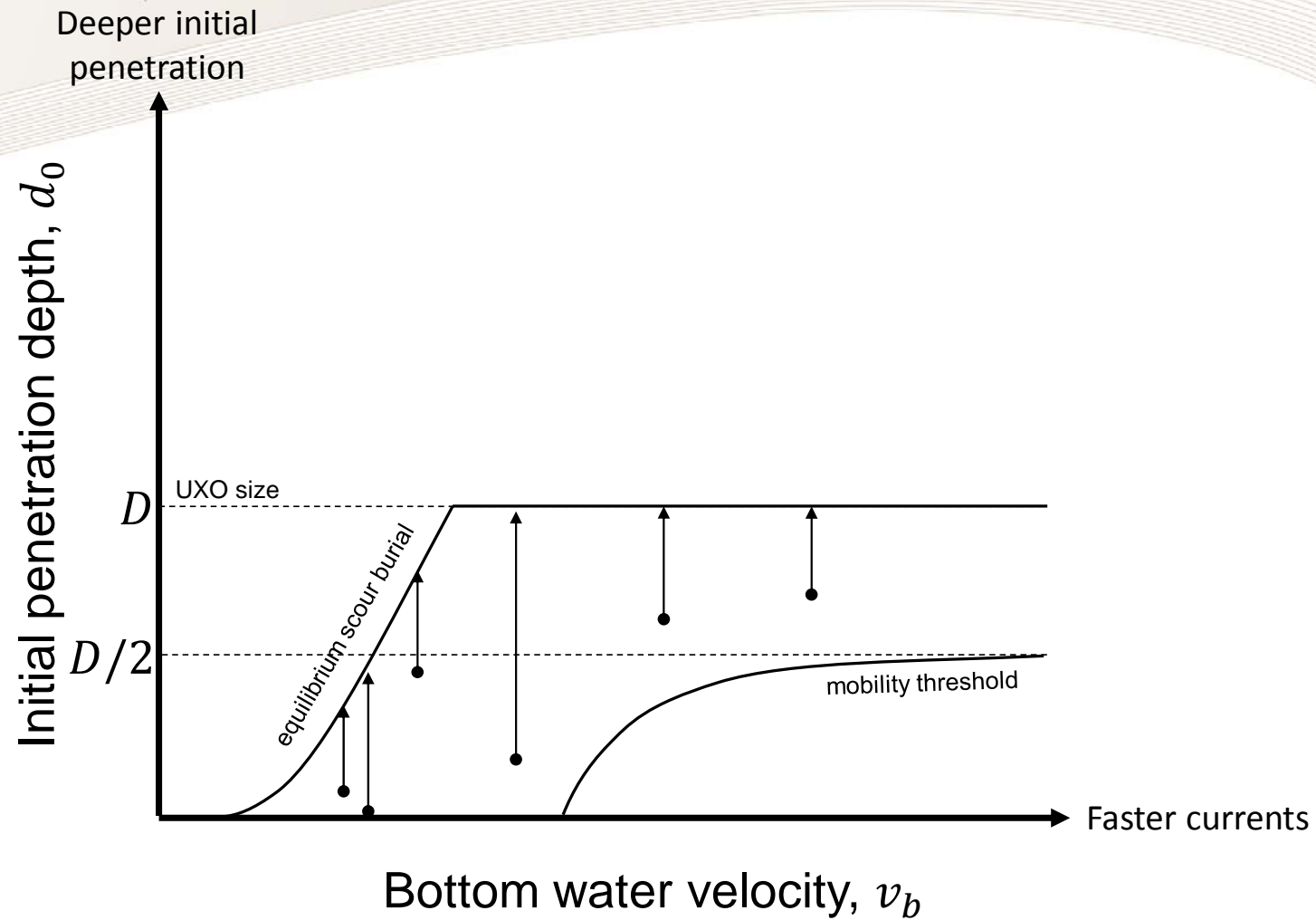
- Mobility models for sandy sediments are for objects on the sea floor (proud).
- Models for partly buried objects are needed.

## **Mobility**

Note that the mobility model developed by IDA (backup slide “Mobility Model: Balance of Moments about Contact Point”) assumes there is no suction effect holding the munition to the sediment bed (e.g., our model was developed with sandy sediments in mind). However, for consolidated mud-like sediments, additional model development is needed.

Furthermore, most mobility models for sandy sediments assume the munition is proud. IDA’s model extends towards partly developed munitions. However, IDA’s model is based on first principles of physics and is therefore relatively simplistic. More sophisticated models and/or associated validation would be useful for partly buried munitions.

## **IDA** | Initial burial regime map: Notional sketch

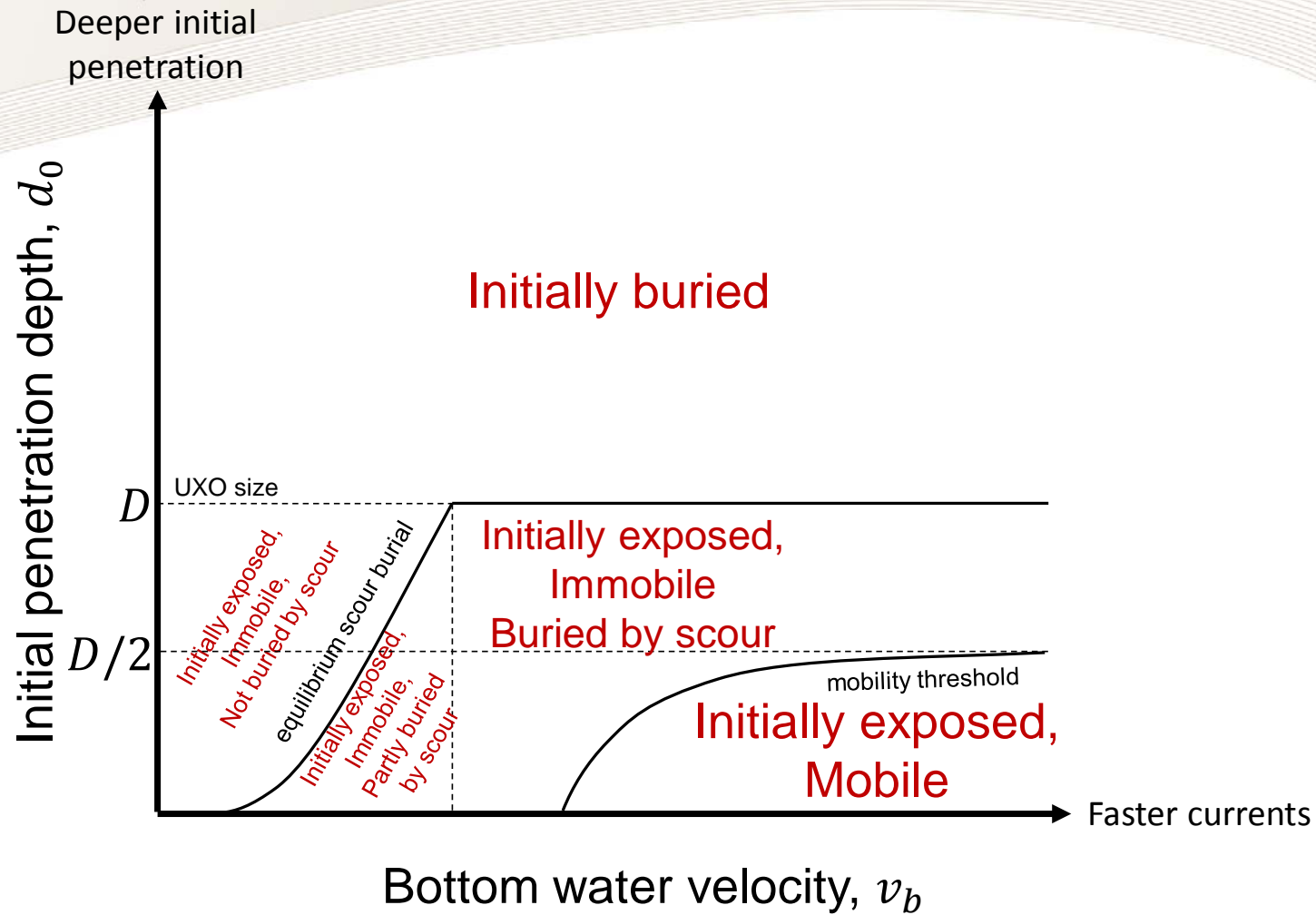


## Scour

Munitions less than fully buried in the sediment protrude into the bottom water currents and perturb them. The perturbed flow can preferentially erode sediment adjacent to the munition and thereby excavate a hole into which the munition falls, further burying it. This phenomenon is known as scour burial. The scour burial process can repeat until the remaining exposed portion of the munition no longer perturbs the flow adequately to bring about further burial. We refer to this level of burial as *equilibrium scour burial*.

The level of equilibrium scour burial is determined by the Shields number, which represents a ratio of the force exerted on sediment particles by dynamic pressure from the circulating current to the gravitational settling force on the same particles mitigated by buoyancy. In other words, it is a ratio of perturbative force to restorative force on the sediment. At a high enough Shields number, the sediment particles will be successfully lofted into the current and removed from around the munition (Rennie and Brandt 2015). This effect occurs over the course of hours to days. If the munition is not mobile in the time frame of scour burial, then a munition less buried than the equilibrium scour burial depth will, over that timescale, reach its equilibrium scour depth, as illustrated by the upward arrows in this map.

## IDA Initial burial regime map: Notional sketch

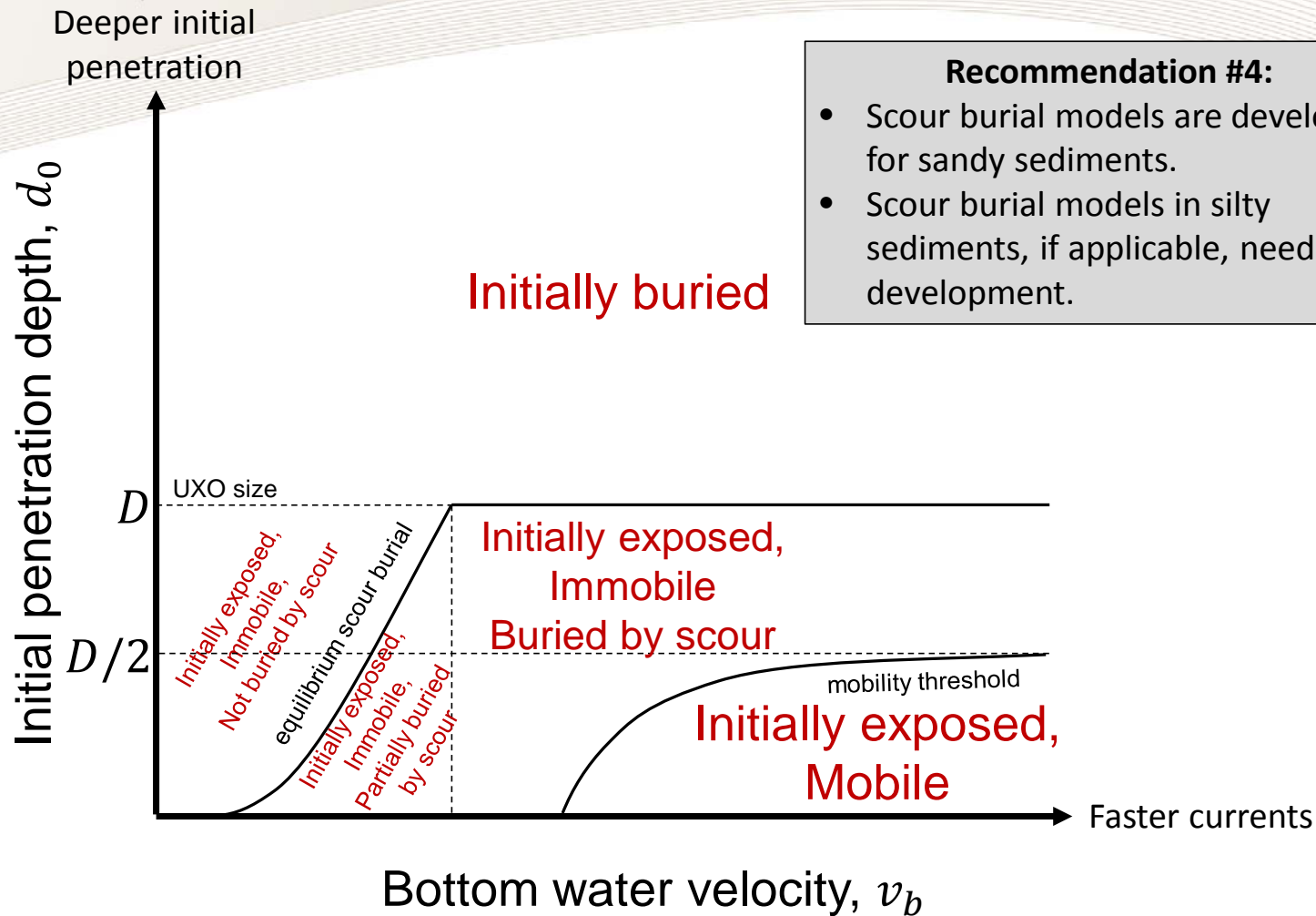




## Scour

Due to scour, the details of the initial impact become irrelevant if the munition penetrates less than the equilibrium scour burial depth. In other words, if we know that the munition lies *anywhere* under the equilibrium scour burial curve but above the mobility threshold curve, in the “Initially exposed, Immobile, Buried by scour” region of the map, then we do not need to know exactly *where* in this region it lies. That is, no further fidelity in initial penetration models is needed.

## IDA Initial burial regime map: Notional sketch



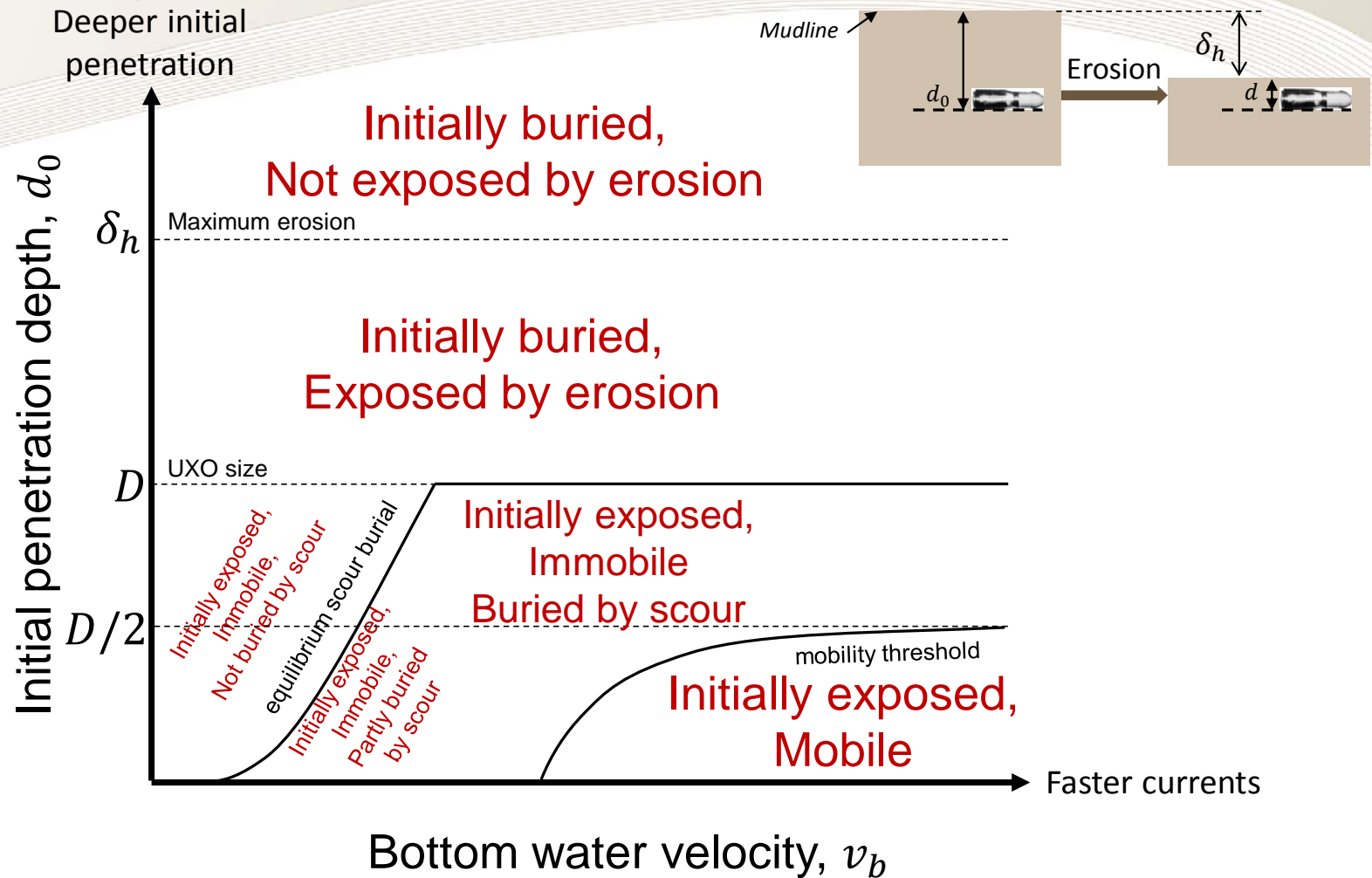
### Recommendation #4:

- Scour burial models are developed for sandy sediments.
- Scour burial models in silty sediments, if applicable, need development.

## **Scour**

Note that scour burial models are built for sandy sediments. For muds and clays, such models need development, if relevant.

## IDA Initial burial regime map: Notional sketch



## Erosion

Over days to decades, the sediment in the vicinity of the munition may experience erosion or accretion as material is removed from or deposited into the neighborhood. The seabed may also experience gross motion, such as migration of formations such as sand bars or mega-ripples. The effect of such erosion/accretion is to alter the degree of burial of the munitions. Other than in energetic events such as storms causing sudden large changes in the sediment, the pace of erosion and accretion is slower than the timescale for scour burial. Therefore, one would expect that such munitions would never be other than transiently more exposed than their equilibrium scour burial depth.

We denote the maximum erosion by  $\delta_h$ , noting that, again, the specification of  $\delta_h$  implicitly captures a specific time duration, and so our map implicitly characterizes a particular location over a particular period of time. Munitions initially buried deeper than this maximum erosion ( $d_0 > \delta_h$ ) will not, over the time duration of interest, be at all exposed. Other munitions will be durably exposed to a degree limited by scour burial.

Our investigation of the literature suggests that the mobility threshold will fall completely below the equilibrium scour burial curve (computed based on mobility thresholds and scour burial models presented in Rennie and Brandt 2015), as depicted in our notional map. Consequently, other-than-energetic erosion events are unlikely to mobilize previously immobile munitions. Rather, scour burial will always keep pace with gradual erosion maintaining the immobility of the munitions. That is, considering the following expressions from Rennie and Brandt 2015:

- Mobility threshold:  $U_{\text{mobility}} = \sqrt{1.2gD^{0.38}d^{0.62}(S_{\text{munition}} - 1)}$ , where  $U$  is the bottom water velocity,  $g$  is gravitational acceleration,  $D$  is the munition diameter,  $S_{\text{munition}}$  is the munition specific gravity, and  $d$  is the bottom roughness (grain diameter).
- Conditions for 100% equilibrium scour burial:  $U_{\text{scour}} = \sqrt{\frac{gd(S_{\text{sediment}} - 1)}{2.95f}}$ , where  $S_{\text{sediment}}$  is the sediment particle specific gravity, and  $f$  is a friction factor.

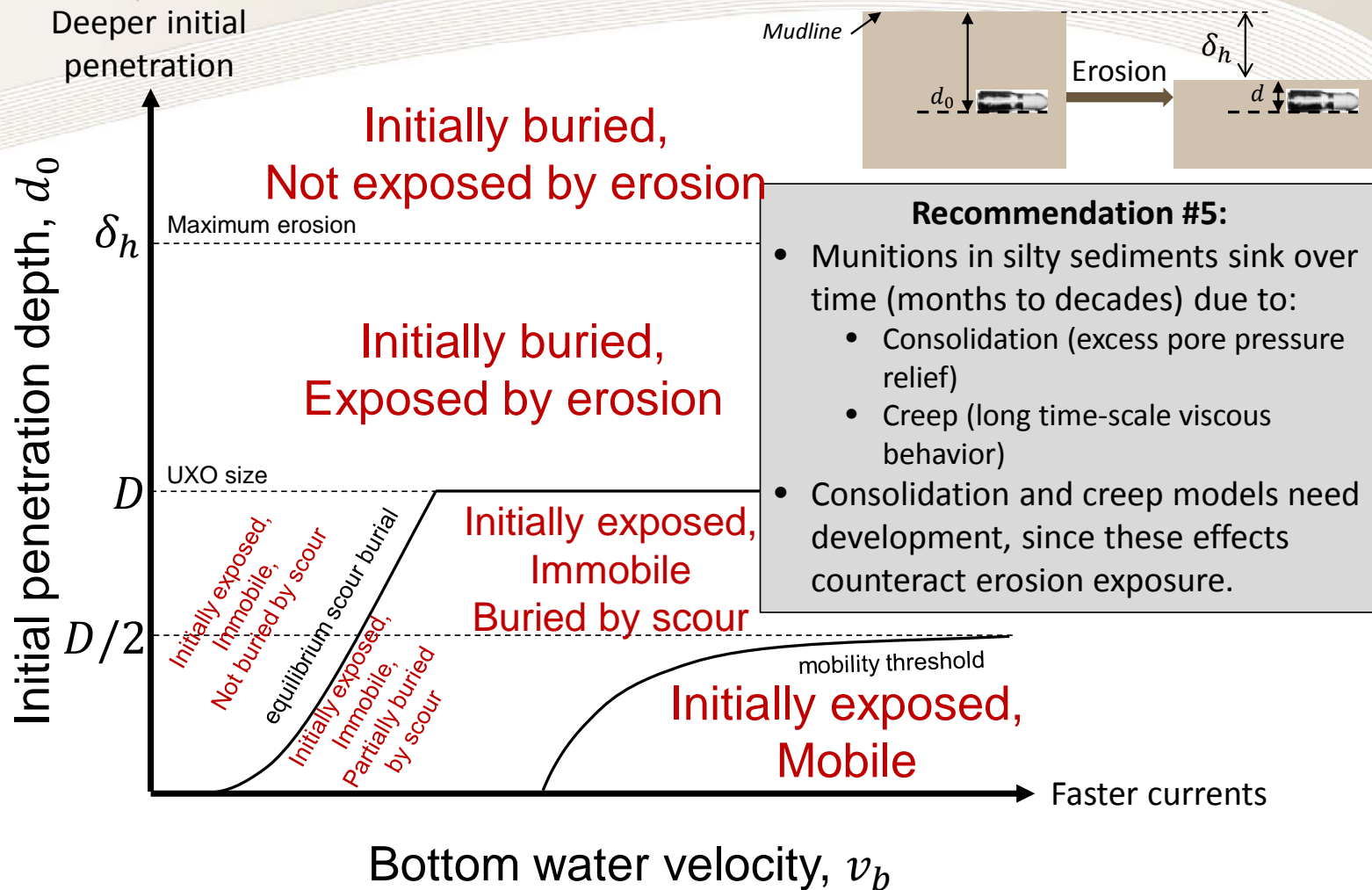
We then evaluate the ratio of the two bottom water velocity thresholds:  $\frac{U_{\text{mobility}}}{U_{\text{scour}}} = \sqrt{3.5f \left(\frac{D}{d}\right)^{0.38} \left(\frac{S_{\text{munition}} - 1}{S_{\text{sediment}} - 1}\right)}$

For munition specific gravities at least as high as sediment specific gravities, and for sediment particle diameters at most 1/60 the munitions diameter (e.g., 10 cm munition, 1 mm sand), the mobility threshold will exceed the threshold for 100% scour burial for friction

factors greater than 0.05. Smaller sediment particles and denser munitions each further increase the mobility threshold relative to the 100% scour burial threshold (i.e., mobility requires a higher velocity than full scour burial at friction factors below 0.05).



## IDA Initial burial regime map: Notional sketch





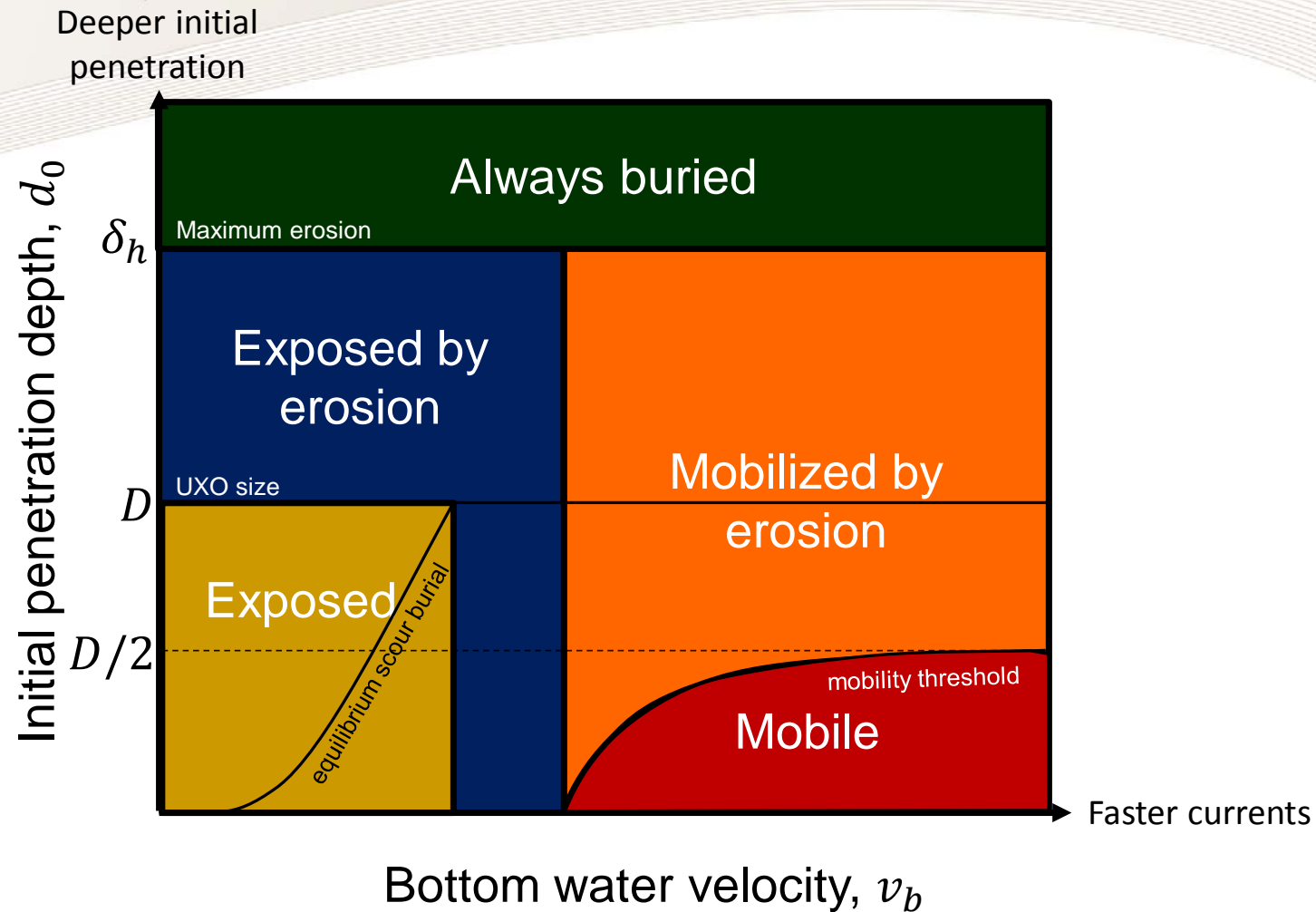
## Erosion

Effects not captured in this map are the long-term behaviors of muddy or clay-like sediments:

- Consolidation refers to the gradual (hours to years) relief of excess pore pressure in the sediment. The forceful entry of the munition into the sediment locally increases pressure in the sediment. Over time, fluid flow through the porous structure of the sediment relieves this excess pressure. The munition can sink further as the resistance exerted by the higher pore pressure abates.
- Such sediments also exhibit viscous behaviors over long timescales, flowing very slowly to relieve applied stresses. This is known as creep. A munition denser than the surrounding sediment will slowly continue to sink into the sediment over years to decades until it reaches density equilibrium.

Any complete picture of munition evolution in sediment would need to account for these effects. More relevant to the present topic: these effects (and uncertainty in these effects) will diminish the sensitivity of the position evolution of the munition to its initial penetration conditions. These effects will also diminish any leverage to improve estimation of such evolution via improving prediction of the munition's initial penetration depth.

## **IDA** | Initial burial regime map: Notional sketch

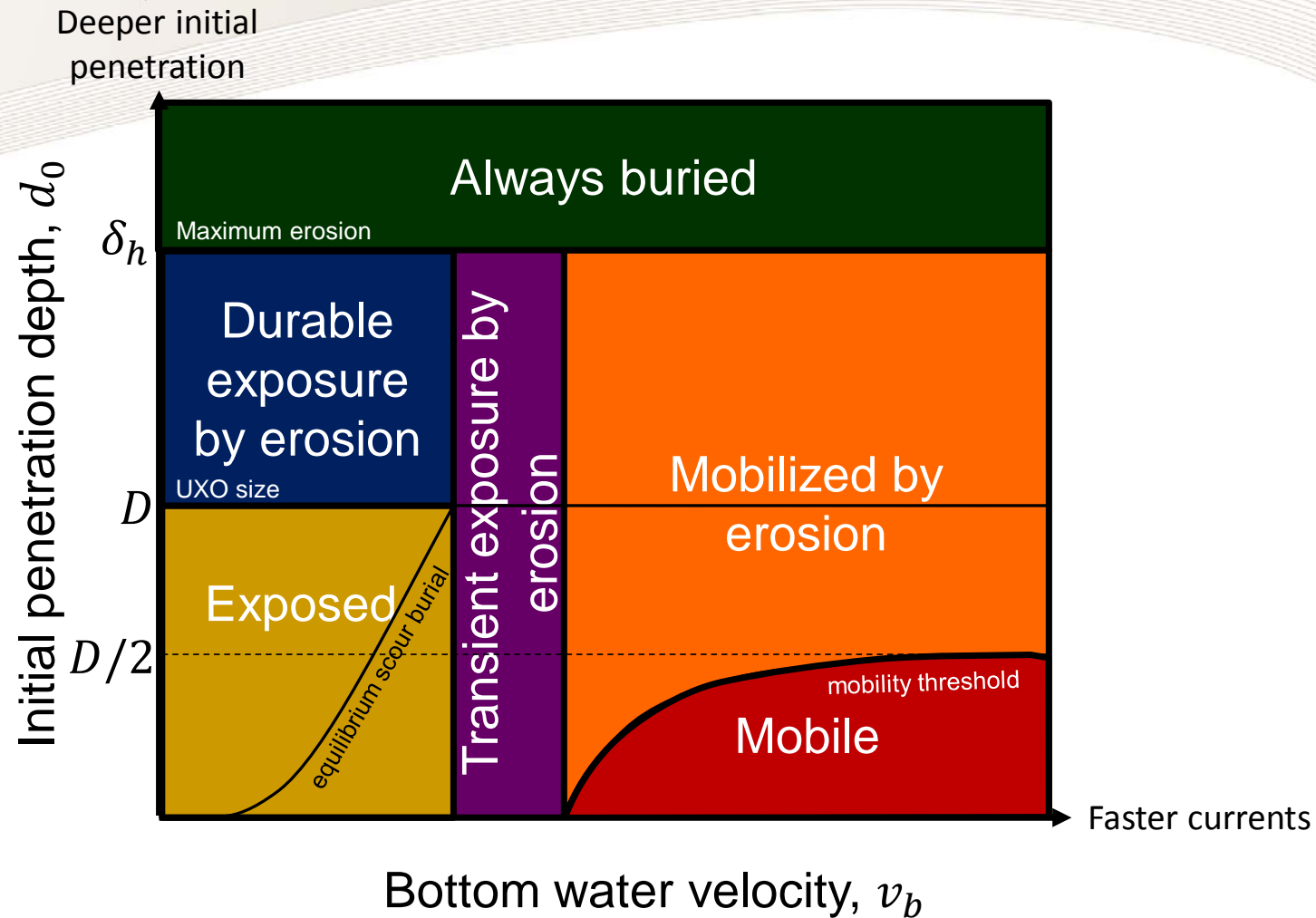


## Combining Effects of Mobility, Scour, and Erosion

Combining the effects discussed so far, we can partition the map into a series of regions relating to distinguishable categories of munition fate as a function of its initial sediment-penetration depth and the bottom water velocity. In most cases, knowing in which region a munition lies is important, but exactly *where* in that region is irrelevant:

- At the top in green (“Always buried”) are munitions buried deeper than the reach of erosion in the time frame of consideration. (Remember, the higher up the vertical axis, the deeper the initial penetration into the sediment.) These munitions will remain continuously buried for the duration of the interval.
- On the bottom right in red (“Mobile”), munitions are moved over a short period of time from their initial location.
- Above that region, in orange (“Mobilized by erosion”), are munitions that would be mobilized by sufficiently rapid erosion. Typically, however, erosion occurs more slowly than scour burial. Therefore, such munitions, if initially exposed, will be scour-buried shortly after initially reaching the sea floor. Otherwise, if not initially exposed, then scour burial will keep them below the sediment surface in the face of gradual erosion.
- On the lower left in yellow (“Exposed”) are munitions partly buried upon impact in waters sufficiently quiescent to leave the munition exposed even after scour effects (i.e., even after reaching the scour equilibrium burial depth). Accretion may fully bury such munitions, but subsequent erosion will leave them exposed. If, over time, erosion relative to the initial sediment level is on the order of the munition size, then irrespective of where in this region a munition initially impacted the sediment, it will end up at its equilibrium scour burial depth during the period of maximum erosion, thus effacing all details of the initial impact within this region. In other words, there is a ratcheting effect—as erosion diminishes the instantaneous burial depth below the equilibrium scour burial depth, scour will restore the equilibrium scour burial depth. Subsequent accretion may bury the munition further, but successive erosion/accretion cycles can only bury the munition deeper.
- The final region, shown in blue (“Exposed by erosion”), second from the bottom on the left and extending to the center bottom, encompasses munitions that were either initially buried or scour buried soon thereafter, but, in either case, not so deeply buried as to be beyond the reach of erosion.

## IDA | Initial burial regime map: Notional sketch



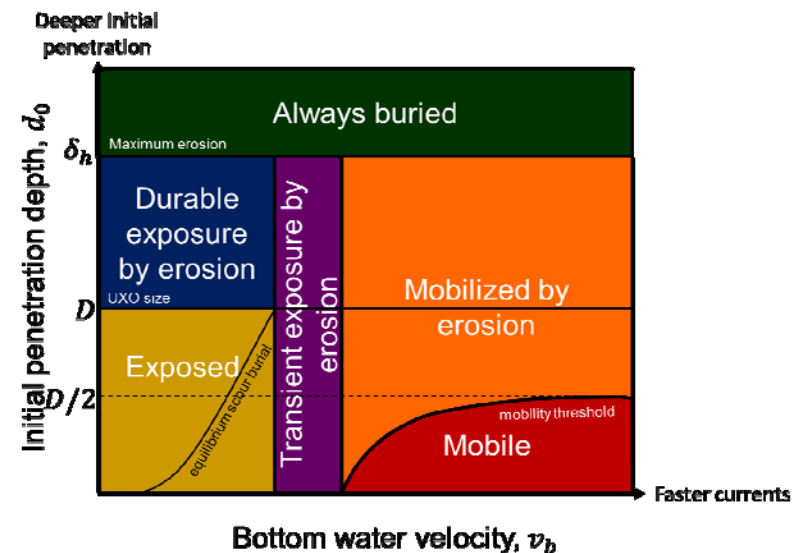
## Combining Effects of Mobility, Scour, and Erosion

It is worthwhile to further subdivide this last region:

- The blue (“Durable exposure by erosion”) region second from the bottom on the left captures munitions initially fully buried but then exposed by erosion. Because the bottom currents in this region of the map are insufficient to fully scour bury the munitions subsequent to exposure by erosion, such munitions will remain durably exposed. Further, such munitions will not remain more exposed than their equilibrium scour burial depth.
- The narrow vertical region in the center of the parameter space shown in purple (“Transient exposure by erosion”) represents munitions that become fully buried over the scour burial timescale even if they were initially exposed. Any erosion to the point of exposure will be mitigated by full scour burial, so although such munitions may surface periodically on the sediment bed, such exposure will be transient subject to scour burial. Nevertheless, barring subsequent accretion, these munitions will remain very shallowly buried, so they may be amenable to detection and remediation efforts.

## IDA | Initial burial regime map: Our assumptions

- Constant bottom water velocity
  - But in reality,  $v_b$  varies with time, and sudden erosion events (e.g., storms) are highly correlated with increases in  $v_b$ .
- Mobility time < scour burial time < erosion time
  - But for some events (e.g., storms): erosion time < scour burial time
- Independent processes
  - But storm events may be correlated with seasonal erosion/accretion cycle
- Deterministic evolution
  - But in reality,  $\delta_h$  is stochastic



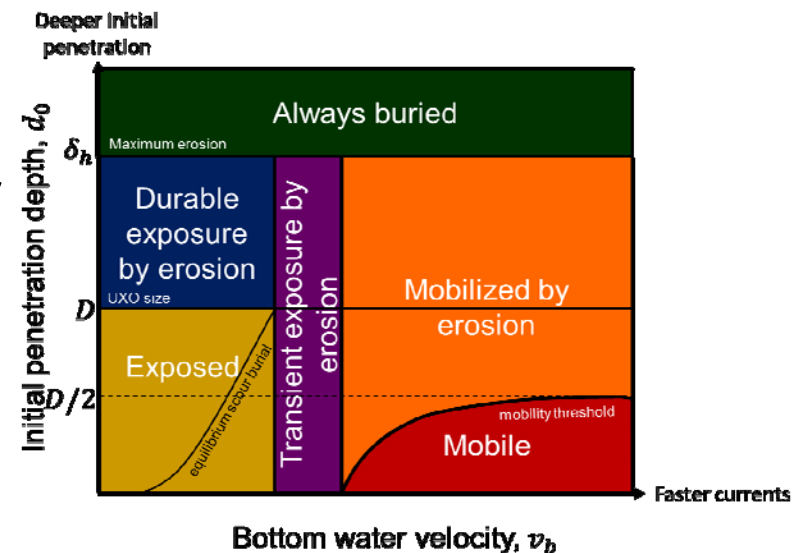
## Map Assumptions

In constructing our parametric partition of this map, we made a series of simplifications. Here we elaborate on when those simplifications might be invalid:

- First, we treated bottom water velocity as time-invariant. Of course, in reality, bottom water velocity varies with time, weather conditions, tides, and more.
- Also, typically, erosion occurs more slowly than scour burial, which, in turn, occurs more slowly than movement of munitions by the current. However, storm events, which may be the greatest source of exposure and mobility risk, violate these assumptions. During storm events, bottom water velocity may increase dramatically, whether due to enhanced currents or due to wave-induced circulation at the seabed. The same effects can create rapid erosion at a timescale shorter than that for scour burial. Thus, during storm events, munitions either insufficiently buried or suddenly exposed by erosion may be mobilized by the temporarily enhanced bottom current.
- Bottom water velocities may also vary seasonally in synchrony with periodic erosion and accretion cycles as well as storm events. Our analysis does not capture the correlation of these processes.
- Bottom water velocity and erosion/accretion are stochastic variables whose randomness is not captured by our deterministic analysis. Our map shows a single maximum degree of erosion  $\delta_h$ . The stochastic nature of  $\delta_h$  adds uncertainty to predictions of munition fate, and assessments of risk probabilities would need to account for the statistical distribution of  $\delta_h$ .

## IDA | Initial burial regime map: Implications

- Burial regime maps are scenario specific.
- Localization to a sector of the map indicates what level of initial burial fidelity is useful:
  - High fidelity may be useful near edges of sectors
  - High fidelity may not be as useful within a sector
- Useful fidelity varies not only with local conditions, but also with burial depth



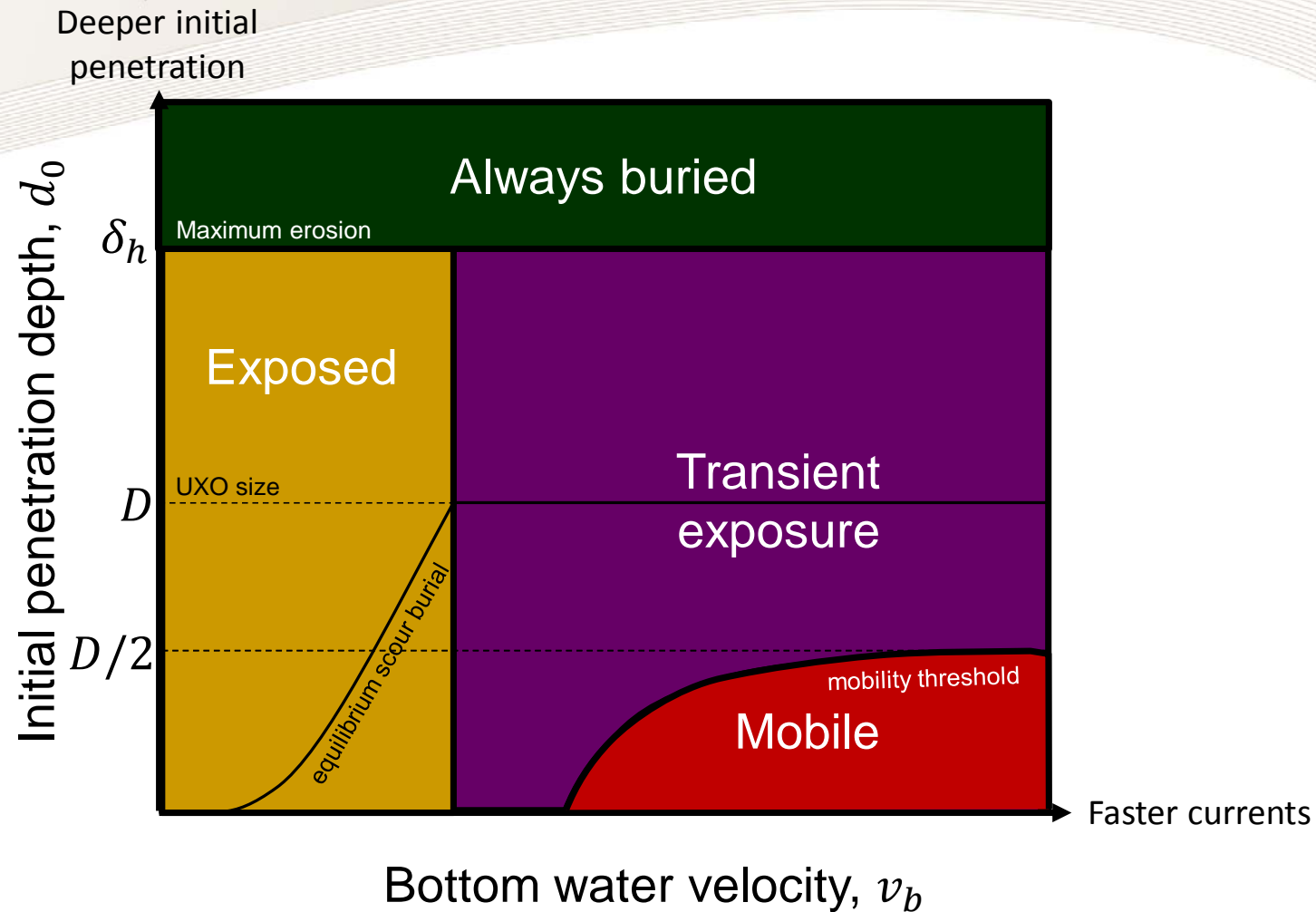


## **Implications**

Every scenario would require its own regime map to capture the local sediment conditions, water depth, currents, erosion profile, and munitions of interest. For each such scenario, the regime map would facilitate considerations of required prediction fidelity for initial sediment penetration. As discussed, identifying in which region of this map the munition lies would be useful, and therefore, high-fidelity initial predictions of penetration depth near the region boundaries may be very useful in some cases. However, far from region boundaries, high-fidelity prediction of initial penetration depth may have little influence on the risk associated with the munition.

The critical observation is that there is no universally useful fidelity for penetration prediction. The useful fidelity varies with penetration depth itself as well as with the local conditions, which determine the locations of the regime boundaries.

## IDA | Initial burial regime map: Risk buckets



## Risk Buckets

One could further simplify the regime map by dividing it into what we call *risk buckets*. Some of the distinguishable fates on the full regime map do not translate into different risks. It may principally be useful to distinguish levels or categories or “buckets” of risk rather than simply distinct fates. This diagram of risk buckets combines the regimes of initially exposed munitions and those durably exposed by erosion into a single risk bucket of stationary munitions exposed for sustained durations. This diagram also combines the map regimes corresponding to transient exposure by erosion and mobilization by erosion. Since those munitions above the mobility curve would typically be reburied by scour before they could be mobilized, in the absence of events generating rapid erosion and high currents, both regimes correspond to munitions temporarily exposed by erosion and remaining shallowly buried thereafter. In that vein, one could equally well think of the four risk buckets as:

- exposed,
- deeply buried,
- shallowly buried, and
- mobile.

## IDA | Initial burial regime map: Sandy Sediment Example

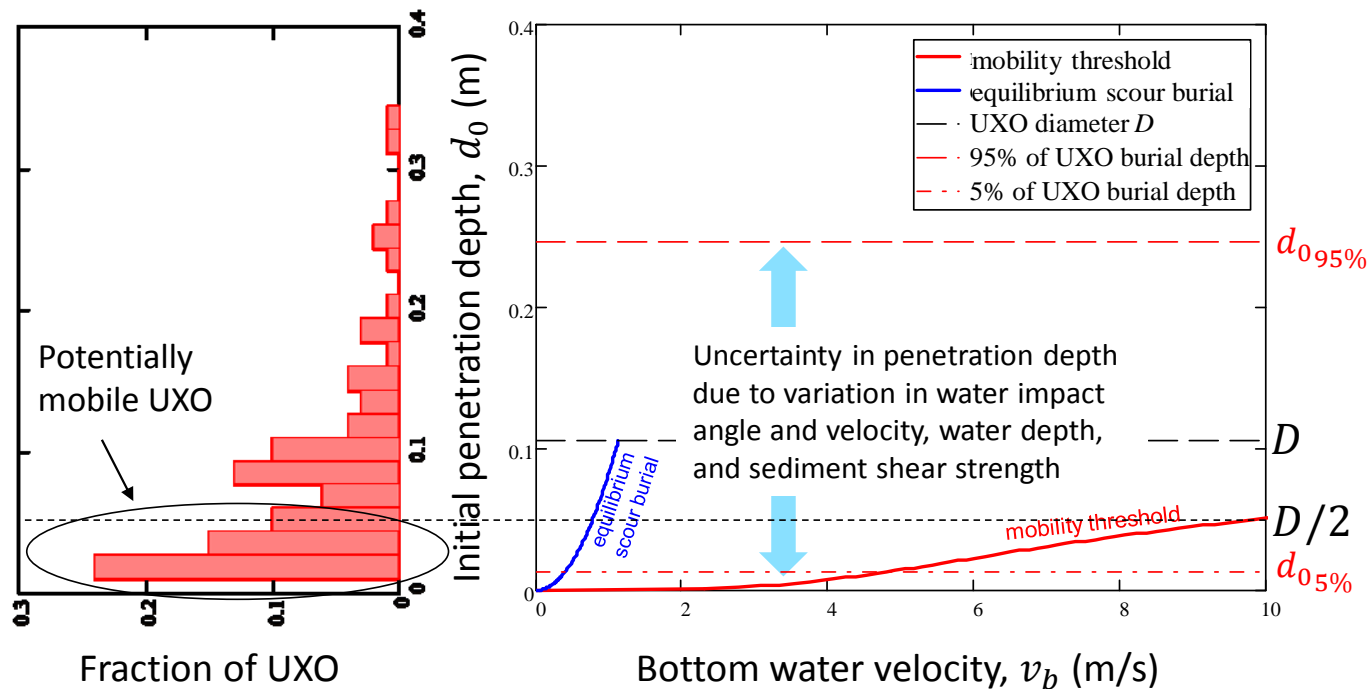
### Broad side impact:

Water depth: uniform distribution, 3 to 5 m

Water impact velocity: uniform distribution, 50 to 300 m/s

Water impact angle: normal distribution,  $45 \pm 15^\circ$

Sediment shear strength: normal distribution,  $20 \pm 5$  kPa



## **A Quantitative Example of the Burial Regime Map**

Here, on the right, we show a quantitative instance of the mobility and scour burial regimes of the map for a particular scenario. We utilized the equilibrium scour burial depth model from Rennie and Brandt 2015 and the IDA mobility threshold model for 100 micron sand (backup slide “Mobility Model: Balance of Moments about Contact Point”). On the left, we show a histogram of initial sediment-penetration depths from a Monte Carlo model discussed later in this briefing. The Monte Carlo simulation randomized over input values as described at the top of this slide. As shown, although the mean initial penetration depth is approximately half the munition diameter, the variability in the penetration depth in this case is large compared with the scale of the regimes on the map. In this case, the benefit of predicting initial penetration depth to high fidelity for any given input conditions would be negated by the high variability in initial penetration depth due to input condition variation. In short, the useful fidelity of initial penetration prediction is bounded by the variability in uncontrolled and unknown initial conditions.

## IDA | Recommendations: Sediment types

### Sandy

- Loose sediment with high bearing strength
- *Scour burial*: Local enhancement of eddy currents further bury munitions
- **Recommendation #1**: Improve sandy sediment penetration models.
- **Recommendation #3**: Develop mobility models for partly buried objects.

### Cohesive (clay, mud)

- Cohesive sediment with low bearing strength
- *Consolidation* (slow relief of pore pressure): Munitions sink over hours to years as excess water pore pressure equilibrates
- *Creep* (viscous behavior at long time scales): Munitions continue to sink over years to decades
- **Recommendation #2**: Develop mobility models for cohesive sediment.
- **Recommendation #4**: Develop scour burial models for cohesive sediment.
- **Recommendation #5**: Improve consolidation and creep models.

Here we consolidate the recommendations found in the preceding section.

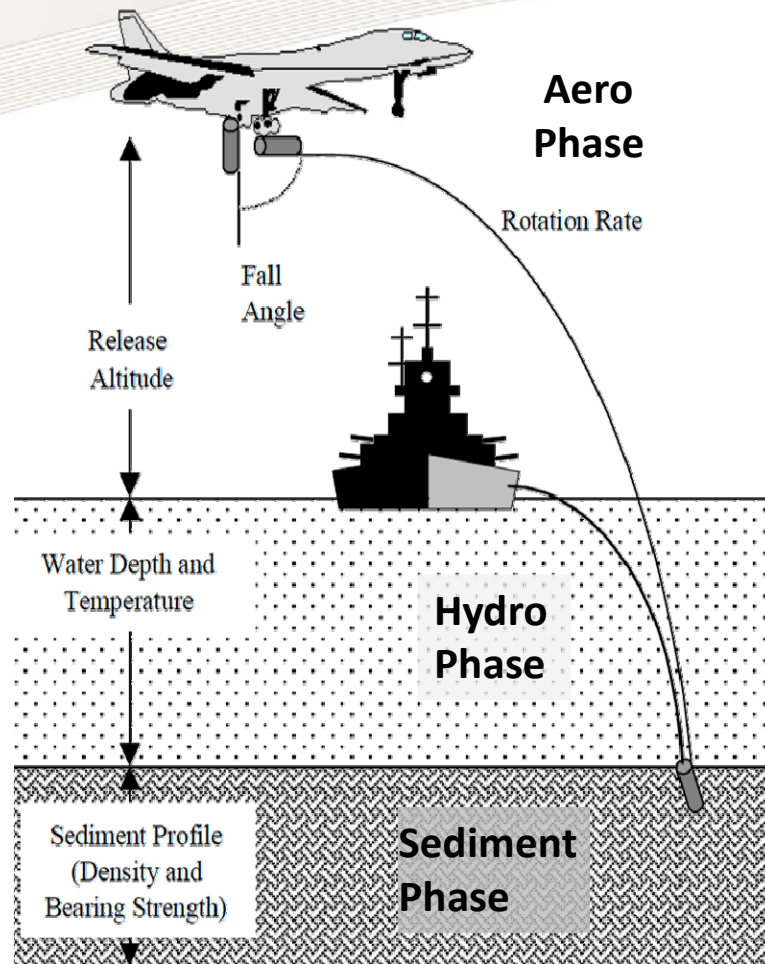
# **ACHIEVABLE FIDELITY OF INITIAL BURIAL DEPTH**



We have now explored what fidelity is *useful* for underwater UXO remediation projects when estimating a munition's initial penetration depth into the sediment.

Next, we will consider our second question: What fidelity is already *achievable* via existing penetration models that have already been developed for underwater mines?

# IDA | Predicting Penetration of Munitions into the Seabed



## Modeling Objective:

Estimate initial sediment penetration of UXO for inputs to models of burial, exposure, and mobility over time with the ultimate goal of predicting risk of UXO exposure and location.

## Existing Models

### Key parameters

- Water Impact velocity vector
- Angle of attack
- Water depth
- Munition drag coefficient
- Sediment Impact velocity vector
- Angle of attack
- Sediment shear strength, density, bearing strength
- Rate dependence of resistance force

MINE6D  
(MIT)

STRIKE35  
(NPS)

IMPACT35  
(NPS)

IMPACT28  
(NRL)

Initial  
Burial  
depth

Figure adapted from P.C. Chu et al., "Mine Burial Prediction Experiment," *J. of Counter-Ordnance Technology* (5th Int. Symp. On Technology and Mine Problem).

The descent of a munition to its final resting position in the sediment proceeds in three phases:

- **AERO PHASE**—For a munition released above the water, there is an aerodynamic or ballistic phase in which the munition, under the influence of gravity and aerodynamic forces and moments, travels from its release point to its water entry point. The initial conditions for the aerodynamic phase are given by the delivery mechanism of the weapon. For a mortar, it might be a muzzle velocity and elevation angle. For a bomb, it might be a release altitude and aircraft velocity. The aerodynamic model follows the projectile through the air and gives its location, orientation, velocity, and dynamics when it hits the waterline. For projectiles designed for aerodynamic stability, the orientation is fixed relative to the trajectory angle with small perturbations. These perturbations, however, can be amplified by asymmetric forces as the projectile transitions into the water.
- **HYDRO PHASE**—Once the projectile begins entering the water, there are interface effects at the waterline. Especially at high velocities, air becomes entrained along with the projectile and enters the water as a cavitation bubble surrounding the projectile. Drag forces, moments, and buoyancy are all affected by the cavitation bubble. The projectile travels through the water column influenced by gravity, buoyancy, and hydrodynamic forces and moments produced by viscous interaction with the water, as well as inertia of the water disturbed by the transit. If an aerodynamically stable projectile enters the water without damage (e.g., with intact fins) and with sufficiently low angle of attack, it may remain hydrodynamically stable during its water transit. A hydrodynamic model follows the projectile from its initial conditions given by the output of the aerodynamic model through its transit of the water column and provides the position, orientation, velocity, and dynamics of the projectile when it hits the so-called mudline, the interface between the water and the sediment.
- **SEDIMENT PHASE**—The sediment model then takes as its initial conditions the output of the hydrodynamic model and tracks the projectile's penetration into the sediment, accounting for gravity and phenomena-generating forces resisting sediment penetration, potentially including buoyancy, friction, inertia, sediment-bearing strength and shear strength, viscosity, pore pressure, etc. These properties may vary with location and depth below the mudline and may themselves be rate dependent. The sediment model tracks the projectile until it comes to a halt and outputs the final resting orientation and position of the projectile, most notably, its penetration depth below the mudline.

In addition to properties of the media, all these models require parameters describing the projectile such as its density and drag, lift, and moment coefficients.

Aerodynamic models generally exist within the ballistics community. These models are necessary because most projectiles do not achieve aerodynamic terminal velocity, so the water-entry velocity must be computed dynamically. Also, the trajectory is not generally perfectly vertical.

One of the primary thrusts of the analysis described in this document was the applicability or extensibility of models from the underwater mine community to the underwater UXO problem. The four models we considered are shown on the lower right of the slide. The ensuing slides will discuss these models further, but briefly: MINE6D developed by the Massachusetts Institute of Technology (MIT) and STRIKE35 developed by the Naval Postgraduate School (NPS) cover only the hydrodynamic phase, and IMPACT28 from the Naval Research Laboratory (NRL) and IMPACT35 from NPS cover the hydrodynamic and sediment-penetration phases as well as a rudimentary treatment of the aerodynamic phase.



## IDA | Brief Description of the Models

Model Name	Description	Validation
<b>2D models</b> predict rigid body motion in the $x$ - $z$ plane including rotation about the $y$ -axis.		
<b>IMPACT25/28</b>	3 DOF model from air-drop through water column. <sup>1</sup> <ul style="list-style-type: none"> <li>• Hydro: Developed to address rotation (absent in 1D predecessor IBPM).</li> <li>• Sediment: Handles multi-layers.</li> </ul>	Limited low velocity mine drops (<10 m/s)
<b>3D models</b> predict rigid body motion in $x,y,z$ coordinates including rotation about the $x,y,z$ axes. All have been compared favorably to limited experimental results/		
<b>MINE6-D</b> (Hydrodynamic only)	6-DOF model <sup>2</sup> designed to accurately capture complex 3D dynamics of mines in the water column.	Limited low velocity mine drops (<10 m/s)
<b>IMPACT35</b>	5-DOF model <sup>3</sup> (neglects rotation about the axis of symmetry) for near cylindrical mines. <ul style="list-style-type: none"> <li>• Hydro: Designed to account for <math>y</math>-direction currents and observed 3D dynamic modes of falling mines.</li> <li>• Sediment: Adds new rate-dependent sediment strength model to IMPACT 25/28.</li> </ul>	Limited low velocity mine drops (<10 m/s)
<b>STRIKE35</b> (Hydrodynamic only)	6-DOF model describes motion of JDAM through a water column. <sup>4</sup> Designed to model high velocity hydrodynamic behavior of a tapered object with fins.	Several high velocity JDAM drops (400 m/s)

Models and experiments show high sensitivity to initial conditions at waterline.

<sup>1</sup>P. Chu, "Mine Impact Burial Prediction From One to Three Dimensions," *Applied Mechanics Review* 62 (January 2009).

<sup>2</sup>J. Mann et al., "Deterministic and Stochastic Predictions of Motion Dynamics of Cylindrical Mines Falling Through Water," *IEEE Journal of Ocean Engineering* 32, no. 1 (2007).

<sup>3</sup>P. Chu and C. Fan, "Mine-Impact Burial Model (IMPACT-35) Verification and Improvement Using Sediment Bearing Factor Method," *IEEE J. of Ocean Eng.* 32, no. 1 (January 2007).

<sup>4</sup>P. Chu, et al., "Modeling of Underwater Bomb Trajectory for Mine Clearance," *Journal of Defense Modeling and Simulation: Applications, Methodology, Technology* 8 (1) (2011): 25–36.

This slide provides a compare-and-contrast of the four models introduced on the previous slide:

- IBPM, the Interim Burial Prediction Model, was a one-dimensional (1D) model that assumed a constant mine orientation. IBPM was expanded into a two-dimensional (2D) model capturing three degrees of freedom (two directions in position and one orientation, all in a single 2D plane). That model was implemented in BASIC as IMPACT25 and in MATLAB as IMPACT28. The IMPACT25/28 model addresses all three phases of descent (aerodynamic, hydrodynamic, and sediment) and accommodates multiple sediment layers with different properties. IMPACT25/28 utilizes a simplified sediment-penetration model based on bearing strength and assuming a simple relationship between bearing strength and shear strength. IMPACT25/28 also incorporates inertial resistance of the sediment, which may not be of critical importance in low-velocity *mine* sediment impacts but could be essential in high-velocity *munition projectile* impacts. IMPACT25/28 includes a cavitation model capturing such aspects as cavity oscillation frequency. Although capturing a lot of cavitation detail, the model requires empirical determination of a number of coefficients.
- IMPACT35 was then developed to incorporate more complex three-dimensional (3D) observed hydrodynamic behavior in descending mines, such as helical motion. A third dimension is also required to account for water currents in directions other than in-plane with the falling projectile. IMPACT35 is a five-degree-of-freedom model incorporating three directions of translation and two of rotation (pitch and yaw, but not roll, which is assumed to be immaterial due to rotation symmetry of the mines under consideration). IMPACT35 implemented what is known as the delta method for sediment-penetration estimation, which incorporates the effect of pore pressure. Further analysis and experiments with low-velocity mine drops suggested a better sediment-penetration model known as the bearing factor method, which was later incorporated into IMPACT35 in lieu of the delta method.
- MINE6D was developed for the same reasons as IMPACT35: to accurately capture the complex 3D dynamics of sinking mines. MINE6D adds the sixth degree of freedom of roll and can accommodate rotationally asymmetric shapes. MINE6D attempts to more rigorously capture the hydrodynamic interaction of the water with the sinking mine.

All three of the preceding models were supported by limited validation experiments with low-velocity mine drops. In mine drop experiments, the mines entered the water gently or were dropped from a low elevation. They typically, therefore, entered the water below hydrodynamic terminal velocity and accelerated as they descended. Contrast this with the UXO problem in which munition projectiles enter the water at velocities far in excess of the hydrodynamic terminal velocity and decelerate as they descend.

Hydrodynamic terminal velocity is the velocity that is asymptotically approached (from above or below) at which the hydrodynamic resistance forces exactly balance buoyancy and gravity to produce zero acceleration. Therefore:

- STRIKE35 was produced to capture the behavior of the high-velocity projectiles. It was developed/validated in conjunction with a set of experiments dropping Joint Direct Attack Munitions (JDAMs) into an instrumented pond. The JDAMs entered the water at roughly 400 m/s. STRIKE35 utilizes simple forward Euler time discretization to model progress through the water. Where STRIKE35 differs most from the other models is in its use of projectile-specific semi-empirical expressions for hydrodynamic lift, drag, and moment coefficients accommodating specifics such as fin geometry. Any of the models could be enhanced with experimentally derived hydrodynamic coefficients at the velocity ranges of interest. STRIKE35 takes as its initial conditions the entry velocity into the water and does not incorporate sediment penetration. STRIKE35 takes an ad hoc approach to cavitation by assuming that cavitation reduces the drag by a factor of 10 and then suddenly ceases when the munition angle of attack exceeds a pre-specified value.





## IDA | Brief Description of the Models

Model Name	Description	Validation
<b>2D models</b> predict rigid body motion in the x-z plane including rotation about the y-axis.		
<b>IMPACT25/28</b>	3-DOF model from air-drop through water column. <sup>1</sup> <ul style="list-style-type: none"> <li>Hydro: Developed to address rotation (absent in 1D predecessor IBPM).</li> <li>Sediment: Handles multi-layers</li> </ul>	Limited low velocity mine drops (<10 m/s)
<b>3D models</b> predict rigid body motion in x,y,z coordinates including rotation about the x,y,z axes. All have been compared favorably to limited experimental results.		
<b>MINE6-D</b> (Hydrodynamic only)	6-DOF model <sup>2</sup> designed to accurately capture complex 3D dynamics of mines in the water column.	Limited low velocity mine drops (<10 m/s)
<b>IMPACT35</b>	5-DOF model <sup>3</sup> (neglects rotation about the axis of symmetry) for near cylindrical mines. <ul style="list-style-type: none"> <li>Hydro: Designed to account for y-direction currents and observed 3D dynamic modes of falling mines.</li> <li>Sediment: Adds new rate-dependent sediment strength model to IMPACT 25/28.</li> </ul>	Limited low velocity mine drops (<10 m/s)
<b>STRIKE35</b> (Hydrodynamic only)	6-DOF model describes motion of JDAM through a water column. <sup>4</sup> Designed to model high velocity hydrodynamic behavior of a tapered object with fins.	Several high velocity JDAM drops (400 m/s)

Models and experiments show high sensitivity to initial conditions at waterline.

### Recommendation #6:

Exercise caution improving hydrodynamic models. Effect of better hydrodynamics may be dwarfed by stochasticity due to unknown precise initial conditions at the water line.

<sup>1</sup>P. Chu, "Mine Impact Burial Prediction From One to Three Dimensions," *Applied Mechanics Review* 62 (January 2009).

<sup>2</sup>J. Mann et al., "Deterministic and Stochastic Predictions of Motion Dynamics of Cylindrical Mines Falling Through Water," *IEEE Journal of Ocean Engineering* 32, no. 1 (2007).

<sup>3</sup>P. Chu and C. Fan, "Mine-Impact Burial Model (IMPACT-35) Verification and Improvement Using Sediment Bearing Factor Method," *IEEE J. of Ocean Eng.* 32, no. 1 (January 2007).

<sup>4</sup>P. Chu, et al., "Modeling of Underwater Bomb Trajectory for Mine Clearance," *Journal of Defense Modeling and Simulation: Applications, Methodology, Technology* 8 (1) (2011): 25–36.

These four models may do an excellent job predicting the progress of a projectile through the water *given initial conditions*. However, for the munition projectiles of interest in underwater UXO remediation, the initial conditions at the waterline may be highly uncertain. Therefore, adding fidelity to the hydrodynamic model may not address the dominant sources of uncertainty in the sediment-penetration prediction. In addition, the details of the projectile's progress through the water column may not have a strong influence on its initial conditions at the mudline and may therefore not strongly influence its sediment-penetration depth. Experiments and models have exhibited strong sensitivity to initial conditions. In experiments with nominally similar mine-release conditions, different falling modalities (e.g., see-saw vs. helical spiral) have been observed, suggesting instabilities not conducive to modeling. The statistics of the mudline impact velocity are more important than identifying which precise initial conditions lead to each descent modality.

Ultimately, caution should be exercised before investing further in high-fidelity hydrodynamic models as the goal is to characterize sediment-penetration depth.

## IDA | Model Features

	Dimensions	DOF	Aerodynamic	Wind	Waterline interface	Hydrodynamic	Cavitation	Fins	Current	Mudline interface	Sediment	Inertial drag
IMPACT25/28	2	3	Y	N	Y	Y	Y	N	N	Y	Y	Y
IMPACT35	3	5	Y	Y	Y	Y	N	N	Y	Y	Y	N
STRIKE35	3	6	N		Y	Y	Y	Y	N	N	N	
MINE6D	3	6	N		Y	Y	Y	N	Y	N	N	

Here we show a tabular breakdown of the features captured by the various models.

## IDA | Model Features

	Dimensions	DOF	Aerodynamic	Wind	Waterline interface	Hydrodynamic	Cavitation	Fins	Current	Mudline interface	Sediment	Inertial drag
IMPACT25/28	2	3	Y	N	Y	Y	Y	N	N	Y	Y	Y
IMPACT35	3	5	Y	Y	Y	Y	N	N	Y	Y	Y	N
STRIKE35	3	6	N		Y	Y	Y	Y	N	N	N	
MINE6D	3	6	N		Y	Y	Y	N	Y	N	N	

### Recommendation #7:

Models (other than STRIKE35) are designed for near-cylindrical mines. For UXO, projectile-specific drag, lift, and moment coefficients are needed for estimating hydrodynamic stability and gross velocity.

### Recommendation #8:

Model modules (aero, hydro, sediment) are nearly independent and could and should be mixed and matched with little effort to choose best-of-breed for each regime (aero, hydro, sediment) for each scenario of interest.

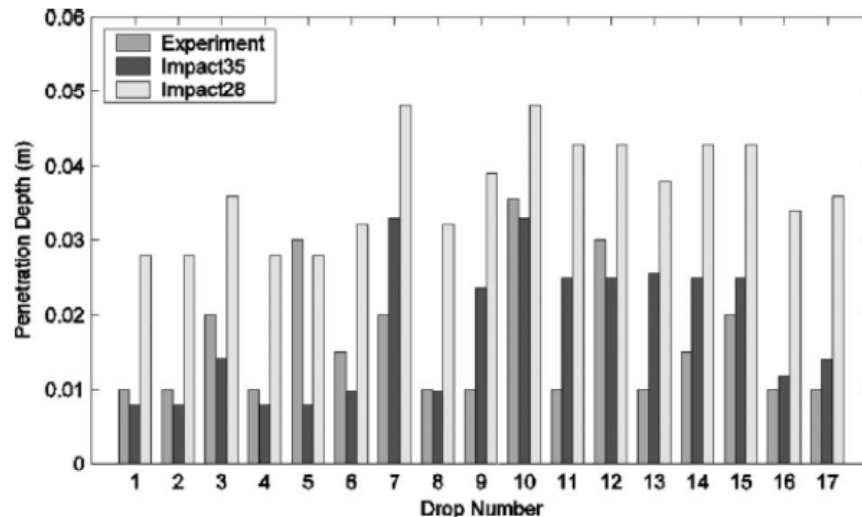
Even though STRIKE35 is the only model to use highly specific empirical hydrodynamic coefficients, it would not be difficult to implement this type of characteristic in any of the hydrodynamic models. The hard work is gathering the empirical data on each class of projectile. If the models other than STRIKE35 are used, the existing hydrodynamic coefficients based on cylindrical mines would likely not adequately capture the hydrodynamic behavior of munition projectiles for good sediment-penetration prediction. In particular, the models ought to capture the hydrodynamic stability of the projectiles, because projectiles penetrating the water column in a stable fashion will exhibit much higher terminal velocities and higher sediment impact velocities than do mines.

Also of note, the models incorporating multiple phases of descent (aerodynamic, hydrodynamic, and sediment) are spliced together in a relatively compartmentalized fashion, allowing the mixing and matching of modules between models with relative ease.

## IDA | Comparing 2D and 3D Burial Prediction models\*

Low-velocity (<10 m/s) mine impacts.

Mines were gently deposited in the water and reached terminal velocity in the water.



Model	Description	Used in
Bearing strength	Naïve weight bearing capacity relationship to shear strength; Inertial drag included	IMPACT25/28
Delta method	Includes shear forces, buoyancy, and water pore pressure	IMPACT35 early version
Bearing factor method	Found to be more accurate than Delta method in low velocity mine experiments	IMPACT35 later version

IMPACT35 matched experimental results more closely than IMPACT28.

### Questions:

- Is this improvement operationally significant?
- How much further improvement is possible?
- How much further improvement would be operationally useful?

\*P. Chu, "Mine Impact Burial Prediction From One to Three Dimensions," *Applied Mechanics Review* 62 (January 2009).



This slide compares a 2D model (IMPACT28) and a 3D model (IMPACT35) for estimating the penetration depth of mines.

The pertinent parameters for the 2D model (IMPACT28) are sediment density and bearing strength. For sediment resistance, the 2D assumes a bearing strength 10 times that of shear strength. The 3D model (IMPACT35) uses the Delta or Bearing factor method:

- The Delta method assumes that the mine pushes the sediment and leaves space in the wake as it penetrates the sediment. This space is refilled by water and the water cavity is produced.
- The Bearing factor method is based on the fact that the shear resistance, which retards the mine propagation, is proportional to the product of the sediment shear strength and the rupture area perpendicular to the velocity with a non-negative bearing factor.

(It was shown that the Bearing factor method gives more accurate predictions than the Delta method.)

The bar chart shown in this slide compares the predictions of the 2D model (IMPACT28, light gray) and 3D (IMPACT35, dark gray) with experimental data (medium gray). The 2D model (IMPACT28) overpredicts the actual sediment-penetration depth by an order of magnitude on average. As can be seen from the chart, the 3D model (IMPACT35) predictions are in better agreement with the experimental data.

It is important to note, however, that the 2D model errors are on the order of 2 to 3 cm, and the question we pose here is: How significant is the improvement in model predictions?

Realizing that there is considerable uncertainty in many other model parameters as well as initial conditions of the mine impact into sediments, we would like to understand to what extent the improvement in modeling predictions can be actually meaningful.

## **IDA | Applying Existing Models to Predict Location of UXO\***

- NRL Stennis developed a prototype framework for risk assessment
  1. Aerodynamic model – NRL in-house
  2. Hydrodynamic model – IMPACT35 + STRIKE35
  3. Sediment penetration model – IMPACT35
  4. Mobility and migration models – UXO MM
- They incorporated this framework into a Bayesian network
- They used a notional Camp Perry scenario to show that they could generate outputs based on a mash-up of pieces of the various codes in a way that could be compared to survey data
  - Their work demonstrates a proof-of-principle of incorporating existing mine models together for munition penetration prediction
  - Their work has not yet been fully validated with empirical data

\*K. Todd Holland, "A Wide Area Risk Assessment Framework for Underwater Military Munitions Response," MR2411 Progress Review, May 2015.

NRL Stennis used several models in tandem to construct a prototype probabilistic framework to statistically categorize spatial distribution of expected initial munitions contamination (Holland 2015). The following modules were assembled together:

- aerodynamic trajectory
- impact with the air-water interface
- free-fall through the water column (Chu and Ray 2006) – IMPACT35
- impact penetration with a sedimentary seabed (Chu and Fan 2007) – IMPACT35
- mobility and migration models (Wilson et al. 2008) – UXO MM

The easting/northing predicted location of the munitions were shown to be in close agreement with available data, which is the density of the UXO “targets” found by an underwater magnetometer survey. The conclusion of this work is that IMPACT35 could be quickly adapted for use in underwater UXO remediation projects, with the addition of ballistic equations and range firing records to simulate impact penetration and to predict a buried UXO population distribution.

Note, however, that to date, the results are limited to validating the easting/northing *location* estimates of the initial munition impacts, not their penetration *depth* into the sediment nor their subsequent mobility.

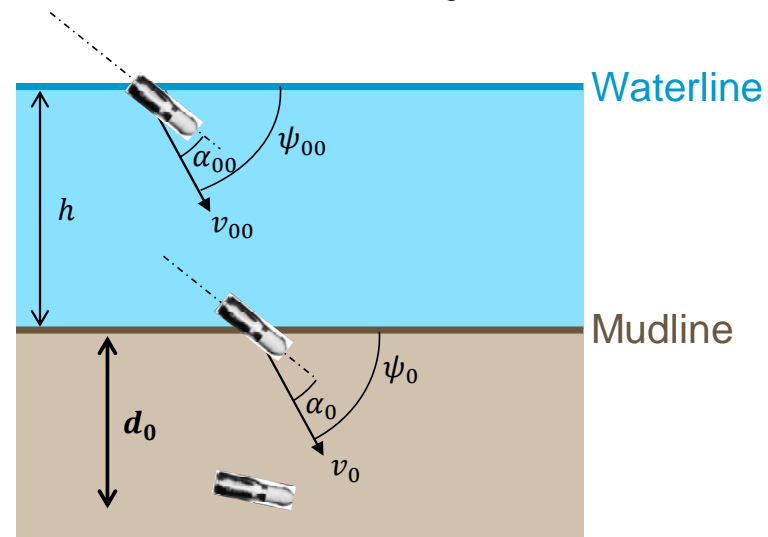
## IDA | Model dependencies

### General Munition Burial Model:

$$d_0 = f\left( \underbrace{\psi_{00}, \alpha_{00}, v_{00}}_{\substack{\text{initial conditions} \\ \text{of munition trajectory}}}, \underbrace{h, \mu}_{\text{environment}}, \underbrace{m, L, D, C_D}_{\text{munition properties}} \right)$$

- Aerodynamic model
  - Outputs:  $v_{00}, \psi_{00}, \alpha_{00}$
- Hydrodynamic model
  - Inputs:  $v_{00}, \psi_{00}, \alpha_{00}, h$
  - Outputs:  $v_0, \psi_0, \alpha_0$
- Sediment penetration model
  - Inputs:  $v_0, \psi_0, \alpha_0, \mu$
  - Output:  $d_0$
- Other properties
  - Air properties, water properties, current, wind, munition properties (lift, drag, density, shape, size)

$d_0$	initial penetration depth
$v_0$	velocity at mudline
$\psi_0$	elevation angle vs. mudline
$\alpha_0$	angle of attack at mudline
$\mu$	sediment shear strength
$h$	water depth
$v_{00}$	velocity at waterline
$\psi_{00}$	elevation angle vs. waterline
$\alpha_{00}$	angle of attack at waterline
$m$	munition mass
$L$	munition length
$D$	munition diameter
$C_D$	munition drag coefficient



Here we begin a mathematical characterization of the fidelity of initial sediment-penetration depth predictions. (Note that by “initial” sediment penetration, we are referring to the munition’s sediment penetration *upon impact*. We are *not* referring to the munition’s sediment penetration due to subsequent mobility, scour, or erosion/accretion.)

Our goal in this exercise is to build a mathematical framework for quantifying the relative contributions of various sources of initial sediment-penetration prediction error. This framework allows us to then explore the comparative value of reducing those error sources. We sought to identify which sources of error were dominant vs. negligible, as well as which sources of error were reducible vs. irreducible.

We start with a functional dependency model. The initial sediment-penetration depth  $d_0$  depends on the initial conditions of the munition’s trajectory (i.e., at the water line), the environment, and the munition’s properties:

- **Initial conditions of munition trajectory:** The moment in time to which the initial conditions are referenced is arbitrary. One could consider the functional model to begin when the projectile is released/expelled from its launching platform. However, it may instead be convenient to consider initial conditions at the moment the munition projectile first contacts the *waterline* from the air. We denote conditions associated with this first waterline contact by a “00” subscript. The munition’s initial conditions are thus its position, orientation, velocity, and rotation rate:
  - Velocity at the waterline is described by a speed  $v_{00}$  and trajectory angle  $\psi_{00}$ .
  - Angle of attack at the waterline is denoted by  $\alpha_{00}$  and captures the munition’s orientation at the waterline relative to its trajectory angle  $\psi_{00}$ . There could also be a yaw angle, but for simplicity we omit that here along with initial rotation rates.
  - Position at the waterline will only affect sediment-penetration depth via local environmental conditions, and therefore we need not explicitly consider the munition’s position at the waterline.
- **Environment:** We can capture the local environmental conditions via several parameters. Here we use two parameters, omitting others for clarity:
  - water depth  $h$  and
  - sediment shear strength  $\mu$ .

- **Munition properties:** We can characterize the munition via several parameters, as well. Here we omit many of those parameters for clarity (such as the munition's mass distribution, center of pressure, detailed shape, lift and moment coefficients, and so forth) and include only its:
  - mass  $m$ ,
  - geometry (length  $L$  and diameter  $D$ ), and
  - drag coefficient  $C_D$ .

Bearing all these parameters in mind, the functional model simply specifies the output (the initial sediment-penetration depth  $d_0$ ) as a function of the inputs. In this case,  $d_0 = f(\psi_{00}, \alpha_{00}, v_{00}, h, \mu, m, L, D, C_D)$ .

The various model regimes (i.e., aerodynamic, hydrodynamic, sediment) link the initial and final conditions (inputs and outputs) in each domain:

- The aerodynamic model takes as its input the munition projectile's release conditions and outputs the “00” conditions at the waterline.
- In turn, these “00” conditions serve as the inputs to the hydrodynamic model, which then computes the “0” conditions at the mudline.
- The “0” conditions then feed the sediment-penetration model, which outputs the initial sediment-penetration depth  $d_0$ .

Because no model perfectly represents the physical world, even with perfectly correct inputs, the output of every model will differ from what an experiment would show. We refer to this as the model error:

- $\varepsilon_{hm}$  for the hydrodynamic model error and
- $\varepsilon_{sm}$  for the sediment model error.

We do not fully consider the aerodynamic model here; we take the “00” waterline initial conditions as the point of entry into our consideration.



## IDA | Sensitivities of General Munition Burial Model

- Sediment penetration model:

$\varepsilon$  = error

$$\varepsilon_{d_0} = \underbrace{\frac{\partial d_0}{\partial v_0} \varepsilon_{v_0} + \frac{\partial d_0}{\partial \psi_0} \varepsilon_{\psi_0} + \frac{\partial d_0}{\partial \alpha_0} \varepsilon_{\alpha_0} + \frac{\partial d_0}{\partial \mu} \varepsilon_{\mu}}_{\text{model sensitivity}} + \varepsilon_{sm}$$

- Hydrodynamic model:

$$\varepsilon_{v_0} = \frac{\partial v_0}{\partial v_{00}} \varepsilon_{v_{00}} + \frac{\partial v_0}{\partial \psi_{00}} \varepsilon_{\psi_{00}} + \frac{\partial v_0}{\partial \alpha_{00}} \varepsilon_{\alpha_{00}} + \frac{\partial v_0}{\partial h} \varepsilon_h + \varepsilon_{hm_v}$$

$$\varepsilon_{\psi_0} = \frac{\partial \psi_0}{\partial v_{00}} \varepsilon_{v_{00}} + \frac{\partial \psi_0}{\partial \psi_{00}} \varepsilon_{\psi_{00}} + \frac{\partial \psi_0}{\partial \alpha_{00}} \varepsilon_{\alpha_{00}} + \frac{\partial \psi_0}{\partial h} \varepsilon_h + \varepsilon_{hm_\psi}$$

$$\varepsilon_{\alpha_0} = \frac{\partial \alpha_0}{\partial v_{00}} \varepsilon_{v_{00}} + \frac{\partial \alpha_0}{\partial \psi_{00}} \varepsilon_{\psi_{00}} + \frac{\partial \alpha_0}{\partial \alpha_{00}} \varepsilon_{\alpha_{00}} + \frac{\partial \alpha_0}{\partial h} \varepsilon_h + \varepsilon_{hm_\alpha}$$

Model error

- Combined model

$$\begin{aligned} \varepsilon_{d_0} = & \frac{\partial d_0}{\partial v_0} \left( \frac{\partial v_0}{\partial v_{00}} \varepsilon_{v_{00}} + \frac{\partial v_0}{\partial \psi_{00}} \varepsilon_{\psi_{00}} + \frac{\partial v_0}{\partial \alpha_{00}} \varepsilon_{\alpha_{00}} + \frac{\partial v_0}{\partial h} \varepsilon_h + \varepsilon_{hm_v} \right) \\ & + \frac{\partial d_0}{\partial \psi_0} \left( \frac{\partial \psi_0}{\partial v_{00}} \varepsilon_{v_{00}} + \frac{\partial \psi_0}{\partial \psi_{00}} \varepsilon_{\psi_{00}} + \frac{\partial \psi_0}{\partial \alpha_{00}} \varepsilon_{\alpha_{00}} + \frac{\partial \psi_0}{\partial h} \varepsilon_h + \varepsilon_{hm_\psi} \right) \\ & + \frac{\partial d_0}{\partial \alpha_0} \left( \frac{\partial \alpha_0}{\partial v_{00}} \varepsilon_{v_{00}} + \frac{\partial \alpha_0}{\partial \psi_{00}} \varepsilon_{\psi_{00}} + \frac{\partial \alpha_0}{\partial \alpha_{00}} \varepsilon_{\alpha_{00}} + \frac{\partial \alpha_0}{\partial h} \varepsilon_h + \varepsilon_{hm_\alpha} \right) \\ & + \frac{\partial d_0}{\partial \mu} \varepsilon_{\mu} + \varepsilon_{sm} \end{aligned}$$

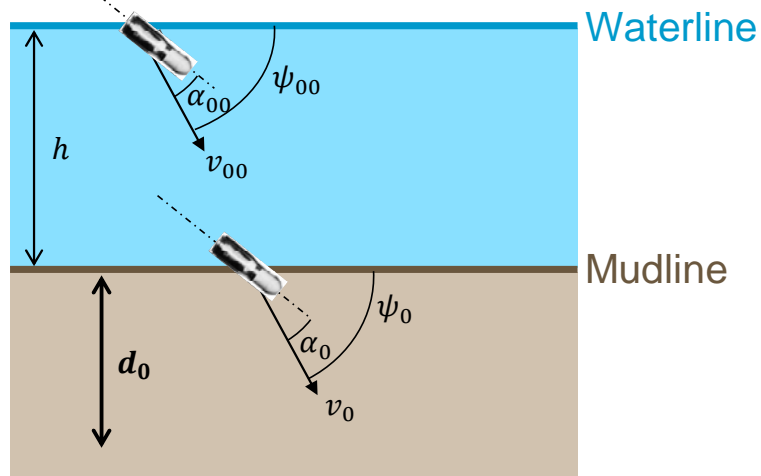


In addition to the model errors  $\varepsilon_{hm}$  and  $\varepsilon_{sm}$ , any implementation of the model will provide imperfect results because the inputs can never be perfectly well known. The sensitivity of the model is the degree to which the outputs are affected by variation (or error) in the inputs. For a high-fidelity model, the sensitivity of the model may be closely approximated by the sensitivity of the underlying physical system to perturbations in the initial conditions. Assuming that the outputs vary smoothly with the input values, for sufficiently small deviations in initial conditions, a linear model describes the sensitivities in terms of derivatives of the functional model. Adopting the nomenclature that  $\varepsilon_x$  is the error in parameter  $x$ , we denote, for example, the error in the input initial trajectory angle at the waterline as  $\varepsilon_{\psi_{00}}$ . Thus, in the hydrodynamic model, for example, the contribution to the error in the prediction of mudline velocity  $\varepsilon_{v_0}$  from error in the input waterline velocity  $\varepsilon_{v_{00}}$  would be given by the product of the input error  $\varepsilon_{v_{00}}$  and the sensitivity  $\frac{\partial v_0}{\partial v_{00}}$ . This framework can be constructed for either single-domain models or for the end-to-end functional model.

The overall output prediction error is given by the sum of the modeling error and the contributions from input errors. The input errors to one domain can be constructed from the input errors to the preceding domain and the modeling error in the preceding domain.

## IDA | Errors and Assumptions

- $\varepsilon_{v_{00}}, \varepsilon_{\alpha_{00}}, \varepsilon_{\psi_{00}}$ : from ballistic/aerodynamic uncertainty.
- $\varepsilon_h$ :
  - Short term: from waves, tide.
  - Long-term: from water level, mudline evolution.
- $\varepsilon_\mu$ : from measurement uncertainty, spatial variation, time evolution



Since our consideration begins at the waterline, we consider the errors in waterline initial conditions to be overall inputs to our system. These errors come from unmeasured variation in the firing and transit conditions of the projectiles as well as errors in the aerodynamic model.

Errors in the water depth can arise from short-term variability in water depth due to waves and tides. A projectile impacting the crest of a wave would experience a different water column depth  $h$  than a projectile impacting the trough of the wave. Water depth  $h$  also varies over long periods of time due to changes in overall absolute water level as well as evolution of the sediment contour (i.e., erosion, accretion, formation movement).

Errors in sediment properties such as shear strength  $\mu$  arise from difficulty making high-fidelity measurements of sediment properties as well as variability over time and from point to point within a region of interest.

## IDA | Errors and Assumptions

- $\varepsilon_{v_{00}}, \varepsilon_{\alpha_{00}}, \varepsilon_{\psi_{00}}$ : from ballistic/aerodynamic uncertainty.

Irreducible (based on variable & unknown firing conditions)

- $\varepsilon_h$ :

Irreducible

- Short term: from waves, tide.
- Long-term: from water level, mudline evolution.

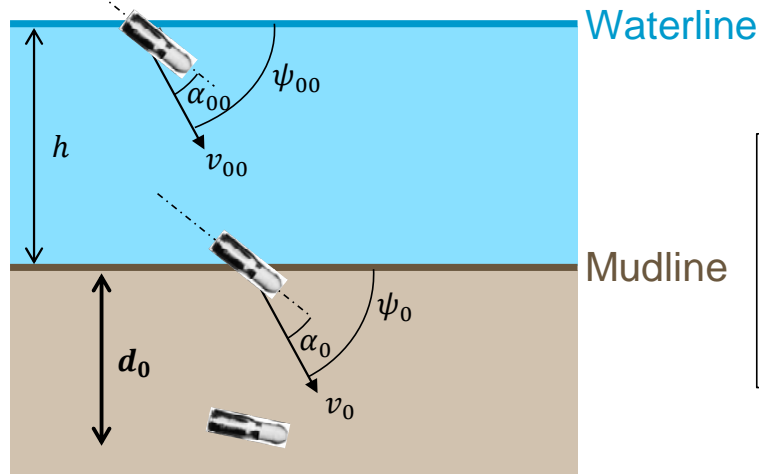
Probably irreducible

Reducible

- $\varepsilon_\mu$ : from measurement uncertainty, spatial variation, time evolution

Irreducible

Probably irreducible



$$\varepsilon \rightarrow \sigma$$

Statistical characterization of error:

$\varepsilon$  = error in one instance

$\sigma$  = average magnitude of error

$$\sigma = \sqrt{E(\varepsilon^2)}$$

Some of these sources of error are reducible and some are irreducible. For example, sediment property measurement error  $\varepsilon_\mu$  might be reduced by development of improved measurement techniques and equipment. On the other hand, for retrospective studies, the particular firing conditions during a time frame decades in the past may be unknown and irrecoverable. If irreducible errors dominate overall uncertainty in sediment-penetration prediction, then there is little overall fidelity to be gained by improving the reducible uncertainties.

Continuing this analysis, we will move from a consideration of the error in one instance (e.g., one munition impacting the sediment) to the statistical characterization of the error over a large number of instances (e.g., a large number of munitions impacting the sediment). We denote the standard deviation of the error  $\sigma$ ; this parameter represents the expected or mean magnitude of the corresponding single-instance error  $\varepsilon$  over a large number of instances.

## IDA | Improving Initial Burial Prediction

- Improving model ( $\sigma_{hm}, \sigma_{sm}$ ) vs. improving measurement ( $\sigma_{\mu}$ )
- Plan:
  - ✓ Evaluate model sensitivities by running models and using low-order analytic approximations
    - Get waterline input errors ( $v_{00}, \psi_{00}, \alpha_{00}$ ) from ballistics community
    - Get  $\sigma_{\mu}$  and  $\sigma_h$  from oceanography community
      - Only measurement contribution to  $\sigma_{\mu}$  can be improved
    - Review validation experiments for hydrodynamic models to estimate model uncertainties ( $\sigma_{hm}, \sigma_{sm}$ )
      - May be different in high-speed regime
  - ✓ Plug everything into sensitivities equation:

$$\epsilon_{d_0} = \underbrace{\frac{\partial d_0}{\partial v_0} \epsilon_{v_0} + \frac{\partial d_0}{\partial \psi_0} \epsilon_{\psi_0} + \frac{\partial d_0}{\partial \alpha_0} \epsilon_{\alpha_0} + \frac{\partial d_0}{\partial \mu} \epsilon_{\mu}}_{\text{model sensitivity}} + \epsilon_{sm}$$

One key question for efficient improvement of a sediment-penetration model is the choice between model improvement and measurement improvement:

- Model improvements could help if the aspects of the physics not captured or poorly captured by the model contribute significantly to the deviation of predicted depths from actual penetration depths.
- On the other hand, if the physics is already adequately captured by the model but there is sensitivity to knowable inputs, measurement improvements could help.

In short, if the dominant uncertainty is due to unknowable inputs, other improvements may have little leverage.

Here we lay out a recipe for considering the relative error contributions for cases of interest. We have exercised the first and last steps for an example case.

We hypothesize that although low-order models may not capture the nuances of the physical world, they do capture the gross behavior of the physical world well enough to identify major sensitivities. These low-order models are well-suited to use in this fashion due to their quick run time and the insight provided by analytic approximations. We derive and evaluate the sensitivities in an example to follow:

- The initial conditions at the waterline ( $v_{00}, \psi_{00}, \alpha_{00}$ ) should be provided by the ballistics community, where as a matter of course in the testing and characterizing of munitions under nominal conditions, there should be an understanding of the scatter in their speed, trajectory, and angle of attack.
- Variability and measurement uncertainty in the environmental parameters ( $\sigma_\mu$  and  $\sigma_h$ ) should be drawn from the oceanographic community regarding water depth (tides, waves, and long-term water-level variation) and sediment properties (composition, spatial variability, variation over time, and measurement errors). In general, only the variance in measurement error of sediment properties will be reducible.

The model uncertainties should be estimated using existing validation experiments where possible. Prediction errors of the models compared with the experiments should provide the scope of the magnitude of the modeling error for the regime tested. Care must be taken to ensure the free model parameters were not set using the same experiments considered for validation. If experiments were only done in the low-speed regime, as is the case for the mine burial models, new experimentation may be required to understand model errors in the high-speed regime. In particular, the use of low-speed drag and moment coefficients may not capture the high-speed hydrodynamic behavior of munition projectiles.

Finally, as we show in our example, the error contribution estimates should be evaluated in the overall sensitivity equation to compare their magnitudes and identify potential opportunities for improvement.





## IDA | Error Budget: Sediment Penetration Model

- **Sensitivity Equation at Mudline:**

$$\varepsilon_{d_0} = \frac{\partial d_0}{\partial v_0} \varepsilon_{v_0} + \frac{\partial d_0}{\partial \psi_0} \varepsilon_{\psi_0} + \frac{\partial d_0}{\partial \alpha_0} \varepsilon_{\alpha_0} + \frac{\partial d_0}{\partial \mu} \varepsilon_{\mu} + \varepsilon_{sm}$$

$$\sigma = \sqrt{E(\varepsilon^2)}$$

- **Assuming low cross-correlation contribution:**

Sediment model sensitivities

$$\sigma_{d_0}^2 = \left( \frac{\partial d_0}{\partial v_0} \right)^2 \sigma_{v_0}^2 + \left( \frac{\partial d_0}{\partial \psi_0} \right)^2 \sigma_{\psi_0}^2 + \left( \frac{\partial d_0}{\partial \alpha_0} \right)^2 \sigma_{\alpha_0}^2 + \left( \frac{\partial d_0}{\partial \mu} \right)^2 \sigma_{\mu}^2 + \sigma_{sm}^2$$

Sediment Modeling Error

Sediment property uncertainty

Errors emerging from hydrodynamic calculation including hydrodynamic modeling error ( $\sigma_{hm}$ ) and input error to hydrodynamic model ( $\sigma_{v_{00}}, \sigma_{\psi_{00}}, \sigma_{\alpha_{00}}$ )

What would each of these terms be?

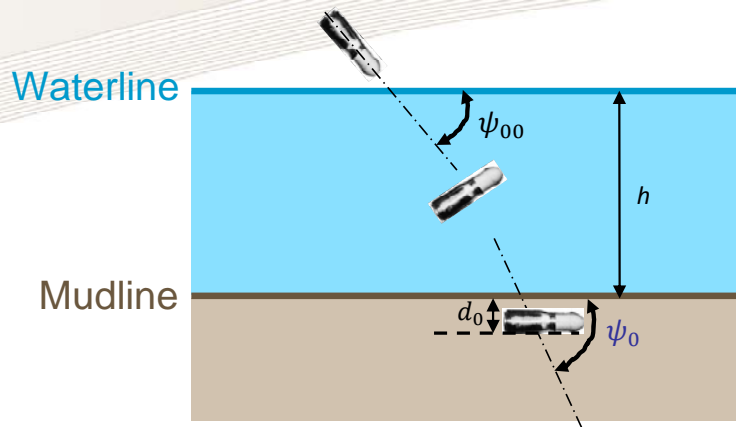
Depends on munitions, sediments...

Looking at the sediment-penetration model, we make the conversion from single-instance errors to standard deviations to form what we call “the sensitivity equation” for the sediment phase. In general, there could be cross-terms in the sensitivity equation involving correlations between the various error sources. For instance, deviations of velocity from the nominal value may be correlated with deviations from the nominal trajectory. For simplicity, we assume that such cross-terms are negligible here. For truly unrelated terms, such as the sediment properties and the munition projectile’s initial conditions at the mudline, this assumption is strongly justified. Regarding the munition projectile’s angle of attack, symmetry might suggest that the cross-terms with the other initial conditions would be zero (e.g., if for every  $\varepsilon_{\psi_0}$  there is equal likelihood of  $+\varepsilon_{\alpha_0}$  and  $-\varepsilon_{\alpha_0}$  then, on average, the product  $\varepsilon_{\psi_0}\varepsilon_{\alpha_0}$  will equal zero because the positive and negative contributions will cancel out by symmetry).

The sensitivities and initial condition uncertainties depend on the so-called operating point—the particular nominal initial conditions and munitions properties. The sediment property uncertainty likewise depends on the sediment properties themselves.

Note that in writing the error budget for the sediment-penetration phase, the errors in the initial conditions at the mudline implicitly depend on uncertainties propagated from the waterline initial conditions via the hydrodynamic model.

## IDA | Stages of a Simplified UXO Burial Depth Model



### Modeling assumptions:

- Presented area and drag coefficient numbers are comparable with those of Strike35 (i.e., munition tumbles upon impact)
- Broadside munition sediment impact
- Known sediment shear strength distributions

1. 2D hydrodynamic model:

$$f_z = \frac{\Delta\rho}{\rho_w} g - \frac{\rho_w A C_d}{2m} v v_z$$

$$f_x = -\frac{\rho_w A C_d}{2m} v v_x$$

2. Aubeny's sediment penetration model<sup>1</sup>

$$f = \begin{cases} c(v)\gamma_1(\mu)(\sqrt{x^2 + z^2})^{b_1} + \frac{1}{2} A C_d \frac{\rho_s}{m} v^2, & z \leq \frac{D}{2} \\ c(v)\gamma_2(\mu)(\sqrt{x^2 + z^2})^{b_2} + \frac{1}{2} A C_d \frac{\rho_s}{m} v^2, & z > \frac{D}{2} \end{cases}$$

where:

$f$  is the force experienced by the munition,

$$c(v) = 1 + \lambda \ln\left(\frac{v}{\varepsilon_0}\right),$$

$$\gamma_1(\mu) = \frac{\mu A f_1}{m D^{b_1}},$$

$f_1, b_1, f_2, b_2, \lambda$  are empirical constants

$$\gamma_2(\mu) = \frac{\mu A f_2}{m D^{b_2}}$$

<sup>1</sup> C. Aubeny and H. Shi, "Effect of Rate-Dependent Soil Strength on Cylinders Penetrating Into Soft Clay," *IEEE J. Oceanic Eng.* 32 (1) (January 2007).

To gain understanding of how a munition projectile propagates through the hydrodynamic and sediment phases, we make simplifying assumptions and solve the resulting equations of motion numerically in 2D. In our formulation, “z” and “x” are the vertical and horizontal directions, respectively.

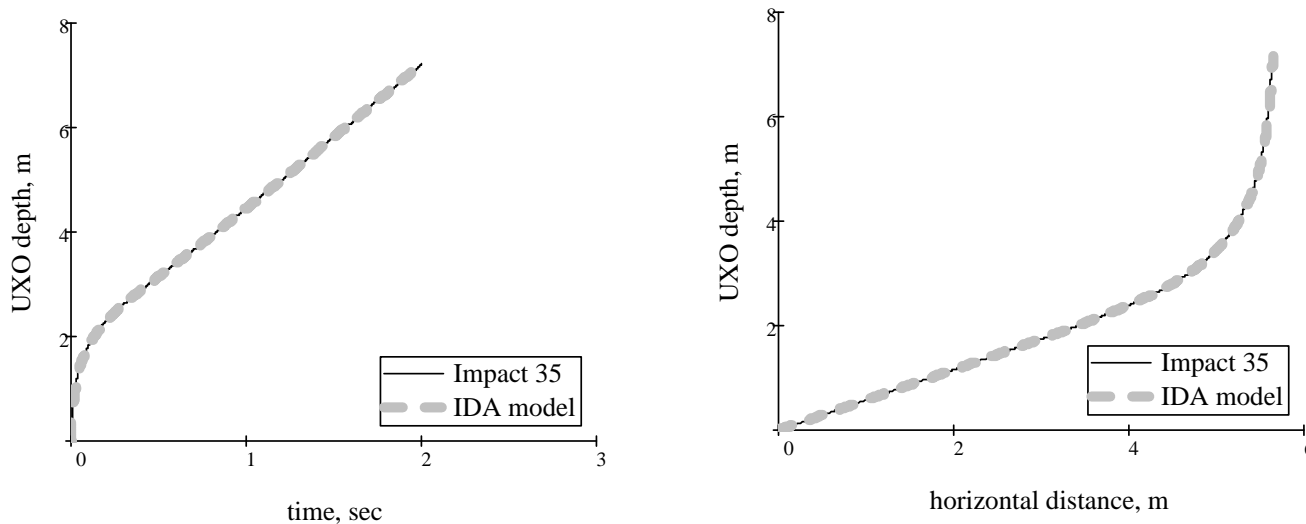
- Hydrodynamic Phase: The differential equations describing the trajectory of the moving munition are given on the chart in part 1 of this slide. The unknowns in these equations are presented area and drag coefficient. We estimate the presented area by assuming that the munition tumbles upon impact. We estimate the value of the drag coefficient by analyzing results of the STRIKE35, as shown in the next chart.
- Sediment Phase: We use Aubeny and Shi’s (2007) equations of a projectile propagating through the sediment phase, given in this chart in part 2. We augment this model by adding a sediment inertial resistance force term. We use the numerical values for the model parameters given by Aubeny and Shi (2007):  $f_1 = 7.41$ ,  $f_2 = 6.34$ ,  $b_1 = .37$ ,  $b_2 = .155$ ,  $\lambda = .022$ . Note that when the sediment-impact velocity is small, on the order of several meters per second, the inertial force effects are also small and can be neglected. This does not remain so, however, as the impact velocity increases.

## IDA | Simplified 2D Hydrodynamic Model vs. IMPACT35 (3D)

### Example: M344

$m = 8.75 \text{ kg}$ ,  $D = 0.106 \text{ m}$ ,  $L = 0.57 \text{ m}$ ,  $C_d = 0.3$ ,  $v_{00} = 200 \text{ m/s}$ ,  $\psi_{00} = 30^\circ$ ,  $\alpha_{00} = 0$

Presented area  $0.045 \text{ m}^2$



It is possible to use simplified 2D hydrodynamic models in place of IMPACT35 (3D).

This simplified model was solved numerically.

## Hydrodynamic Phase

Here we numerically solve the 2D hydrodynamic phase equations of motion for a particular case with the impact conditions and munitions parameters as shown. The trajectories predicted by our simplified 2D model (dashed gray line) and STRIKE35 (solid black line) are in good agreement, lending confidence to using our simplified 2D model for subsequent analyses of munition trajectory through the water.

## IDA | Even Simpler 1D Hydrodynamic Model

- An analytic model is an exact solution to a simplified problem and can be used to:
  - Compute partial derivatives (for the sensitivities equation).
  - Scope the area of parameter space in which some variables do not contribute (e.g., terminal velocity).

$$\sigma_{v_0}^2 = \left( \frac{\partial v_0}{\partial v_{00}} \right)^2 \sigma_{v_{00}}^2 + \left( \frac{\partial v_0}{\partial \psi_{00}} \right)^2 \sigma_{\psi_{00}}^2 + \left( \frac{\partial v_0}{\partial \alpha_{00}} \right)^2 \sigma_{\alpha_{00}}^2 + \left( \frac{\partial v_0}{\partial h} \right)^2 \sigma_h^2 + \sigma_{hm_v}^2$$

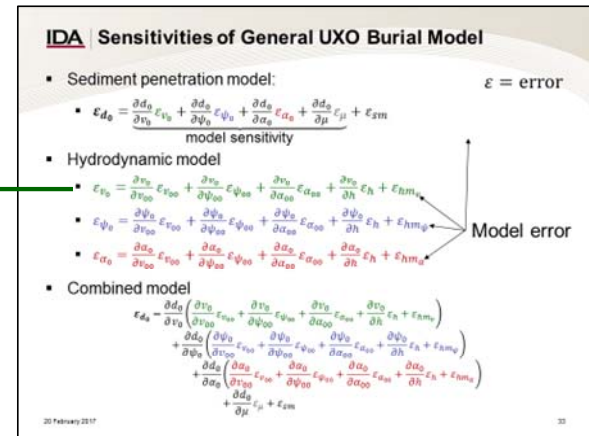
- In a regime far above terminal velocity in water, the forces on the descending munition will be dominated by hydrodynamic form drag:

$$m \frac{dv}{dt} = -\frac{1}{2} \rho_w v^2 C_d A$$

where

$$v = v_0 e^{\beta z}$$

$$\beta \equiv \frac{\rho_w C_d A}{2m}$$





## Hydrodynamic Phase

In contrast to computational models (which are in some sense like a black box, a mysterious enclosed device, where one can explore behavior by adjusting inputs and observing outputs), analytical models provide a mathematical formula, that can be examined to produce insight. For instance, as shown on the bottom of this slide, the analytical solution to a hydrodynamic model,  $v = v_0 e^{\beta z}$ , suggests that projectile velocity at the mudline will be proportional to projectile velocity at the waterline (with a constant of proportionality that will vary with projectile properties). This solution may be inaccurate because it solves a simplified problem stripped of some of the important physics such as projectile rotation, but assuming it captures the dominant physical features, the insights it yields should hold approximately true. Thus, without doing many computational experiments, one could understand how projectile velocity at the mudline depends on other factors.

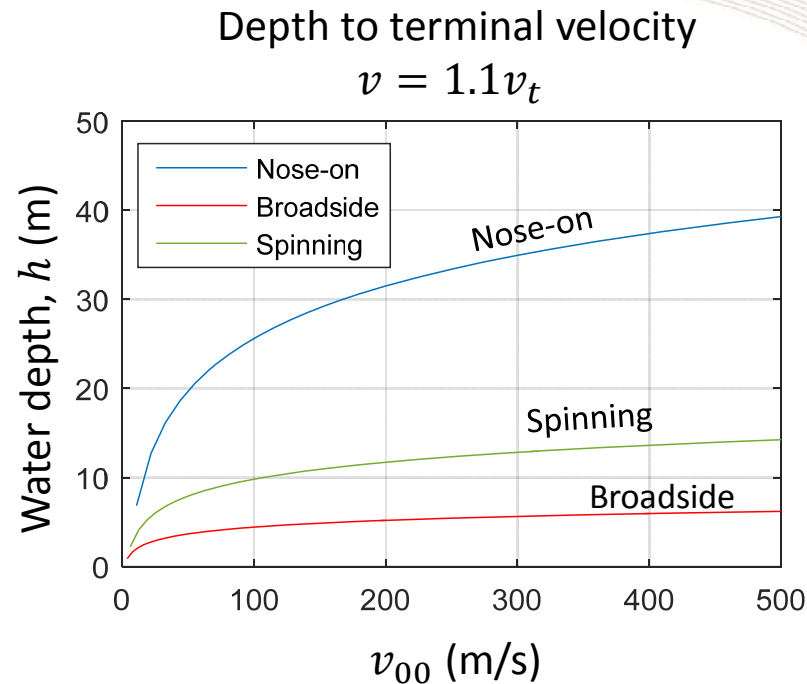
This analytical model can be used to compute mathematical expressions for the sensitivities in the error budget (e.g.,  $\frac{\partial v_{00}}{\partial v_0}$ ). It can also be used to carve out areas of parameter space (sets of operating points) where variables may be unimportant. For instance, for sufficiently deep water, munitions will reach terminal velocity (the velocity at which vertical forces are in equilibrium and the object remains at a constant velocity) before hitting the mudline. In such water depths, the munition's velocity at the waterline no longer affects its velocity at the mudline, and improved hydrodynamic models to capture detailed projectile dynamics during the early phases of water entry are wasted with regard to sediment-penetration depth prediction. Therefore, the analytic model can help determine how deep is “sufficiently deep” such that the sediment-penetration depth is independent of the initial conditions at the waterline.

The particular model shown on this slide ( $v = v_0 e^{\beta z}$ ) assumes that the projectile travels only vertically (i.e., in 1D) and presents a constant projected area and drag coefficient. In this case, the projectile velocity decreases exponentially with depth in the water column. In the backup slides (“Angled Trajectories”) we show a more nuanced analytical model that captures horizontal motion of a 2D trajectory.

## IDA | Even Simpler 1D Hydrodynamic Model: Example

$$v = v_0 e^{\beta z}$$

- M344
- Specific gravity:  $S = 4$
- $C_d = 0.3$
- Aspect ratio = 6
- Diameter = 0.106 m
- Presented area depends on dynamics
  - Nose on
  - Spinning
  - Broadside



Here we use an even simpler 1D hydrodynamic model  
in place of IMPACT35.

We solved this model analytically.

This model delineates a region of parameter insensitivity  
due to terminal velocity ( $v_t$ ).

## Hydrodynamic Phase

As suggested on the previous slide, here we exploit the 1D analytical hydrodynamic model ( $v = v_0 e^{\beta z}$ ) to identify the depth at which the munition's terminal velocity is achieved and its subsequent behavior is independent of the initial conditions ( $\frac{\partial v_0}{\partial v_{00}} = \frac{\partial \psi_0}{\partial v_{00}} = \frac{\partial \alpha_0}{\partial v_{00}} = 0$ ). Since, in this model, terminal velocity is approached asymptotically, we consider achievement of 110% of terminal velocity sufficient to remove the effect of initial conditions. We take a set of munitions parameters associated with the M344 shell. See backup slide “M344” for more information on this particular type of projectile.

We consider three possibilities for the projectile dynamics in the water (parametrically, since the model does not allow projectile rotations):

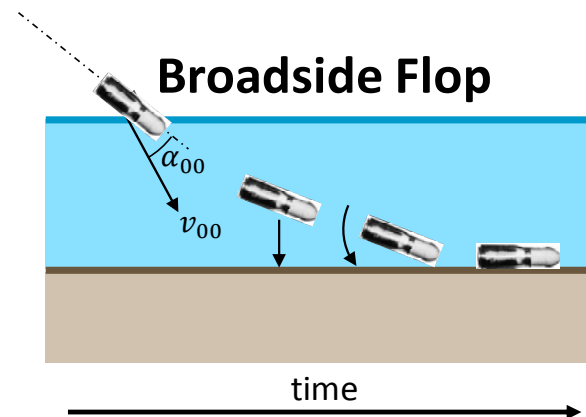
- nose-on,
- spinning, and
- broadside.

The presented area of a projectile is minimized when traveling nose-on and maximized when traveling broadside, so results for those two conditions should bound the behavior in other cases. For a projectile that spins through the water column, one can show that the analytical solution holds with the presented-area-drag-coefficient product replaced by its time-averaged value,  $\overline{C_d A} = \frac{1}{t} \int_0^t C_d(t') A(t') dt'$ ,  $\beta = \frac{\rho_w \overline{C_d A}}{2m}$ .

The analysis then shows that for this projectile, if unstable in the water column (either broadside or spinning), initial conditions at the waterline do not influence sediment-penetration depth in water deeper than 15 m. In contrast, if this projectile transits the water stably nose-on, it would need 30–40 m depth to wash out initial waterline conditions.

## IDA | Hydrodynamic Instability

- If fins break off or with a large enough angle of attack at the waterline ( $\alpha_{00}$ ), the projectile can tumble or turn **broadside**.
  - In our computational studies, we utilize a **broadside** projectile as the worst case for UXO exposure (i.e., shallowest sediment penetration).
- Angle of attack at mudline
  - Stable:
    - $\alpha_0 = 0 \pm \sigma_{\alpha_0}$
  - Unstable: **flips broadside** on sediment impact
    - $\alpha_0 = -\psi_0 \pm 0$
  - Unstable: random impact
    - $\alpha_0 = 0 \text{ to } 2\pi (\pi \pm \pi)$



## Hydrodynamic Phase

The UXO of greatest concern will be those most shallowly buried. Due to the increased hydrodynamic and sediment-penetration resistance, these will be munitions that impact the sediment broadside. Munitions that meet the water at a sufficiently high angle of attack or those that break one or more fins are likely to tumble or turn broadside in the water. Therefore, for our computational studies, except where otherwise noted, we examined munitions traveling broadside through the water.

We considered three possibilities for munitions behavior at the water-sediment interface:

- For munitions moving stably nose-on through the water, we presume they maintain a low angle of attack in a narrow distribution with a mean of zero (perfectly nose-on) until mudline contact.
- For spinning munitions, the angle of attack at the mudline will be random—for these munitions, the differential formulation of the sensitivity (with partial derivatives) will not accurately capture the effect and finite differences should be considered.
- For angle of attack sufficiently deviating from nose-on, the munition is likely to flip broadside to the sediment interface due to the torque exerted by the sediment resistance at the munition's point of first contact.

Again, to consider the worst case for UXO risk, we assume the last case, what we call “the broadside flop,” unless otherwise stated in our analysis. The broadside flop also fixes  $\alpha_0$  ( $\sigma_{\alpha_0} = 0$ ), so sensitivity to  $\alpha_0$  is irrelevant (it gets multiplied by zero in the sensitivity equation).

## IDA | Simplified Sediment Model

Sensitivity Equation:

$$\sigma_{d_0}^2 = \left( \frac{\partial d_0}{\partial v_0} \right)^2 \sigma_{v_0}^2 + \left( \frac{\partial d_0}{\partial \psi_0} \right)^2 \sigma_{\psi_0}^2 + \left( \frac{\partial d_0}{\partial \alpha_0} \right)^2 \sigma_{\alpha_0}^2 + \left( \frac{\partial d_0}{\partial \mu} \right)^2 \sigma_{\mu}^2 + \sigma_{sm}^2$$

Burial depth estimate from simplified sediment model (Aubeny and Shi 2007<sup>1</sup>):

$$d_0 = \sin \psi_0 \left[ \frac{(b+1)m v_0^2}{2c_1 \mu D^{1-b} k L (D \sin \alpha_0 + L \cos \alpha_0)} \right]^{\frac{1}{b+1}}$$

Details available  
in backup

Sensitivities of penetration depth estimate to initial conditions at mudline:

$$\frac{\partial d_0}{\partial v_0} = \frac{2}{b+1} \frac{d_0}{v_0} \qquad \frac{\partial d_0}{\partial \alpha_0} = -\frac{1}{b+1} d_0 \frac{(D \cos \alpha_0 - L \sin \alpha_0)}{(D \sin \alpha_0 + L \cos \alpha_0)}$$

$$\frac{\partial d_0}{\partial \psi_0} = -d_0 \cot \psi_0 \qquad \frac{\partial d_0}{\partial \mu} = -\frac{1}{b+1} \frac{d_0}{\mu}$$

Now plug these derivatives back into the Sensitivity Equation...

<sup>1</sup>C. Aubeny and H. Shi, "Effect of Rate-Dependent Soil Strength on Cylinders Penetrating Into Soft Clay," *IEEE J. Oceanic Eng.* 32 (1) (Jan. 2007).

## **Sediment Phase**

To evaluate the sensitivities in the sensitivity equation for the sediment phase, we take the velocity-dependent resistance model published by Aubeny and Shi (2007). The velocity (i.e., rate dependence) prevents derivation of an analytic solution to Aubeny and Shi's model. However, this rate dependence is weak, and by considering the range of the rate-dependent contribution, bounding analytic solutions (upper and lower bounds to the penetration predicted by the full rate-dependent Aubeny and Shi model) can be derived as we do in the backup slides (see "Simplified Sediment Model"). The form of the solution is shown on the current slide. This expression is amenable to taking derivatives. We do so and utilize the resulting expressions in the sensitivity equation.

## IDA | Simplified Sediment Model

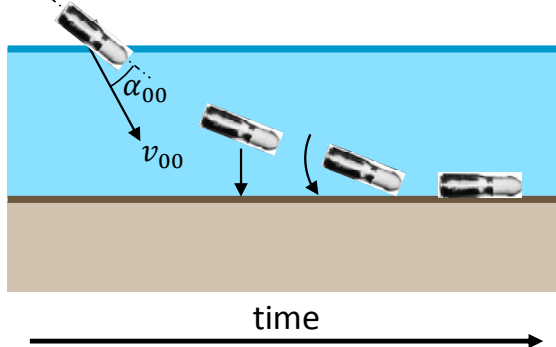
Sensitivity equation:

$$\sigma_{d_0}^2 = \left( \frac{\partial d_0}{\partial v_0} \right)^2 \sigma_{v_0}^2 + \left( \frac{\partial d_0}{\partial \psi_0} \right)^2 \sigma_{\psi_0}^2 + \left( \frac{\partial d_0}{\partial \alpha_0} \right)^2 \sigma_{\alpha_0}^2 + \left( \frac{\partial d_0}{\partial \mu} \right)^2 \sigma_{\mu}^2 + \sigma_{sm}^2$$

With derivatives plugged in...

$$\begin{aligned} \sigma_{d_0}^2 = & \left( \frac{2}{b+1} \frac{d_0}{v_0} \right)^2 \sigma_{v_0}^2 + (d_0 \cot^2 \psi_0)^2 \sigma_{\psi_0}^2 \\ & + \left( \frac{1}{b+1} d_0 \frac{(D \cos \alpha_0 - L \sin \alpha_0)}{(D \sin \alpha_0 + L \cos \alpha_0)} \right)^2 \sigma_{\alpha_0}^2 + \left( \frac{1}{b+1} \frac{d_0}{\mu} \right)^2 \sigma_{\mu}^2 + \sigma_{sm}^2 \end{aligned}$$

For an unstable, **broadside flop**: By definition, we know  $\alpha_0 = -\psi_0$  and so  $\sigma_{\alpha_0}^2 = 0$



Therefore:

$$\frac{\sigma_{d_0}^2}{d_0^2} \approx 4 \frac{\sigma_{v_0}^2}{v_0^2} + \left( \frac{\pi}{2} - \psi_0 \right)^2 \sigma_{\psi_0}^2 + \frac{\sigma_{\mu}^2}{\mu^2} + \frac{\sigma_{sm}^2}{d_0^2}$$



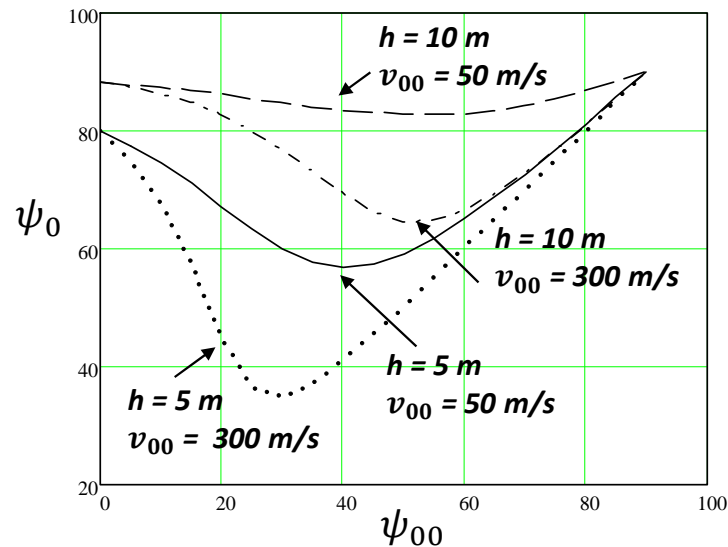
## **Sediment Phase**

To evaluate the sensitivities in the sensitivity equation for the sediment phase, we take the velocity-dependent resistance model published by Aubeny and Shi (2007). The velocity (i.e., rate dependence) prevents derivation of an analytic solution to Aubeny and Shi's model. However, this rate dependence is weak, and by considering the range of the rate-dependent contribution, bounding analytic solutions (upper and lower bounds to the penetration predicted by the full rate-dependent Aubeny and Shi model) can be derived as we do in the backup slides (see "Simplified Sediment Model"). The form of the solution is shown on the current slide. This expression is amenable to taking derivatives. We do so and utilize the resulting expressions in the sensitivity equation.

## IDA | Estimating Errors in Initial Conditions at Mudline

Use computational hydrodynamic model to evaluate  $\sigma_{v_0}$  and  $\sigma_{\psi_0}$ :

E.g., compute  $\psi_0$  as a function of  $\psi_{00}$ , holding  $h$  and  $v_{00}$  constant:



**IDA | Stages of a Simplified UXO Burial Depth Model**

**1. 2-D hydrodynamic model:**

$$f_z = \frac{\Delta \rho}{\rho_w} g - \frac{\rho_w A C_d}{2m} v v_z$$

$$f_x = -\frac{\rho_w A C_d}{2m} v v_x$$

**2. Aubeny's sediment penetration model**

$$f = \begin{cases} c(v) \gamma_1(\mu) (\sqrt{x^2 + z^2})^{b_1} + \frac{1}{2} A C_d \frac{\rho_w}{m} v^2, & z \leq \frac{D}{2} \\ c(v) \gamma_2(\mu) (\sqrt{x^2 + z^2})^{b_2} + \frac{1}{2} A C_d \frac{\rho_w}{m} v^2, & z > \frac{D}{2} \end{cases}$$

where  $f$  is the force experienced by the munition

$$c(v) = 1 + \lambda \ln\left(\frac{v}{v_0}\right)$$

**Modeling assumptions:**

- Presented area and drag coefficient numbers are comparable with those of Strike 35 (i.e. UXO tumbles upon impact)
- Broadside UXO sediment impact
- Known shear strength distributions

$\gamma_1(\mu) = \frac{\mu A f_1}{m D^{b_1}}$ ,  $\gamma_2(\mu) = \frac{\mu A f_2}{m D^{b_2}}$ ,  $f_1, b_1, f_2, b_2, \lambda$  are empirical constants

22 February 2017

Monte Carlo  
 $h, v_{00}, \psi_{00}$

$\sigma_{\psi_0}$

and likewise  
for  $\sigma_{v_0}$

## Combine Hydrodynamic and Sediment Phases

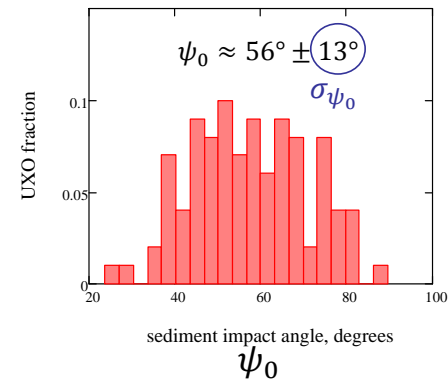
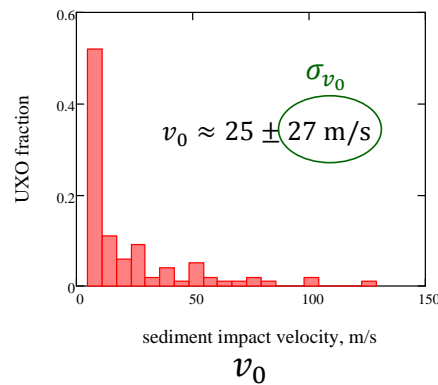
This slide shows the sediment impact angle  $\psi_0$  as a function of water impact angle  $\psi_{00}$  for two water depths  $h$ : 5 and 10 m, and two water impact velocities  $v_{00}$ : 50 and 300 m/s. As can be seen from the figure, the sediment impact angle  $\psi_0$  varies from about 35 degrees (when the water depth  $h$  is lowest, water impact velocity  $v_{00}$  is highest, and water impact angle  $\psi_{00}$  is about 30 degrees) to 90 degrees (when the water impact angle  $\psi_{00}$  is also 90 degrees).

We proceed to utilize our simplified 2D hydrodynamic model to estimate distributions of the sediment impact angle  $\psi_0$  and velocity  $v_0$  by performing Monte Carlo simulations for various water depths  $h$  and water impact angle  $\psi_{00}$  and velocity  $v_{00}$  values.

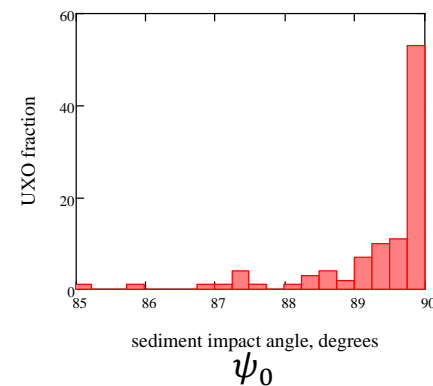
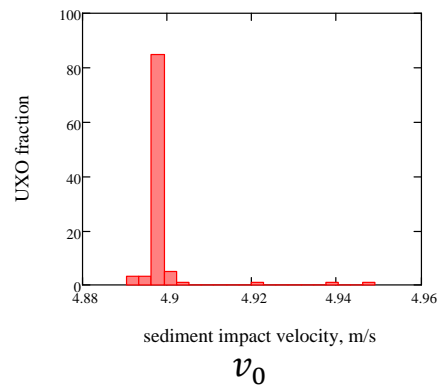
# IDA | Monte Carlo Results: Estimates of $\sigma_{v_0}$ and $\sigma_{\psi_0}$

$v_{00}$  uniformly distributed, 50 to 300 m/s  
 $\psi_{00}$  normally distributed,  $45 \pm 15^\circ$

Shallow water:  
 Uniformly  
 distributed 1–10 m



Deep water:  
 Uniformly  
 distributed 15–30 m



## Combine Hydrodynamic and Sediment Phases

To account for unknown initial conditions of munitions impacting the water surface, we assume that water depth  $h$ , water impact angle  $\psi_{00}$ , and water impact velocity  $v_{00}$  can be represented by probability distributions with parameters shown on this slide. We distinguish two fundamentally different cases: shallow water (water depth  $h$  varies uniformly from 1 to 10 m) and deep water (uniform water depth  $h$  variation from 15 to 30 m):

- In deep water (bottom row), the sediment impact velocity  $v_0$  centers around its terminal velocity value with very a small deviation, while the sediment impact angle  $\psi_0$  is very close to 90 degrees. The simulations show at that at a water depth  $h$  of 15 m and higher, the effect of the waterline impact conditions is practically negligible, and the sediment impact can be approximated by the munition's terminal velocity with vertical impact angle.
- In shallow water (top row), both the sediment impact velocity  $v_0$  and angle  $\psi_0$  are widely distributed with the mean and standard deviations shown on the figure. Clearly, in this case, the sediment-penetration depth predictions will be much more uncertain than those for the case of deep water.

## IDA | Our Example: Unstable, Broadside Flop

$$\frac{\sigma_{d_0}^2}{d_0^2} \approx 4 \frac{\sigma_{v_0}^2}{v_0^2} + \left(\frac{\pi}{2} - \psi_0\right)^2 \sigma_{\psi_0}^2 + \frac{\sigma_{\mu}^2}{\mu^2} + \frac{\sigma_{sm}^2}{d_0^2}$$

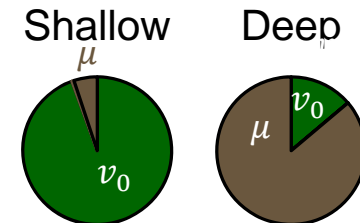
Operating Point and Initial Condition Uncertainty							
Cases	$v_0$ m/s	$\sigma_{v_0}$ m/s	$\psi_0$	$\sigma_{\psi_0}$	$\alpha_0$	$\sigma_{\alpha_0}$	$\frac{\sigma_{\mu}}{\mu}$
Shallow	25	$\pm 27$	56°	$\pm 13^\circ$	50°	$\pm 0$	$\pm 50\%^*$
Deep	4.9	$\pm 0.5$	70°	$\pm 0.7^\circ$	90°		
Contribution to Initial Burial Depth Uncertainty							Total
Shallow	216%		15%	0		50%	222%
Deep	20%		0%	0			54%

e.g., 27 m/s error in  $v_0$  leads to a 216% error in  $d_0$

For the Unstable, **Broadside Flop** case:

- In shallow water: Uncertainty in  $v_0$  dominates the uncertainty in  $d_0$
- In deep water: Uncertainty in  $\mu$  dominates the uncertainty in  $d_0$

Total square error contribution



\*Rennie and Brandt, "SERDP Project MR-2227 Interim Report," August 2015.

## Combine Hydrodynamic and Sediment Phases

Using results from the Monte Carlo analysis and the scientific literature to evaluate the operating points and the variance of the mudline initial conditions (only the contribution from initial waterline condition variation), we evaluate the sensitivity equation and compare the error contributions:

- In shallow water, the waterline projectile velocity  $v_{00}$  significantly influences the mudline projectile velocity  $v_0$ , so variation in sediment impact velocity  $\sigma_{v_0}$  is not erased by water depth  $h$ . Uncertainty in the projectile velocity at the mudline  $\sigma_{v_0}$  then dominates the uncertainty in the sediment-penetration depth  $\sigma_{d_0}$ . Improving the penetration model would only help if the fractional model error  $\sigma_{sm}/d_0$  exceeds 100%. Since the velocity uncertainty considered here,  $\sigma_{v_0}$ , ultimately stems from the munition firing condition variation, it is irreducible. Additional improvements in measurement or modeling will only be useful if their current contribution exceeds a 100% fractional error.
- In deep water, where the effect of the irreducible uncertainties of the firing conditions are effaced by the achievement of terminal velocity, uncertainty in the sediment properties  $\sigma_\mu$  dominates the overall sediment-penetration prediction uncertainty  $\sigma_{d_0}$ . If the uncertainty in sediment properties  $\sigma_\mu$  stems from measurement error, then better measurement techniques might improve sediment-penetration prediction accuracy. On the other hand, if  $\sigma_\mu$  is dominated by point-to-point spatial variation in the sediment properties over the local region of interest, then  $\sigma_\mu$  will be irreducible, and further model or measurement enhancements will do little to improve the accuracy of sediment-penetration prediction.

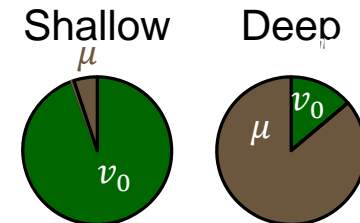
## IDA | Our Example: Unstable, Broadside Flop

$$\frac{\sigma_{d_0}^2}{d_0^2} \approx 4 \frac{\sigma_{v_0}^2}{v_0^2} + \left(\frac{\pi}{2} - \psi_0\right)^2 \sigma_{\psi_0}^2 + \frac{\sigma_{\mu}^2}{\mu^2} + \frac{\sigma_{sm}^2}{d_0^2}$$

Operating Point and Initial Condition Uncertainty							
Cases	$v_0$ m/s	$\sigma_{v_0}$ m/s	$\psi_0$	$\sigma_{\psi_0}$	$\alpha_0$	$\sigma_{\alpha_0}$	$\frac{\sigma_{\mu}}{\mu}$
Shallow	25	$\pm 27$	56°	$\pm 13^\circ$	50°	$\pm 0$	$\pm 50\%^*$
Deep	4.9	$\pm 0.5$	70°	$\pm 0.7^\circ$	90°		
Contribution to Initial Burial Depth Uncertainty							Total
Shallow	216%		15%	0		50%	222%
Deep	20%		0%	0			54%

e.g. 27 m/s error in  $v_0$  leads to a 216% error in  $d_0$

Total square error contribution



### Recommendation #9:

Use simplified models with sensitivity analytic framework to understand when and how initial sediment penetration predictions can be improved.



## **Combine Hydrodynamic and Sediment Phases**

As we have illustrated by this example, the analytical models can be a powerful tool to reveal opportunities (or lack thereof) for improving sediment-penetration prediction. Higher fidelity models, where they exist and are sufficiently validated, can also be used to evaluate the sensitivity equation, where feasible.

## IDA | Irreducible Uncertainty in Burial Depth

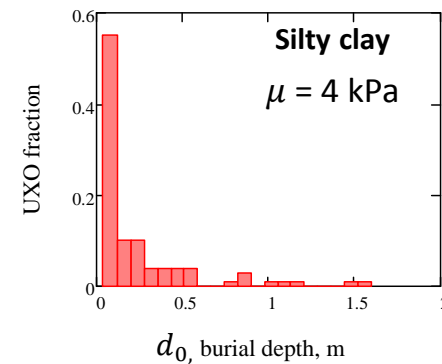
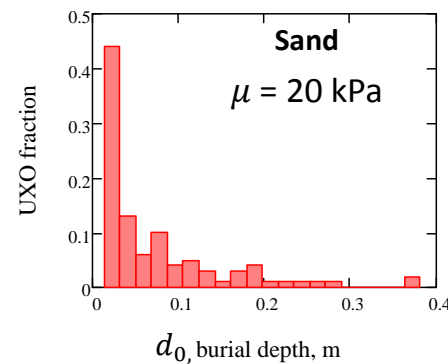
$v_{00}$  uniformly distributed, 50 to 300 m/s

$\psi_{00}$  normally distributed,  $45 \pm 15^\circ$

$\mu$  fixed and known

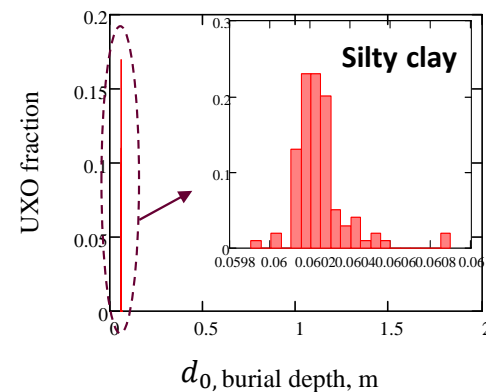
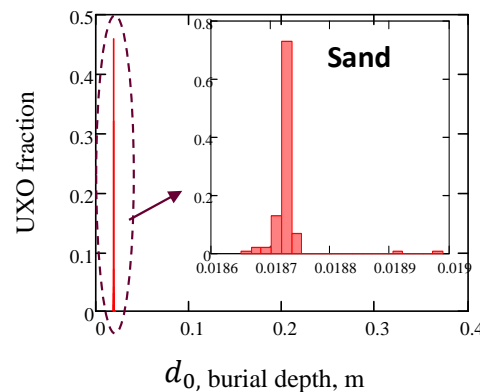
*In shallow water, initial conditions greatly affect the uncertainty in sediment penetration depth.*

Shallow water  
1–10 m



*In deep water, the effect of initial conditions on sediment penetration depth is negligible.*

Deep water  
15–30 m



## Combine Hydrodynamic and Sediment Phases

Having estimated variability in sediment-impact conditions, we proceed to estimate variability of predicted sediment-penetration depths. As an example, we consider two sediments representative of low sediment shear strength (silty clay) vs. high sediment shear strength (sand).

As we have shown on the previous slide, there are two fundamentally different regimes that we have to consider: deep water and shallow water:

- In deep water, the water impact conditions have negligible effect on the predicted sediment-penetration depth  $d_0$ ; they are instead controlled by the munition terminal velocity and sediment shear strength  $\mu$ .
- This is not so for the shallow case: the sediment-penetration depth  $d_0$  is distributed from near zero to 0.4 m values in sand and up to 1.5 m in silty clay. Note that in the shallow-water case, these resulting depth distributions ultimately arise from the unknown water impact conditions, and the predicted depth uncertainty is therefore irreducible.

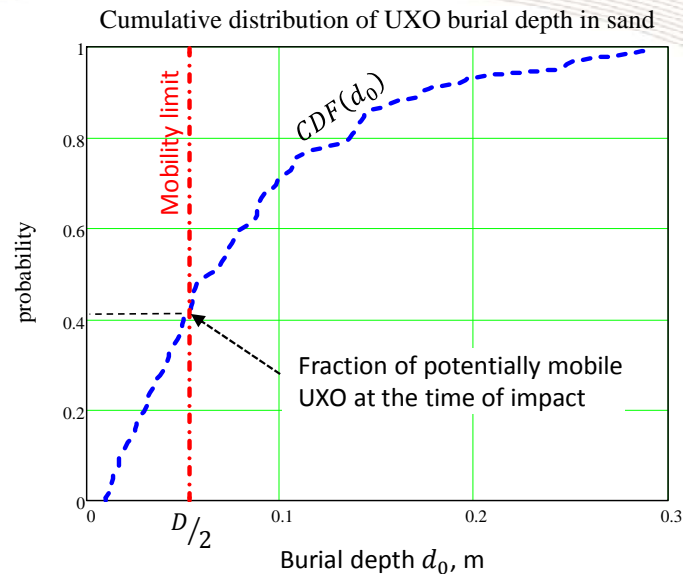
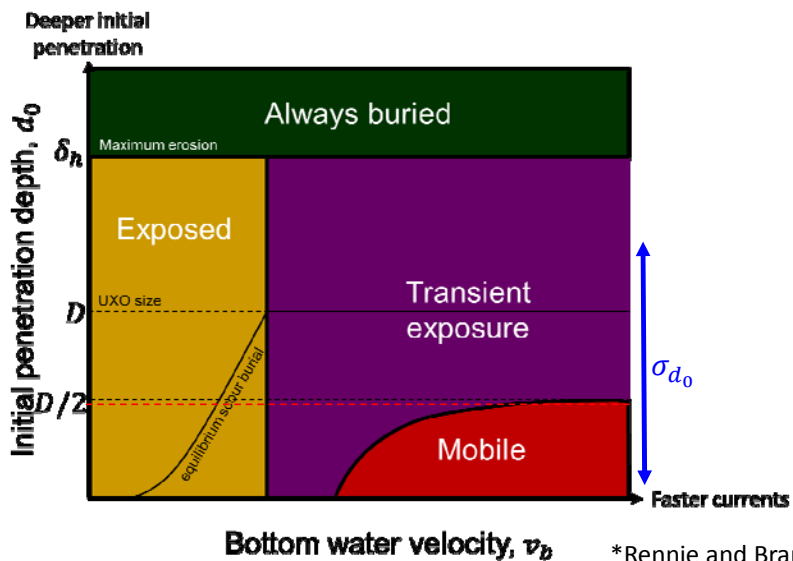
# **WHERE WOULD **ADDITIONAL** FIDELITY HELP?**

We have now explored:

- What fidelity (i.e., accuracy and precision) is useful for underwater UXO remediation projects when estimating a munition's initial penetration depth into the sediment.
- What fidelity is already achievable via existing penetration models that have already been developed for underwater mines.

We will now consider our third and final question: Where (and when) would *additional* fidelity be helpful for underwater UXO remediation projects?

## Connecting Useful Fidelity to Achievable Fidelity: Shallow Water Example



- Improving the model will not fully eliminate uncertainty in initial sediment penetration depth  $d_0$  due to irreducible uncertainty in environmental conditions ( $\mu$ ) and initial impact conditions at the waterline ( $v_{00}$ , etc.).

\*Rennie and Brandt, "SERDP Project MR-2227 Interim Report," August 2015.

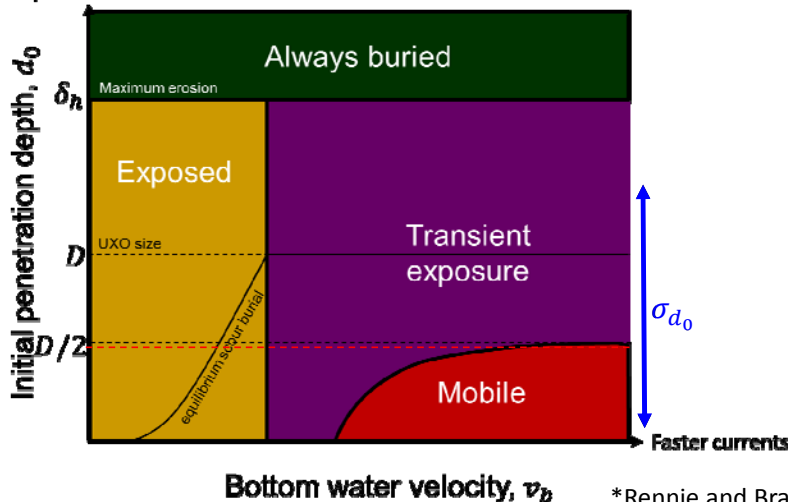
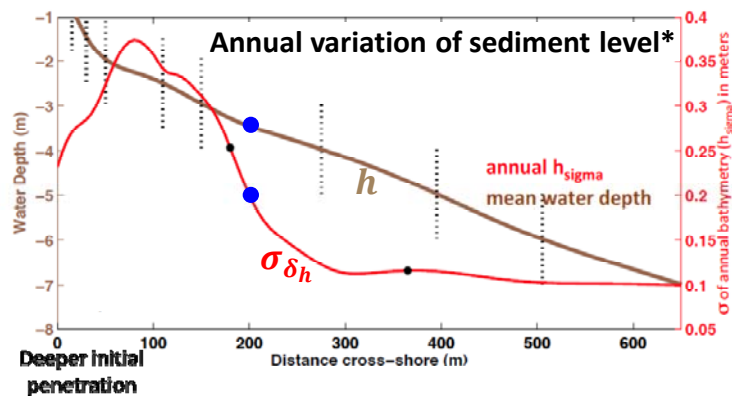
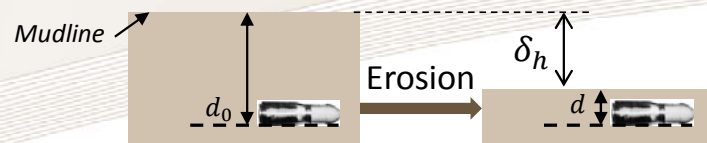
Consider, as an example, a particular case of munitions buried in sand in shallow water depths, 3–5 m. In the upper right figure, we show the cumulative distribution of the buried depth, in this case based on the uncertainties in:

- the waterline impact velocity  $v_0$  (we assume a uniform distribution, 50 to 300 m/s),
- the waterline impact entrance angle  $\psi_0$  (we assume a normal distribution with mean =  $\pi/4$  and standard deviation =  $\pi/12$ ) and,
- the sediment shear strength  $\mu$  (we assume a normal distributed with mean = 20 MPa and standard deviation = 5 MPa).

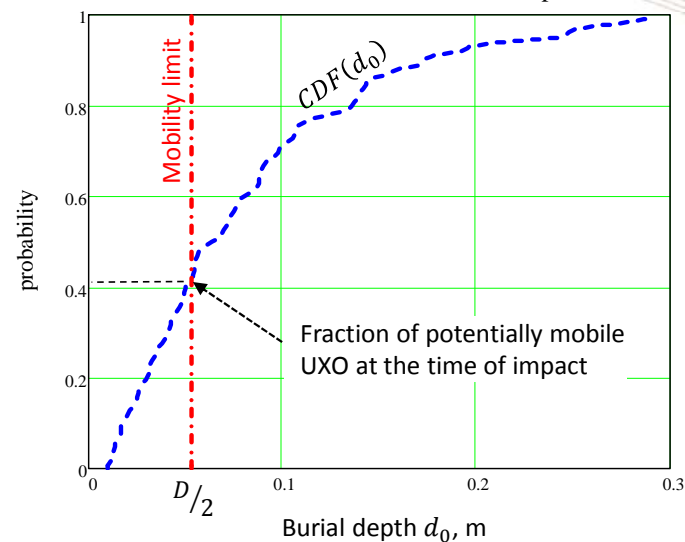
As can be seen from the upper right figure, slightly more than 40% of munitions will have a sediment-penetration depth less than  $1/2$  the diameter  $D$ , making them potentially mobile. In other words, our simplified models predict that about 40% of the munitions will be initially mobile.

Note that the spread of the cumulative distribution in the upper right figure stems from the uncertainty in the waterline initial conditions and the sediment shear strength and is therefore irreducible. We can overlay this irreducible uncertainty on the burial regime map developed in the first part of our analysis, as we show in the bottom left corner by a blue arrow. (The magnitude of  $\sigma_{d_0}$  is estimated from the cumulative distribution to be about 1.5 times the munition diameter  $D$ .) If the munition lands in an map regime where the bottom water velocity is not high enough to make the munition mobile, then the munition will remain stable. Improving the accuracy of the model (either in the hydrodynamic or sediment phases or in both) will not lead to improving our knowledge of the fate of this munition, given this large (irreducible) uncertainty in its initial sediment-penetration depth  $d_0$ .

## Connecting Useful Fidelity to Achievable Fidelity: Shallow Water Example



Cumulative distribution of UXO burial depth in sand



- Improving the model will not fully eliminate uncertainty in initial sediment penetration depth  $d_0$  due to irreducible uncertainty in environmental conditions ( $\mu$ ) and initial impact conditions at the waterline ( $v_{00}$ , etc.).

\*Rennie and Brandt, "SERDP Project MR-2227 Interim Report," August 2015.



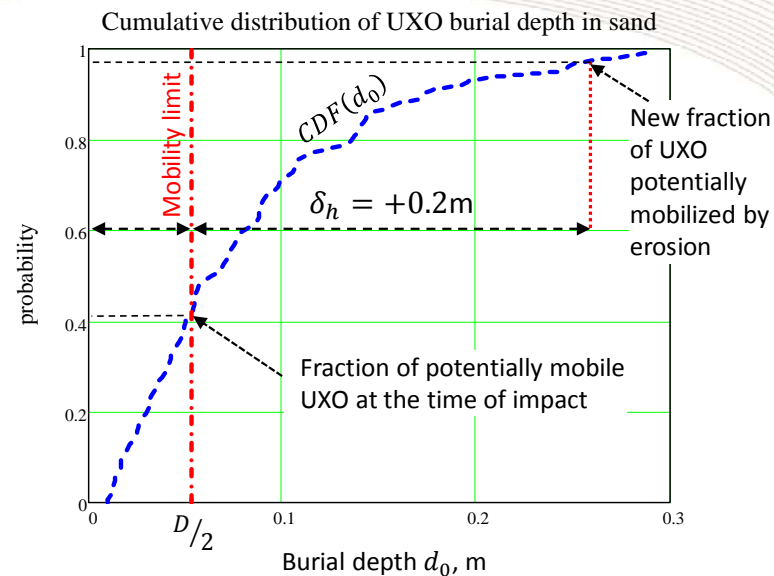
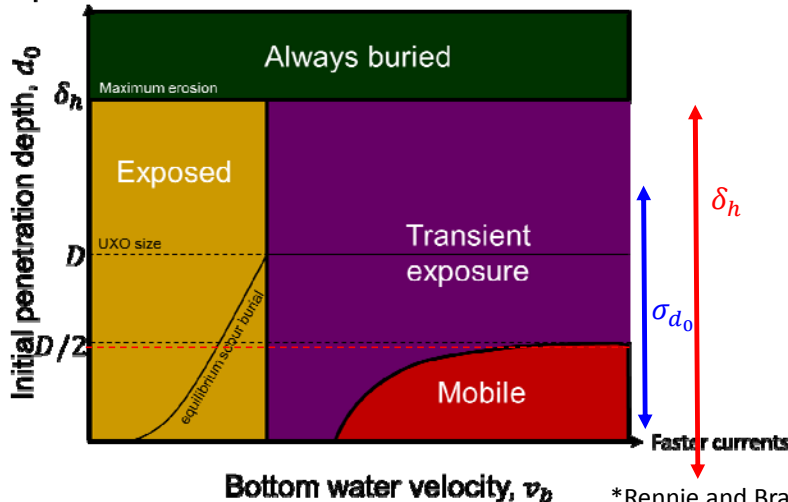
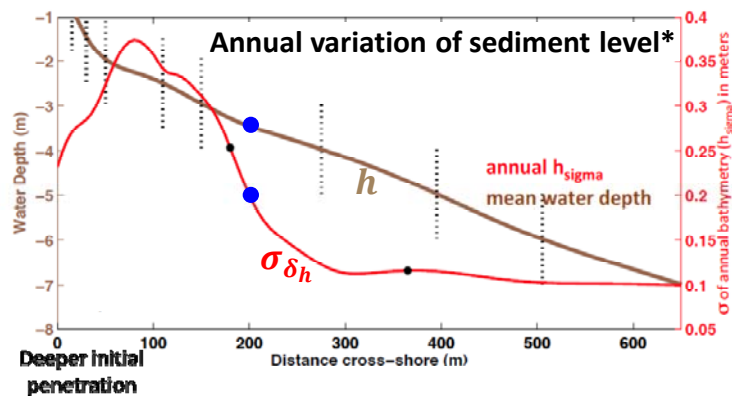
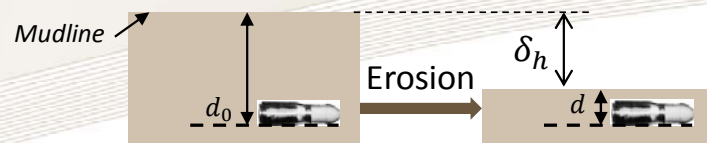
Here we show the effect of sediment floor height variation on the munition burial depth  $d$ . Consider, as an example, a particular case of munitions buried at a specific location: Duck, North Carolina. Shown on the upper left corner is Duck's reported yearly variation of sediment height, quantified as:

- the water depth  $h$  versus distance from shore (brown curve, vertical axis on left) and
- the variation in the water depth  $\delta_h$  versus distance from shore (red curve, vertical axis on right).

In shallow water depths (i.e., about  $h = 5$  m), the variation in water depth is about  $\delta_h = 0.2$  m. One can think of this variation  $\delta_h$  as either the variation in the water depth or as the variation in the sediment level.

We ask the following question: How will this variation in sediment level,  $\delta_h$ , affect the uncertainty in the penetration depth of munitions,  $\sigma_d$ ?

## Connecting Useful Fidelity to Achievable Fidelity: Shallow Water Example



- Improving the model will not fully eliminate uncertainty in initial sediment penetration depth  $d_0$  due to irreducible uncertainty in environmental conditions ( $\mu$ ) and initial conditions at the waterline ( $v_{00}$ , etc.).
- Sediment floor erosion/accretion  $\delta_h$  will wipe out the effect of uncertainty in initial penetration depth  $d_0$ .

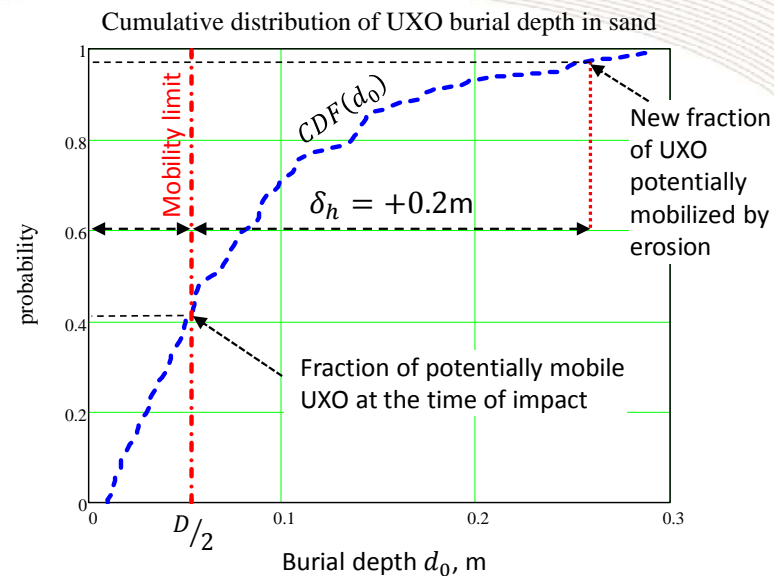
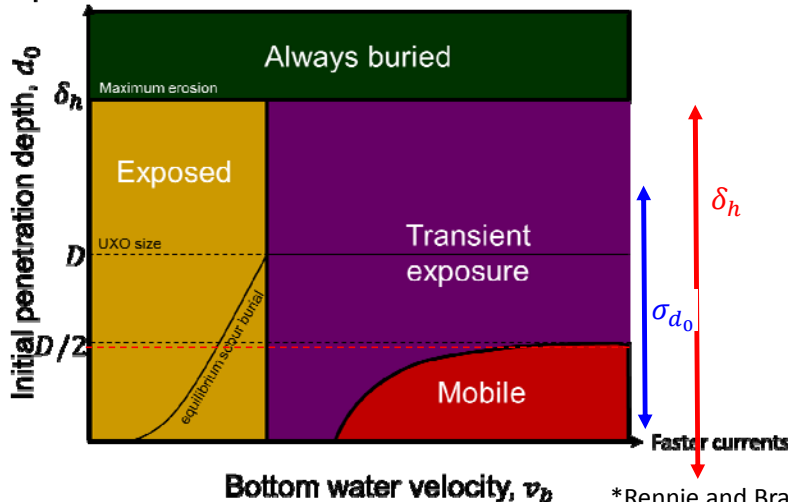
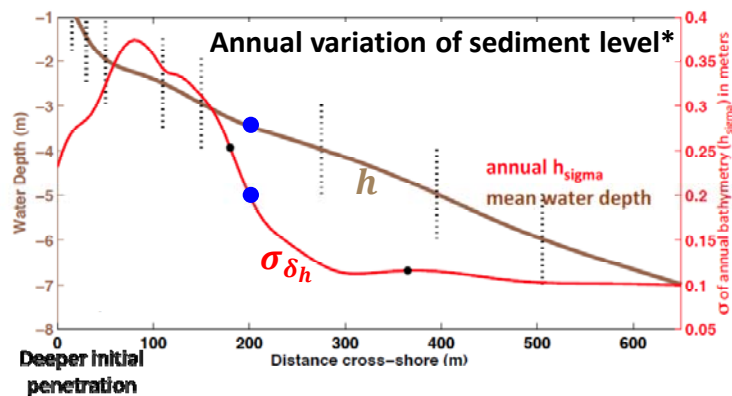
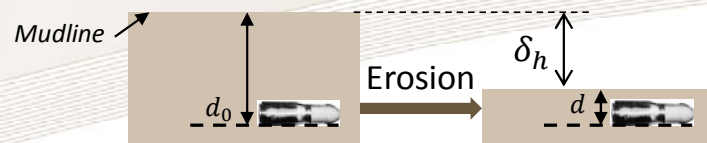
\*Rennie and Brandt, "SERDP Project MR-2227 Interim Report," August 2015.

If the local bottom floor conditions are such that these munitions are initially immobile, the scour process and local sediment floor variation (i.e., accretion) may bury the munition, making the magnitude of initial sediment-penetration depth  $d_0$  irrelevant. On the other hand, the sediment-level variation  $\delta_h$  can also expose the munition and make it potentially mobile if it takes place on the timescale shorter than that of the scour process. For example, at a water depth of about  $h = 5$  m, a sediment-level variation of about  $\delta_h = 0.2$  m may expose initially buried munitions and increase the percentage of the munitions that are mobile (from just over 40% to about 97%, as shown in the upper right figure).

We use a red arrow to represent the sediment-level variation  $\delta_h$  in the burial regime map in the bottom left. We observe that, in addition to the uncertainty in initial burial depth  $\sigma_{d_0}$ , the sediment-level variation  $\delta_h$  contributes irreducible uncertainty in increasing (or decreasing) the munition penetration depth  $d$ . Improving the model accuracy will unlikely be useful in this case.

This example demonstrates that under certain conditions, the depth of the munition's initial penetration into the sediment  $d_0$  does not affect its subsequent exposure and mobility; in this case, an improvement in the accuracy of the munition's initial penetration prediction does not lead to more accurate assessment of the munition's fate.

## Connecting Useful Fidelity to Achievable Fidelity: Shallow Water Example



- Improving the model will not fully eliminate uncertainty in initial sediment penetration depth  $d_0$  due to irreducible uncertainty in environmental conditions ( $\mu$ ) and initial conditions at the waterline ( $v_{00}$ , etc.).
- Sediment floor erosion/accretion  $\delta_h$  will wipe out the effect of uncertainty in initial penetration depth  $d_0$ .
- The only risk bucket sensitive to model fidelity is initial mobility.

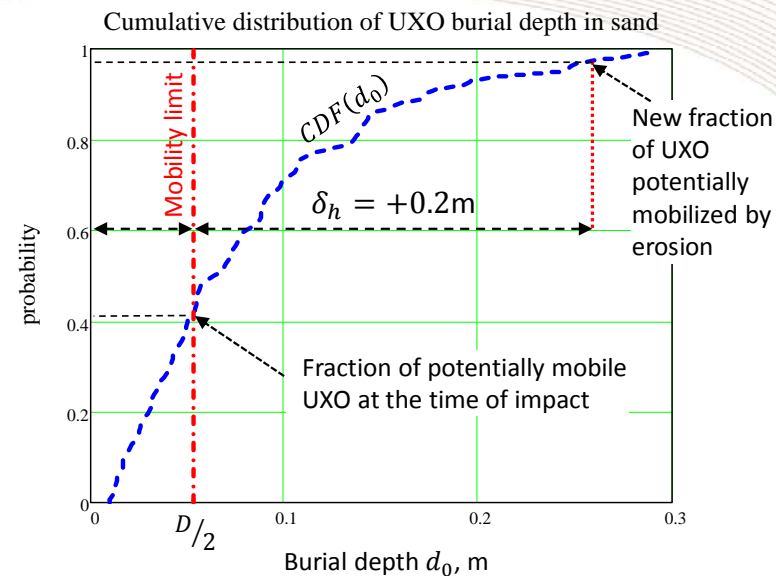
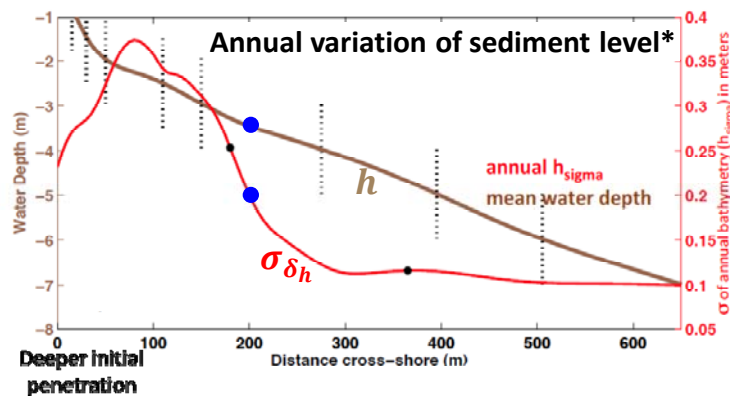
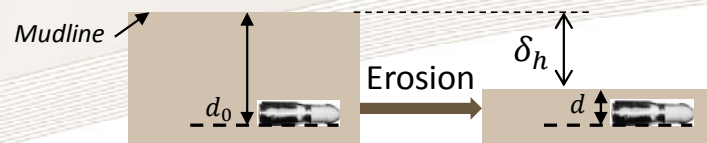
\*Rennie and Brandt, "SERDP Project MR-2227 Interim Report," August 2015.

The burial regime maps can help to answer the question: When will additional improvements in model accuracy be useful?

- If the bottom water velocity is low and the munition remains immobile after the impact, then the scour processes and sediment floor depth variations will control the fate of the munition and erase the effect of the initial sediment-penetration depth, reducing the usefulness of the model fidelity improvements.
- If, on the other hand, the bottom water velocity is such that the munition can be mobile, then the munition's mobility is determined by its initial sediment-penetration depth, and the accuracy of the penetration predictions is very important because it will influence the mobility and fate of the munition.

These considerations show that usefulness of improving model accuracy depends on the particular case of interest. In our example, accurately predicting the initial mobility of munitions may help estimate the fraction of potentially mobile munitions, even though there is considerable irreducible uncertainty in their initial sediment-penetration depths.

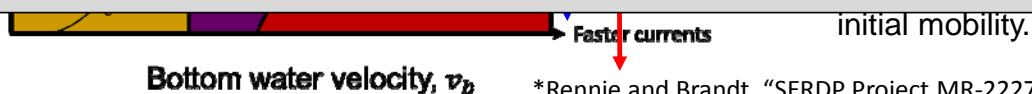
## Connecting Useful Fidelity to Achievable Fidelity: Shallow Water Example



- Improving the model will not fully eliminate uncertainty in initial sediment penetration depth  $d_0$  due to irreducible uncertainty in environmental conditions ( $\mu$ ) and initial conditions at the waterline ( $v_{00}$ , etc.).

### Recommendation #10:

Use regime map to evaluate whether proposed improvements in model fidelity will have operational utility.



\*Rennie and Brandt, "SERDP Project MR-2227 Interim Report," August 2015.

Thus, our final recommendation is to use a burial regime map to evaluate whether proposed improvements in model fidelity will have operational utility.

# **FINDINGS AND RECOMMENDATIONS**



We now summarize our findings and recap our recommendations.

## **IDA | Findings**

- In deep water, initial conditions at the waterline ( $v_{00}$ ,  $\psi_{00}$ ,  $\alpha_{00}$ ) do not influence the initial sediment penetration depth ( $d_0$ ).
  - Terminal velocity ( $v_t$ ) is the dominant influence on the initial conditions at the mudline ( $v_0$ ,  $\psi_0$ ,  $\alpha_0$ ), which, in turn, influence the munition's initial sediment penetration depth ( $d_0$ ).
  - $v_t$ , and therefore  $d_0$ , is sensitive to the hydrodynamic model and, in particular, the munition's drag coefficient.
- In shallow water, much of the uncertainty in the munition's initial sediment penetration depth ( $d_0$ ) stems from the variability in initial conditions at the waterline ( $v_{00}$ ,  $\psi_{00}$ ,  $\alpha_{00}$ ).
  - This variability is based on the original firing conditions and is irreducible.

## **IDA | Findings**

- Sediment shear strength ( $\mu$ ) significantly influences the munition's initial sediment penetration depth ( $d_0$ ).
  - Geographic variability in  $\mu$  within a region of interest produces irreducible uncertainty in  $d_0$ , putting a lower bound on the achievable precision in  $d_0$ .
  - In deep water, where  $\sigma_{v_0}$  is low,  $\sigma_\mu$  has strong influence on  $d_0$ .
- Erosion/accretion  $\delta_h$  strongly affects exposure/mobility.
  - Uncertainty in  $\delta_h$  puts an upper bound on the useful fidelity in  $d_0$ .
- A simple mathematical framework (i.e., “the sensitivity equation”) coupled with simple analytical models can be applied to specific cases to compare the present-day, achievable model errors to what is useful.

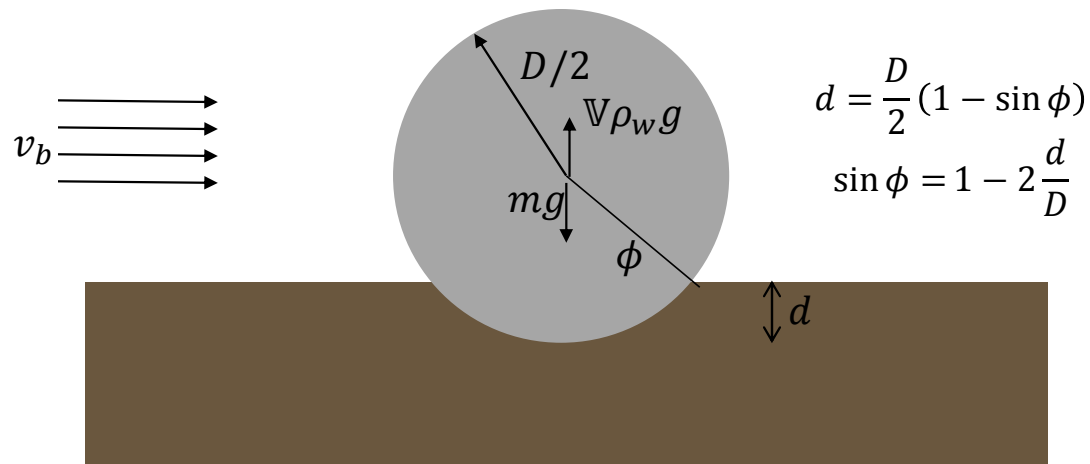
## **IDA | Recommendations**

1. Improve sandy sediment-penetration models.
2. Develop mobility models for silt.
3. Develop mobility models for partly buried objects.
4. Develop scour burial models for silt.
5. Improve models of consolidation and creep.
6. Exercise caution in improving hydrodynamic models to support initial sediment-penetration estimates—the effect of better hydrodynamics may be dwarfed by stochasticity due to unknown precise initial conditions at the waterline.
7. Existing sediment-penetration models (other than STRIKE35) are designed for near-cylindrical mines—for munitions, however, projectile-specific drag, lift, and moment coefficients are needed for estimating hydrodynamic stability and gross velocity.
8. Modules of existing depth penetration models are nearly independent and could and should be mixed and matched with little effort to choose best-of-breed for each phase (aero/hydrodynamic/sediment).
9. Use simplified models within the sensitivity analytical framework to understand when and how initial sediment-penetration predictions can be improved.
10. Use burial regime map to evaluate whether proposed improvements in model fidelity will have operational utility.

## **IDA | Backups**

## IDA | Mobility Model: Balance of Moments about Contact Point

Expand existing mobility model to include partial burial



Equilibrium of moments:

$$\Delta \rho \nabla g \frac{D}{2} \cos \phi = \frac{1}{4} \rho_w U^2 C_d L \left( \frac{D}{2} (1 + \sin \phi) \right)^2$$

$$U = \sqrt{\frac{\Delta \rho \pi g D}{\rho_w C_d}} \left( \frac{\frac{d}{D}}{1 - \frac{d}{D}} \right)^{\frac{1}{4}} \frac{1}{\sqrt{1 - \frac{d}{D}}}$$

IDA developed our own model for predicting mobility thresholds, consistent with the phenomenological model quoted in section 4.2 of Rennie and Brandt (2015) for fully unburied munitions but extending to partly buried munitions via physics first principles.

## IDA | Simplified Sediment Model

- Used the Bearing Factor Model (from IMPACT28 and IMPACT35)
- Net retarding force =  
     Buoyancy + Hydrodynamics + Sediment shear resistance + Inertial drag
- For dominant sediment shear resistance:
  - $\frac{dv}{dt} = -cd^b \left(1 + \lambda \ln \frac{v}{\tilde{v}}\right)$ , where  $c = c_1 \frac{\mu D^{1-b}}{m} (D \sin \alpha_0 + L \cos \alpha_0)$
  - Based on data from Aubeny, the term in parentheses  $\left(1 + \lambda \ln \frac{v}{\tilde{v}}\right)$  ranges in value from 1 to 1.5.
  - Therefore, we can bound the solution by setting that term to a constant:  $\left(1 + \lambda \ln \frac{v}{\tilde{v}} = k\right)$ , where  $k = 1, 1.5$ :  $\frac{dv}{dt} = -kcd^b$
  - Integrating the equation once:  $v = \sqrt{v_0^2 - \frac{2kcd^{b+1}}{b+1}}$
  - And therefore,  $d_0 = \sin \psi_0 \left[ \frac{(b+1)mv_0^2}{2c_1\mu D^{1-b}k(D \sin \alpha_0 + L \cos \alpha_0)} \right]^{\frac{1}{b+1}}$



This slide describes IDA's simplified sediment model, adapted from Aubeny and Shi (2007).

To do the first integration of the resulting simplified differential equation  $\frac{dv}{dt} = -kcd^b$ , we first multiply both sides by  $v$ :

$$v \frac{dv}{dt} = -kcvd^b$$

Noting that  $v = \frac{dd}{dt}$ , it becomes apparent that both sides of this nonlinear equation are exact time differentials. Integrating both sides with respect to time and applying the initial condition that when  $d = 0$ ,  $v = v_0$  then yields:

$$\frac{1}{2}v^2 = \frac{1}{2}v_0^2 - \frac{kcd^{b+1}}{b+1}$$

or

$$v = \sqrt{v_0^2 - \frac{2kcd^{b+1}}{b+1}}.$$

The initial burial depth is the vertical projection of the penetration distance at the time when the velocity goes to zero:

$$d_0 = \sin \psi_0 \left( \frac{(b+1)v_0^2}{2kc} \right)^{\frac{1}{b+1}}.$$

In the Aubeny and Shi model, the exponent  $b$  changes when the object is half-buried, so for burial deeper than  $\frac{D}{2}$ , one would need to apply a two-step solution, first solving for the velocity at half-burial and then treating that as the initial condition for further burial. In our computations, we used a single set of Aubeny constants equivalent to those used in IMPACT35.

For  $b = 0.155$  (Aubeny and Shi's value for more than half-buried cylinders), the bounding estimates for  $d_0$  differ by 30% (i.e., for  $k = 1.5$ , the initial burial depth will be 70% of the initial burial depth for  $k = 1$ , and the model with continuously varying shear strength based on instantaneous velocity will give an intermediate result).

At high sediment-impact velocities, inertial drag (form drag or dynamic pressure) becomes a significant contributor to dynamics and should not be ignored. Inertial drag is dominant when

$$\rho_{\text{sediment}} v^2 C_d \gg \mu \left( \frac{d}{D} \right)^b k c_1.$$

For example, for a drag coefficient of  $\sim 1/3$ , sediment density of  $3000 \text{ kg/m}^3$ ,  $\mu \sim 10 \text{ kPa}$ ,  $kc_1 \sim 10$ , and  $\frac{d}{D} \sim 1$ , inertial forces would dominate for  $v \gg 10 \text{ m/s}$ . In this region, the velocity will exponentially decay with depth in the same fashion as discussed in the hydrodynamic terminal velocity model on backup slide “1D Projectile Dynamics”:

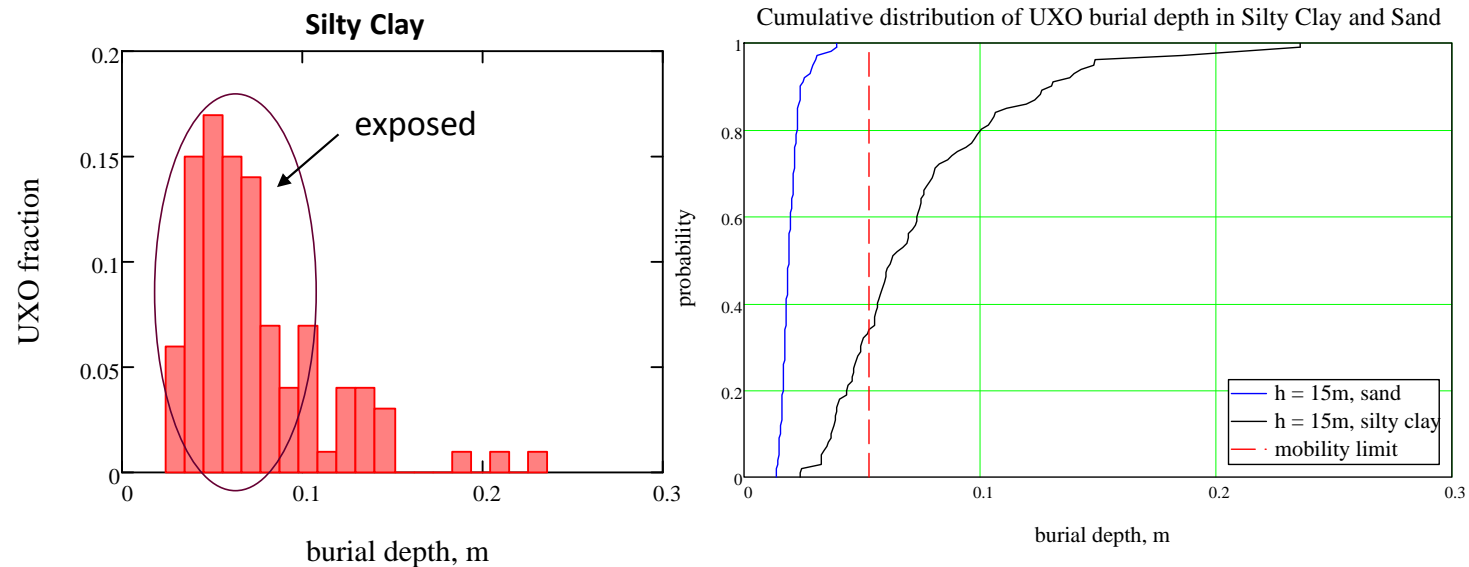
$$v = v_0 e^{-\frac{\rho_s A C_d d}{2m}} .$$



## IDA | Penetration Depth in Sandy and Silty Clay: Deep Water

### Broadside impact:

- $v_{00}$  uniformly distributed, 50 to 300 m/s
- $\psi_{00}$  normally distributed,  $45 \pm 15^\circ$



- In sand, all UXO may be mobile, hence scour models are needed in low bottom water velocity areas; mobility models are needed in high bottom water velocity areas; sediment penetration at impact is important to understanding in which regime the UXO is; therefore, accurate models for penetration into sand at velocity close to terminal are useful.
- In silty clays, knowledge of shear strength, as well as accurate scour, mobility, and long-term sediment penetration models, are important for assessing the fate of UXO.

This slide demonstrates selected results regarding the deep-water case:

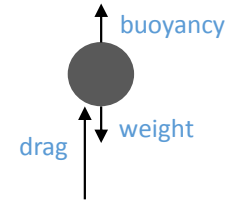
- In sandy areas, most if not all munitions are exposed and potentially mobile. When the sediment level variations take place on the timescale longer than that of scour, a munition's equilibrium scour burial depth will be determined by the scour process. A model with an accurate description of these phenomena is needed.
- In silty clay areas, fewer than half of all munitions will be immobile after sediment impact. In this case, more accurate measurements of silty clay shear strength, as well as models of the scour process and long-term creep and consolidation processes, are needed for more accurate estimates of the munition's fate.

## IDA | 1D Projectile Dynamics

Conservation of momentum:

$$m \frac{dv}{dt} = -\frac{1}{2} \rho_w v^2 A C_d + \Delta \rho \mathbb{V} g$$

↑ Drag
↑ Combined weight and buoyancy



Terminal velocity: Net force = 0

$$v^* = \sqrt{\frac{2\Delta\rho\mathbb{V}g}{\rho_w A C_d}}$$

Exact solution:

$$\frac{v}{v^*} = \sqrt{1 + \left( \frac{v_0^2}{v^{*2}} - 1 \right) e^{-2\frac{z}{L^*}}}$$

$$L^* \equiv \frac{2m}{\rho_w A C_d}$$

$\rho_w$	water density
$\Delta\rho$	projectile density - $\rho_w$
$m$	projectile mass
$A$	projectile cross-sectional area
$C_d$	drag coefficient
$\mathbb{V}$	projectile volume
$g$	gravitational acceleration
$v_{00}$	projectile velocity at waterline

When inertial drag dominates gravitational forces (buoyancy and weight) and viscous forces,

$$m \frac{dv}{dt} = -\frac{1}{2} \rho_w v^2 A C_d .$$

This differential equation can be separated to form

$$-\frac{\rho_w A C_d}{2m} dt = \frac{dv}{v^2} ,$$

which can be integrated to form

$$v = \frac{1}{\frac{\rho_w A C_d}{2m} t + \frac{1}{v_0}} .$$

Integrating once more to find the depth  $z$  as a function of time,

$$z = \frac{2m}{\rho_w A C_d} \ln \left( \frac{\rho_w A C_d}{2m} t + \frac{1}{v_0} \right) + c = \frac{2m}{\rho_w A C_d} \ln \left( \frac{v_0}{v} \right) .$$

This demonstrates exponential decay of velocity with depth,

$$v = v_0 e^{-\frac{\rho_w A C_d}{2m} z} .$$

Even at a velocity of 1 m/s, for a 10 cm diameter munition, the Reynolds number of flow through the water would be on the order of

$$Re = \frac{\rho_w v D}{\mu_w} \sim 10^5 ,$$

so inertial drag is expected to dominate viscous drag.

Terminal velocity occurs when the resistive drag forces balance the driving gravitational forces:

$$\frac{1}{2}\rho_w v^{*2} AC_d = \Delta\rho \mathbb{V}g .$$

Solving for the terminal velocity  $v^*$  yields

$$v^* = \sqrt{\frac{2\Delta\rho \mathbb{V}g}{\rho_w AC_d}} .$$

For a shape approximating a cylinder,  $\mathbb{V} = \frac{\pi}{4}D^2\ell$ ,  $A = \frac{\pi}{4}D^2 \cos \alpha + \frac{\ell}{D}D^2 \sin \alpha$ . Thus, the terminal velocity scaling with munition size is revealed as

$$v^* = \sqrt{\frac{\frac{\pi}{2}\Delta\rho Dg}{\rho_w C_d}} f\left(\frac{\ell}{D}, \alpha\right) .$$

In the exponential-decay model, this velocity is reached after a finite period of time at a depth

$$z^* = \frac{2m}{\rho_w AC_d} \ln\left(\frac{v_0}{v^*}\right) .$$

Let us denote the length scale  $L^* \equiv \frac{2m}{\rho_w AC_d}$ .

In a more nuanced model where buoyancy and weight act throughout, terminal velocity is only approached asymptotically. Solving the full conservation of momentum equation

$$m \frac{dv}{dt} = -\frac{1}{2}\rho_w v^2 AC_d + \Delta\rho \mathbb{V}g$$

or

$$L^* \frac{dv}{dt} = v^{*2} - v^2$$

which can be separated to form



$$\frac{dt}{L^*} = \frac{dv}{v^{*2} - v^2}$$

and then integrated to yield

$$\frac{v}{v^*} = \coth \left[ \frac{v^* t}{L^*} + \tanh^{-1} \frac{v^*}{v_0} \right].$$

This can be integrated again to yield

$$\frac{z}{L^*} + c = \ln \sinh \left( \frac{v^* t}{L^*} + \tanh^{-1} \frac{v^*}{v_0} \right) = -\ln \sqrt{\frac{v^2}{v^{*2}} - 1},$$

which with the initial conditions becomes

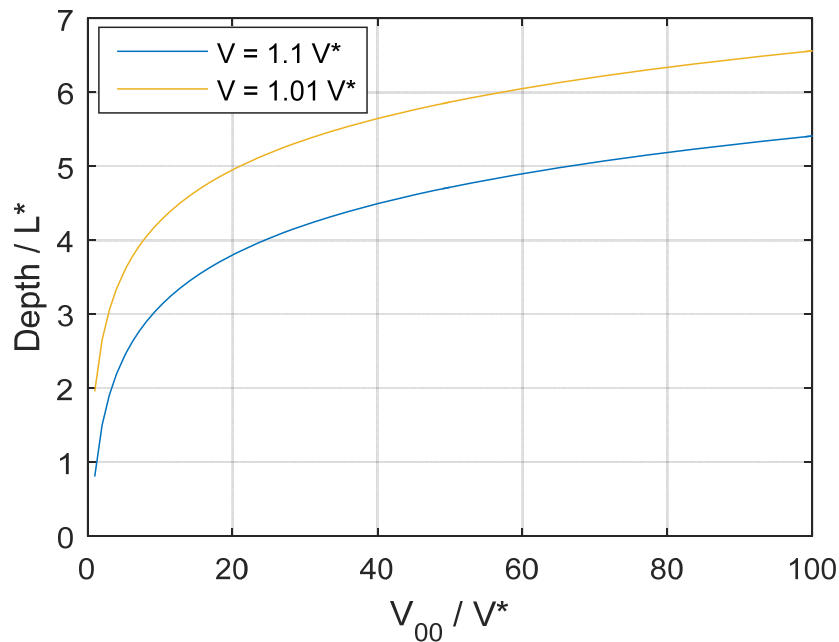
$$\frac{v}{v^*} = \sqrt{1 + \left( \frac{v_0^2}{v^{*2}} - 1 \right) e^{-2\frac{z}{L^*}}}.$$

This expression only allows for asymptotic approach to the terminal velocity, as predicted. To compare this model to the previous inertia-only forces with finite time to terminal velocity, let us substitute the expression for the depth to terminal velocity in the prior model and compute the velocity achieved at the same depth in the more accurate model:

$$\frac{v}{v^*} = \sqrt{2 - \frac{v^{*2}}{v_0^2}}.$$

In the limit of high initial velocities, the inertia-only model predicts terminal velocity achievement at a depth where the velocity would actually be 40% higher.

## IDA | Depth to Terminal Velocity



$\rho_w$  water density  
 $\Delta\rho$  projectile density -  $\rho_w$   
 $m$  projectile mass  
 $A$  projectile cross-sectional area  
 $C_d$  drag coefficient  
 $\mathbb{V}$  projectile volume  
 $g$  gravitational acceleration  
 $v_{00}$  projectile velocity at waterline

$$L^* = \frac{2m}{\rho_w A C_d} \quad v^* = \sqrt{\frac{2\Delta\rho \mathbb{V} g}{\rho_w A C_d}}$$

For projectiles traveling straight downward, here we show, relative to the scale length  $L^*$ , how deep the projectile would have to penetrate the water to achieve come within 10% or 1% of terminal velocity as a function of its initial velocity at the waterline (as a multiple of terminal velocity).

How can the drag coefficient be treated for a projectile spinning during its descent? In the inertia-only model, the drag coefficient can be represented as a function of time  $C_d(t)$ ,

$$m \frac{dv}{dt} = -\frac{1}{2} \rho_w v^2 A C_d(t).$$

Integrating the separated equation now takes a slightly different form:

$$\frac{\rho_w A C_d}{2m} \int_0^t C_d(t') dt' = \frac{1}{v} - \frac{1}{v_0}.$$

For a projectile experiencing many cycles of rotation, the integrated drag coefficient can be taken as a time-invariant average multiplied by the total time,  $\overline{C_d} = \int_0^t C_d(t') dt'$ . The derivation then continues as before with  $C_d$  replaced by  $\overline{C_d}$ . Thus, the drag coefficient can just be treated as its time averaged value in the final expressions.

STRIKE35 employs an expression for the drag-coefficient-area product (treated as drag coefficient variation with a constant nominal presented area) for the Joint Direct-Attack Munition (JDAM), whose dependence on angle of attack is given by a coefficient equal to  $e^{-2(\alpha - \frac{\pi}{2})^2}$  (Chu et al. 2011). For a projectile with a similar angle-of-attack dependence, spinning would sample all angles of attack equally leading to

$$\overline{C_d} = \frac{2}{\pi} \int_0^{\frac{\pi}{2}} e^{-2(\alpha - \frac{\pi}{2})^2} d\alpha = \frac{1}{\sqrt{2\pi}} \operatorname{erf} \frac{\pi}{\sqrt{2}} \approx 0.4.$$

Thus, for this type of angle of attack dependence, the effective drag coefficient of a spinning projectile will be 40% of its broadside value.

## IDA | Angled Trajectories

- Only a component of gravity ( $g \cos \psi$ ) counteracts drag. The remainder moves the trajectory angle closer to vertical.
- Therefore, the path length to terminal velocity is less than the depth to terminal velocity for a vertical velocity.

- Depth to terminal velocity can be bounded:

$$z^* < \ell^* \sin \psi_0 + \frac{1}{2} g \frac{\Delta \rho}{\rho_p} t^{*2}$$

where  $\ell^*$  is the path length to terminal velocity in the vertical trajectory case.

If the trajectory of the projectile is not straight downward, at every point along the trajectory, gravity acts with a component along the trajectory counteracting drag and a component perpendicular to the trajectory acting to turn the trajectory further downward. The action of the gravitational forces along the trajectory will therefore always be less than for a straight downward trajectory as considered in the full model on p. 138 and more than in the model discussed in the notes from the same chart ignoring gravitational forces entirely.

Let  $\ell^*$  be the depth to terminal velocity without gravitational forces in the straight downward case. A lower bound to the depth to terminal velocity will be  $z^* > \ell^* \sin \psi_0$ . We are more interested in an upper bound to identify regions of phase space where projectile initial conditions at the waterline do not contribute to initial burial depth. A simple upper bound can be derived by assuming that the gravity-free depth ( $\ell^* \sin \psi_0$ ) is augmented by the gravitational contribution with no additional drag force due to the associated higher velocity. The vertical travel of sinking projectile absent drag will be given by  $\frac{1}{2} g \frac{\Delta \rho}{\rho_p} t^{*2}$  (using  $t^*$  from the straight downward case) leading to the simple but overly loose upper bound

$$z^* < \ell^* \sin \psi_0 + \frac{1}{2} g \frac{\Delta \rho}{\rho_p} t^{*2} .$$

For a more sophisticated bound, consider that with a downward curving trajectory,  $\psi(t) > \psi_0$  and thus,  $\sin \psi(t) > \sin \psi_0$ . Next consider an uncurving angled trajectory accounting for drag and the tangential component of gravitational forces. Let us call the associated drag forces  $F_{D_0}(t)$ . The real trajectory would curve downward leading to larger gravitational components in the along-trajectory direction, larger velocities, and therefore larger drag forces,  $F_D(t) > F_{D_0}(t)$ . Consider the conservation of vertical momentum equation:

$$m \frac{dv_z}{dt} = -F_D(t) \sin \psi(t) + mg \frac{\Delta \rho}{\rho_p} < -F_{D_0}(t) \sin \psi_0 + mg \frac{\Delta \rho}{\rho_p} .$$

In other words, the right-hand side of the approximation is less negative than the exact right-hand side, so in the approximation, the projectile will decelerate more gradually and reach terminal velocity at a deeper point making it a valid upper bound.

$F_{D_0}(t)$  comes from a solution to the along-trajectory momentum equation with a fixed trajectory:

$$m \frac{d\tilde{v}}{dt} = -\frac{1}{2} \rho_w \tilde{v}^2 AC_d + mg \frac{\Delta \rho}{\rho_p} \sin \psi_0 ,$$

the solution to which is found on p. 141 to be

$$\frac{\tilde{v}}{\tilde{v}^*} = \coth \left[ \frac{\tilde{v}^* t}{L^*} + \tanh^{-1} \frac{\tilde{v}^*}{v_0} \right]$$

where

$$\tilde{v}^* = \sqrt{\frac{2\Delta\rho V g \sin \psi_0}{\rho_w A C_d}} = v^* \sqrt{\sin \psi_0}.$$

The drag force is given by

$$F_{D_0}(t) = \frac{1}{2} \rho_w \tilde{v}^2 A C_d = \frac{1}{2} \rho_w A C_d \tilde{v}^{*2} \coth^2 \left[ \frac{\tilde{v}^* t}{L^*} + \tanh^{-1} \frac{\tilde{v}^*}{v_0} \right].$$

Substituting this into the bounding differential equation for vertical velocity

$$\frac{dv_z}{dt} = -\frac{\tilde{v}^{*2}}{L^*} \coth^2 \left[ \frac{\tilde{v}^* t}{L^*} + \tanh^{-1} \frac{\tilde{v}^*}{v_0} \right] \sin \psi_0 + g \frac{\Delta\rho}{\rho_p}$$

This can be integrated to yield

$$v_z(t) = g \frac{\Delta\rho}{\rho_p} \cos^2 \psi_0 t + \tilde{v}^* \coth \left[ \frac{\tilde{v}^* t}{L^*} + \tanh^{-1} \frac{\tilde{v}^*}{v_0} \right] \sin \psi_0$$

and integrated again to yield

$$z(t) = \frac{1}{2} g \frac{\Delta\rho}{\rho_p} \cos^2 \psi_0 t^2 + L^* \ln \left[ \sinh \left[ \frac{\tilde{v}^* t}{L^*} + \tanh^{-1} \frac{\tilde{v}^*}{v_0} \right] \sqrt{\frac{v_0^2}{\tilde{v}^{*2}} - 1} \right] \sin \psi_0,$$

which then gives the depth-to-terminal-velocity-bounded approximation by substitution of  $t^*$  from the straight-downward case (including gravitational forces):

$$t^* = \frac{L^*}{v^*} \left[ \coth^{-1}(1 + \epsilon) - \coth^{-1} \frac{v_0}{v^*} \right],$$

where  $\epsilon$  is the proximity to true terminal velocity considered sufficient in the asymptotic approach:  $(1 + \epsilon)v^* \approx v^*$ .

# IDA | M344

**Type :** High Explosive Anti Tank Recoiless

**Origin :** United-Kingdom

**Body :** Aluminum & Steel Base

**Color :** Old – Olive Drab, New – Dark

**Marking :** Yellow or White

**Total weight :** 16,88 kg

**Total length :** 99,84 cm

**Diam :** 105,0 mm

**Muzzle velocity :** 503 m/s

**Max range :** 3000 m

**Projectile weight :** M344 – 8,75 kg, T295 – 8,3 kg

**Length :** 71,5 cm

**Tracer :** No

**Filler :** 1,260 kg COMP B

**Fuze :** PI Bd M509 A1/A2, M530

**Penetration :** 480 mm

**Case :** Perforated Plastic lined steel

**Case weight :** 6,0 kg

**Case Length :** 61,0 cm

Projectile



JCAMMO.com



This slides describes the properties of the M344. With fins broken off, we treated the total length as 57 cm, divided equally between a cylindrical and conical section.

## **IDA | Errors: Definitions and Assumptions**

### **Definitions:**

- $\varepsilon_{v_{00}}, \varepsilon_{\alpha_{00}}$ : from ballistic/aerodynamic uncertainty
- $\varepsilon_{\psi_{00}}$ : from ballistic/aerodynamic uncertainty + uncertainty in slope of waterline (waves)
- $\varepsilon_h$ :
  - Short term: waves, tide
  - Long term: water level, mudline evolution
- $\varepsilon_{\mu}$ : measurement uncertainty, spatial variation, time evolution

### **Assumptions:**

- Errors are uncorrelated except maybe  $\varepsilon_{\psi_{00}}$  and  $\varepsilon_{v_{00}}$
- Errors are unbiased except  $\varepsilon_{\psi_{00}}$ 
  - Flight-path angle transformation to elevation vs. waterline may be biased by obscuration of the back side of waves
- Errors in models ( $\varepsilon_{hm}, \varepsilon_{sm}$ ) can include unmodeled parameters like rate-dependent sediment strength

These next few slides describe our use of the sensitivity equation.

## IDA | Error Budget: The Sensitivity Equation

Assuming low cross-correlation between terms:

$$\begin{aligned}\sigma_{d_0}^2 = & \left( \frac{\partial d_0}{\partial v_0} \frac{\partial v_0}{\partial v_{00}} + \frac{\partial d_0}{\partial \alpha_0} \frac{\partial \alpha_0}{\partial v_{00}} + \frac{\partial d_0}{\partial \psi_0} \frac{\partial \psi_0}{\partial v_{00}} \right)^2 \sigma_{v_{00}}^2 \\ & + \left( \frac{\partial d_0}{\partial v_0} \frac{\partial v_0}{\partial \psi_{00}} + \frac{\partial d_0}{\partial \psi_0} \frac{\partial \psi_0}{\partial \psi_{00}} + \frac{\partial d_0}{\partial \alpha_0} \frac{\partial \alpha_0}{\partial \psi_{00}} \right)^2 \sigma_{\psi_{00}}^2 \\ & + \left( \frac{\partial d_0}{\partial v_0} \frac{\partial v_0}{\partial \alpha_{00}} + \frac{\partial d_0}{\partial \alpha_0} \frac{\partial \alpha_0}{\partial \alpha_{00}} + \frac{\partial d_0}{\partial \psi_0} \frac{\partial \psi_0}{\partial \alpha_{00}} \right)^2 \sigma_{\alpha_{00}}^2 \\ & + \left( \frac{\partial d_0}{\partial v_0} \frac{\partial v_0}{\partial h} + \frac{\partial d_0}{\partial \psi_0} \frac{\partial \psi_0}{\partial h} + \frac{\partial d_0}{\partial \alpha_0} \frac{\partial \alpha_0}{\partial h} \right)^2 \sigma_h^2 \\ & + \left( \frac{\partial d_0}{\partial \mu} \right)^2 \sigma_\mu^2 \\ & + \sigma_{sm}^2\end{aligned}$$

## IDA | Error Budget: Deriving Sensitivity Terms

The Sensitivity Equation at the mudline:

$$\sigma_{d_0}^2 = \left( \frac{\partial d_0}{\partial v_0} \right)^2 \sigma_{v_0}^2 + \left( \frac{\partial d_0}{\partial \psi_0} \right)^2 \sigma_{\psi_0}^2 + \left( \frac{\partial d_0}{\partial \alpha_0} \right)^2 \sigma_{\alpha_0}^2 + \left( \frac{\partial d_0}{\partial \mu} \right)^2 \sigma_{\mu}^2 + \sigma_{sm}^2$$

Aubeny and Shi's sediment penetration model:

$$d_0 = \sin \psi_0 \left[ \frac{(b+1)mv_0^2}{2c_1\mu D^{1-b}kL(D \sin \alpha_0 + L \cos \alpha_0)} \right]^{\frac{1}{b+1}}$$

Deriving sensitivity terms from Aubeny and Shi's model:

- $\frac{\partial d_0}{\partial v_0} = \frac{2}{b+1} \frac{d_0}{v_0}$
- $\frac{\partial d_0}{\partial \psi_0} = -d_0 \cot \psi_0$
- $\frac{\partial d_0}{\partial \alpha_0} = -\frac{1}{b+1} d_0 \frac{(D \cos \alpha_0 - L \sin \alpha_0)}{(D \sin \alpha_0 + L \cos \alpha_0)}$
- $\frac{\partial d_0}{\partial \mu} = -\frac{1}{b+1} \frac{d_0}{\mu}$

**Stable case:**

$$\frac{\partial d_0}{\partial \alpha_0} = -\frac{1}{b+1} d_0 \frac{D}{L}$$

**Unstable broadside flop case:**

$$\sigma_{\alpha_0} = 0$$

**Unstable random case  
( $\Delta$  between  $\alpha_0 = 0, \pi/2$ ):**

$$\frac{\Delta d_0}{d_0} = 1 - \left( \frac{D}{L} \right)^{\frac{1}{b+1}}$$

## Error Budget: Comparative Contributions: stable case

The sensitivity equation at the mudline:

$$\sigma_{d_0}^2 = \left( \frac{\partial d_0}{\partial v_0} \right)^2 \sigma_{v_0}^2 + \left( \frac{\partial d_0}{\partial \psi_0} \right)^2 \sigma_{\psi_0}^2 + \left( \frac{\partial d_0}{\partial \alpha_0} \right)^2 \sigma_{\alpha_0}^2 + \left( \frac{\partial d_0}{\partial \mu} \right)^2 \sigma_{\mu}^2 + \sigma_{sm}^2$$

Plugging in sensitivity terms from Aubeny and Shi's model (stable case):

$$\sigma_{d_0}^2 = d_0^2 \left[ \left( \frac{2}{b+1} \frac{1}{v_0} \right)^2 \sigma_{v_0}^2 + (\cot^2 \psi_0)^2 \sigma_{\psi_0}^2 + \left( \frac{1}{b+1} \frac{D}{L} \right)^2 \sigma_{\alpha_0}^2 + \left( \frac{1}{b+1} \frac{1}{\mu} \right)^2 \sigma_{\mu}^2 \right] + \sigma_{sm}^2$$

where  $b = 0.155$ , so prefactors are  $O(1)$ , and  $\cot \psi_0 \approx \frac{\pi}{2} - \psi_0$ , and so:

$$\frac{\sigma_{d_0}^2}{d_0^2} \approx 4 \frac{\sigma_{v_0}^2}{v_0^2} + \left( \frac{\pi}{2} - \psi_0 \right)^2 \sigma_{\psi_0}^2 + \left( \frac{D}{L} \right)^2 \sigma_{\alpha_0}^2 + \frac{\sigma_{\mu}^2}{\mu^2} + \frac{\sigma_{sm}^2}{d_0^2}$$

### Example:

- 10% velocity errors.
- 50% shear strength errors.
- Trajectories within 30 degrees of vertical plus or minus 15 degrees.
- Angle of attack errors less than 10 degrees. With aspect ratios  $> 5:1$ .
- Shear strength errors overall dominant among sensitivities, but if model had 100% error, model error would dominate.

## Error Budget: Comparative Contributions: unstable case

The sensitivity equation at the mudline:

$$\sigma_{d_0}^2 = \left( \frac{\partial d_0}{\partial v_0} \right)^2 \sigma_{v_0}^2 + \left( \frac{\partial d_0}{\partial \psi_0} \right)^2 \sigma_{\psi_0}^2 + \left( \frac{\partial d_0}{\partial \alpha_0} \right)^2 \sigma_{\alpha_0}^2 + \left( \frac{\partial d_0}{\partial \mu} \right)^2 \sigma_{\mu}^2 + \sigma_{sm}^2$$

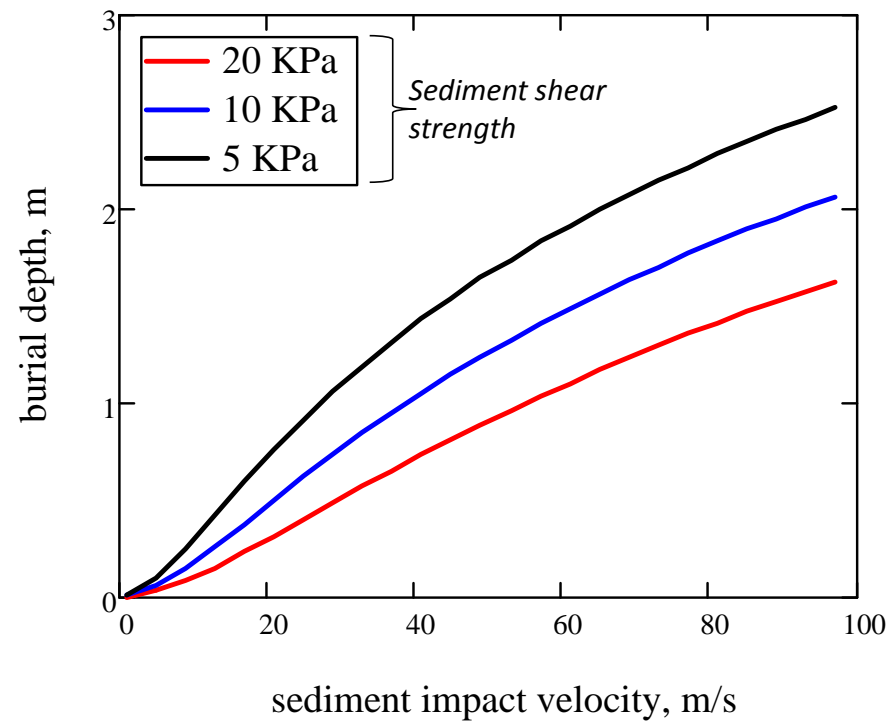
Plugging in sensitivity terms from Aubeny and Shi's model (unstable case):

$$\sigma_{d_0}^2 = d_0^2 \left[ \left( \frac{2}{b+1} \frac{1}{v_0} \right)^2 \sigma_{v_0}^2 + (\cot^2 \psi_0)^2 \sigma_{\psi_0}^2 + \left( \frac{\partial d_0}{\partial \alpha_0} \right)^2 \overset{0}{\cancel{\sigma_{\alpha_0}^2}} + \left( \frac{1}{b+1} \frac{1}{\mu} \right)^2 \sigma_{\mu}^2 \right] + \sigma_{sm}^2$$

where  $b = 0.155$ , so prefactors are  $O(1)$ , and  $\cot \psi_0 \approx \frac{\pi}{2} - \psi_0$ , and so:

$$\frac{\sigma_{d_0}^2}{d_0^2} \approx 4 \frac{\sigma_{v_0}^2}{v_0^2} + \left( \frac{\pi}{2} - \psi_0 \right)^2 \sigma_{\psi_0}^2 + \frac{\sigma_{\mu}^2}{\mu^2} + \frac{\sigma_{sm}^2}{d_0^2}$$

## IDA | Sediment-Penetration Model

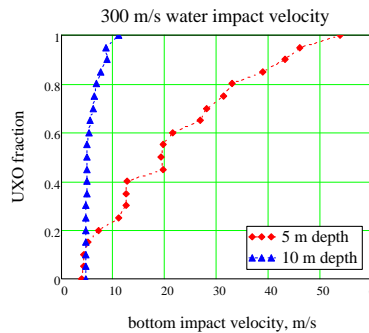
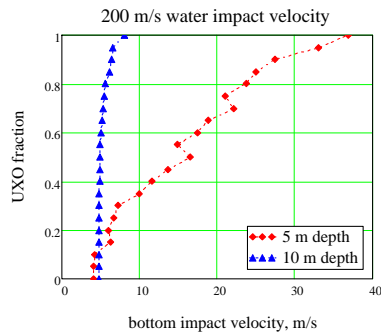
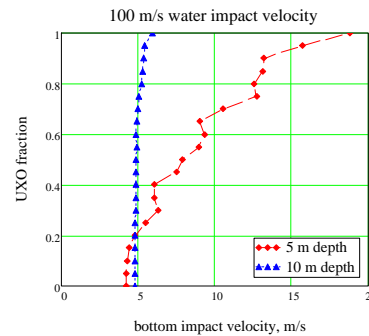
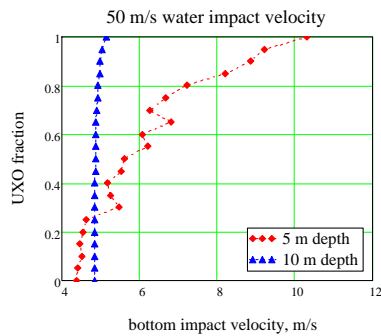




This chart shows munition burial depth as a function of sediment impact velocity and shear strength. We utilized Aubeny and Shi's sediment-penetration model with the addition of inertial terms, as we described in the main text. The munition in this case has a mass of 20 kg and 0.045m<sup>2</sup> presented area.

# Terminal Velocity in Computational Model: Effect of Water Depth and Munition's Impact Velocity at Waterline on Munition's Vertical Velocity at Sediment

Impact angle  $\psi_{00}$  is normally distributed with mean  $\overline{\psi_{00}} = 45^\circ$ , std. dev.  $\sigma_{\psi_{00}} = 15^\circ$ ; drag coefficient  $C_d = 0.3$ ;



## When the water depth is $h = 10$ m:

- the projectile vertical velocity at the mudline  $v_{0z}$  deviates only slightly from the terminal velocity of 4.9 m/s
- the largest deviation occurs at  $v_{00} = 300$  m/s:  $v_{0z}$  varies from about 5 to 10 m/s.

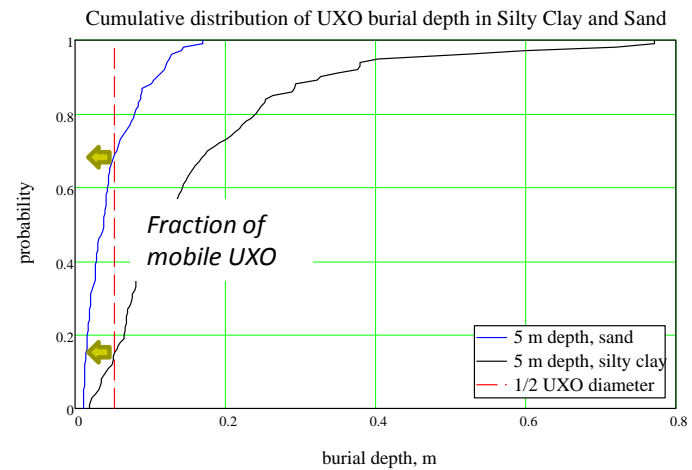
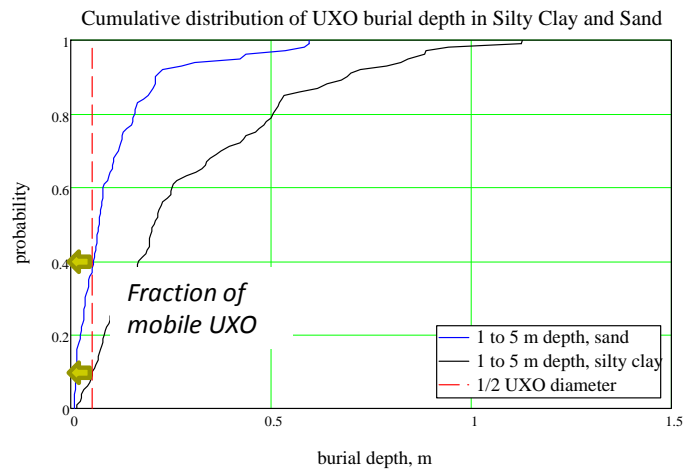
## In $h = 5$ m water depth:

- when  $v_{00}$  changes from 50 to 300 m/s, the  $v_{0z}$  changes from about 1 to 55 m/s
- the largest changes are, as expected, at  $v_{00} = 300$  m/s

This slide demonstrates the effect of water depth and the munition's impact velocity at the waterline on the vertical component of the munition's impact velocity at the sediment:

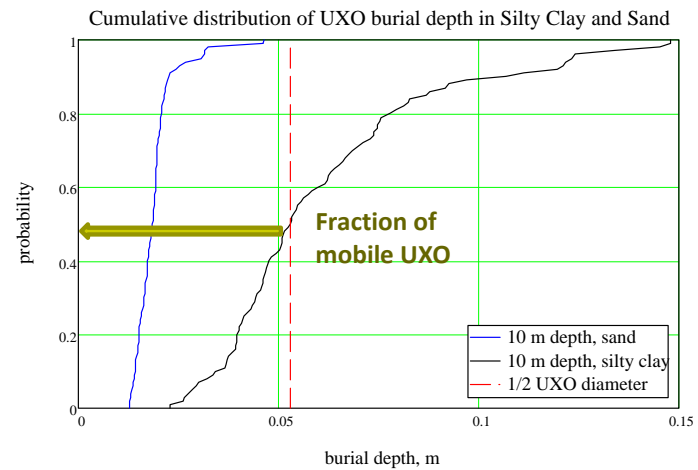
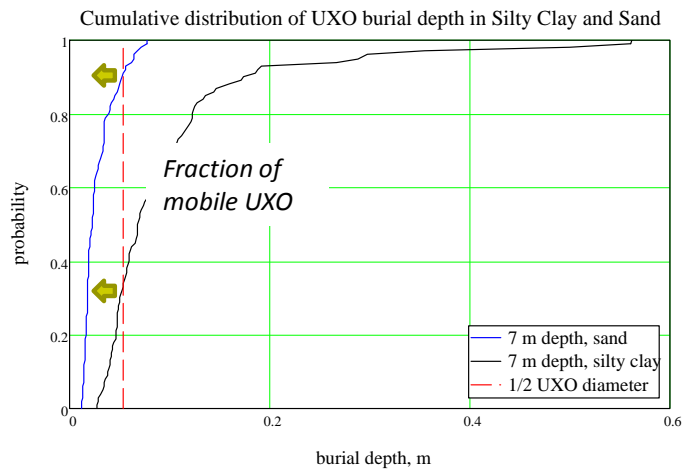
- In 10 m water depth, the vertical component of the munition's impact velocity at the sediment is very close to the terminal velocity, and the munition's impact velocity at the waterline has a negligible contribution.
- In contrast, in 5 m water depth, the vertical component of the munition's impact velocity at the sediment is quite sensitive to the variation in its impact velocity at the waterline.

## Selected Results: Fraction of Mobile Munitions in Silty Clay and Sand



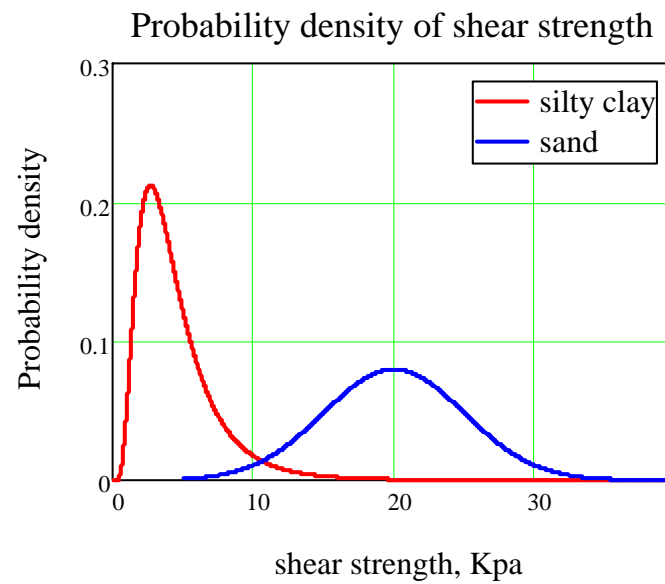
Under the assumption that the munition is potentially mobile if its sediment-penetration depth is less than one-half its diameter, the cumulative distributions of a munition's penetration depth can be used to determine the fraction of immobile/potentially mobile munitions, as shown on this slide. In this example, we are considering a uniform distribution of water depths from 1 to 5 m (left) and exactly 5 m depth (right). As can be seen from these figures, the water depth has a larger effect in sand, where the fraction of munitions that are potentially mobile changes from about 40% (1 to 5 m depth) to 70% (5 m depth). The fraction of potentially mobile munitions in silty clay remains under 20% in both cases.

## Selected Results: Fraction of Mobile Munitions in Silty Clay and Sand



As the water depth increases, so does the fraction of potentially mobile munitions. When the water depth is 7 m, about 90% of the munitions in sand and 30% in silty clay are potentially mobile. When the water depth is 10 m, all of the munitions in sand and about 50% of the munitions in silty clay are potentially mobile.

## IDA | Shear Strength



### **Silty clay:**

Lognormal with mean 4.3 kPa and standard deviation 1.8 kPa

### **Sand:**

Normal with mean 20 kPa and standard deviation 5 kPa



This slides shows the assumed probability density distributions of shear strength for sand and silty clay used in this analysis.

# IDA | Estimating Errors in Munition's Initial Conditions at Mudline

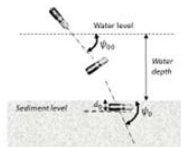
## Hydrodynamic Phase Sensitivities

$\frac{\partial \psi_0}{\partial v_{00}}$	$\frac{\partial v_0}{\partial v_{00}}$	$\frac{\partial \alpha_0}{\partial v_{00}}$
$\frac{\partial \psi_0}{\partial \psi_{00}}$	$\frac{\partial v_0}{\partial v_{00}}$	$\frac{\partial \alpha_0}{\partial \psi_{00}}$
$\frac{\partial \psi_0}{\partial \alpha_{00}}$	$\frac{\partial v_0}{\partial \alpha_{00}}$	$\frac{\partial \alpha_0}{\partial \alpha_{00}}$
$\frac{\partial \psi_0}{\partial h}$	$\frac{\partial v_0}{\partial h}$	$\frac{\partial \alpha_0}{\partial h}$

**IDA | Benefits of simplified models**

**Stages of the UXO Burial Depth Model**

1. 2-D hydrodynamic model



$$f_x = \frac{\Delta p}{\rho_w} = \frac{\rho_w A C_d}{2m} (v_x^2 + v_z^2)$$

$$f_y = -\frac{\rho_w A C_d}{2m} (v_x^2 + v_z^2)$$

2. Aubert's sediment penetration model

$$f = \begin{cases} c(v) \gamma_1(u) (\sqrt{v^2 + z^2})^{\frac{1}{2}} + \frac{1}{2} A C_d \frac{\rho_w}{m} (v_x^2 + v_z^2), & x \leq \frac{D}{2} \\ c(v) \gamma_2(u) (\sqrt{v^2 + z^2})^{\frac{1}{2}} + \frac{1}{2} A C_d \frac{\rho_w}{m} (v_x^2 + v_z^2), & x > \frac{D}{2} \end{cases}$$

where

$$c(v) = 1 + 3.8 \left( \frac{v}{v_{cr}} \right)^{1.5}, \quad \gamma_1(u) = \frac{\mu A C_d}{m \omega D^2}, \quad \gamma_2(u) = \frac{\mu A C_d}{m \omega D^2}$$

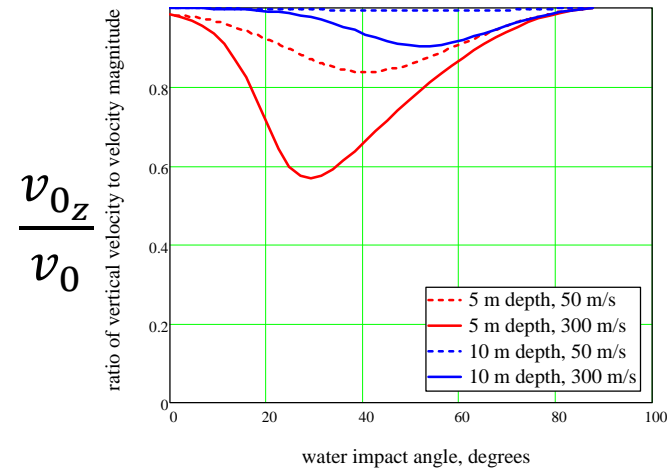
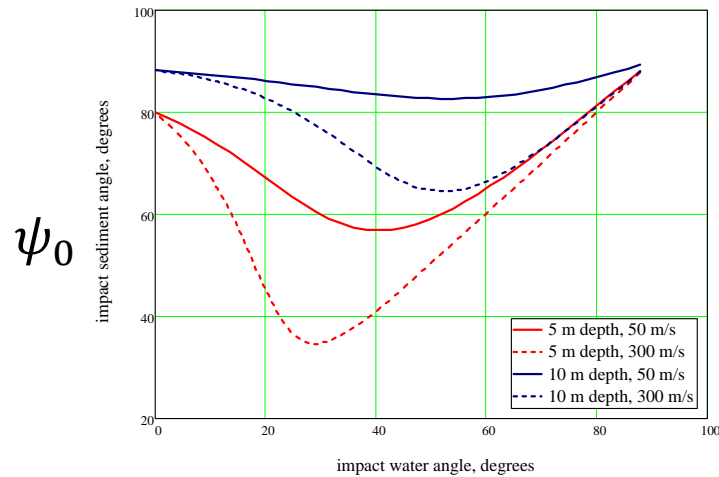
$f_x, f_y, f_z, \rho_w, A$  are constants (empirical)

**Modeling assumptions**

- Assume presented area and drag coefficient numbers to be comparable with those of Strike 35 (i.e. UXO tumbles upon impact)
- Broadside UXO sediment impact
- Known shear strength distributions

14 February 2017

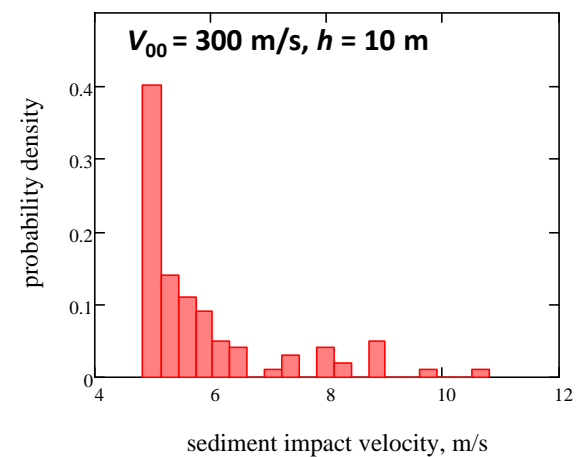
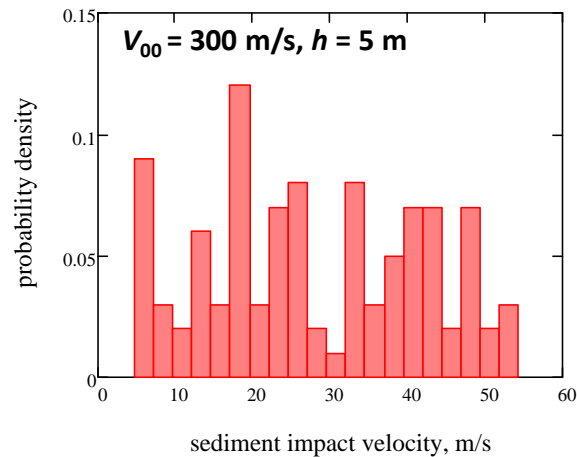
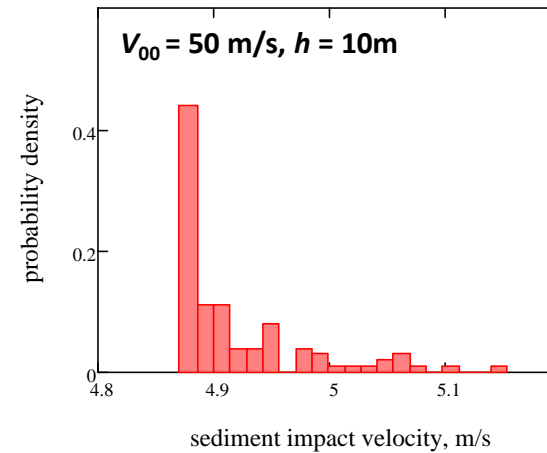
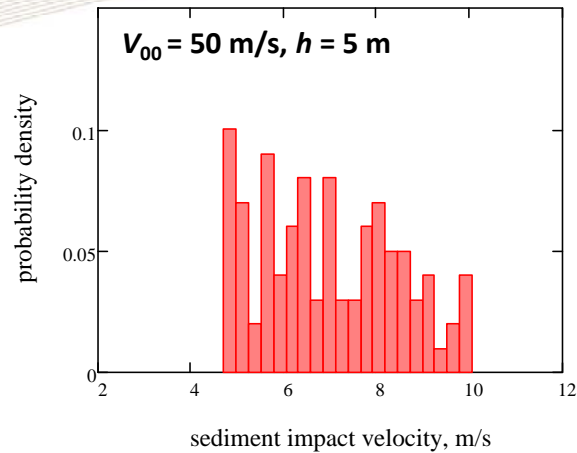
## Use computational hydrodynamic model



This slides gives example results from our sensitivity analysis. We exercised the simplified 2D model of the munition's propagation in water and sediment to compute the terms in the sensitivity matrix shown in the slide. Selected examples are also given: the munition's impact angle at the sediment (left) and the magnitude of the vertical component of the munition's impact velocity at the sediment, normalized by the total magnitude of the munition's impact velocity at the sediment (right). Both these quantities are plotted as a function of the munition's impact velocity at the waterline, for various impact conditions.

## **IDA** | Estimating Velocity Errors in Munition's Initial Conditions at Mudline

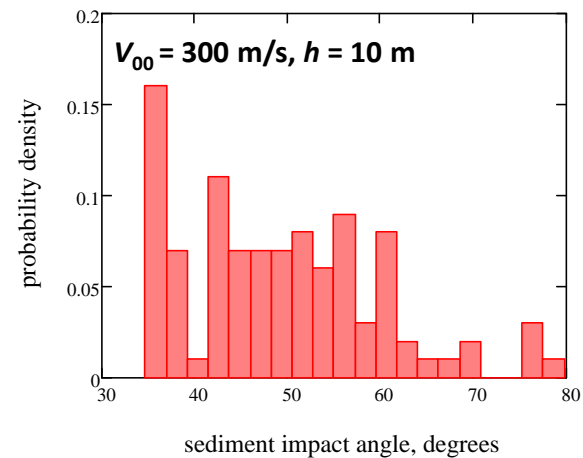
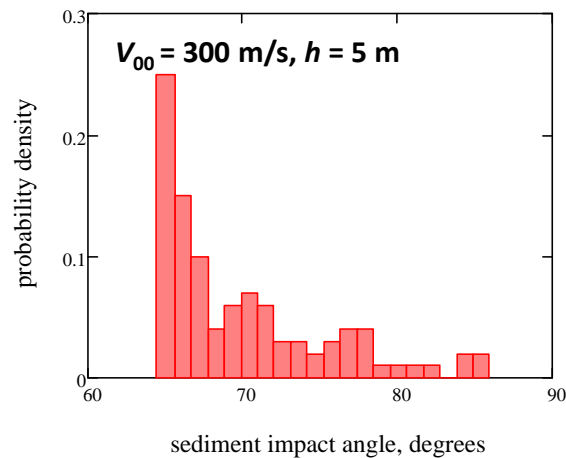
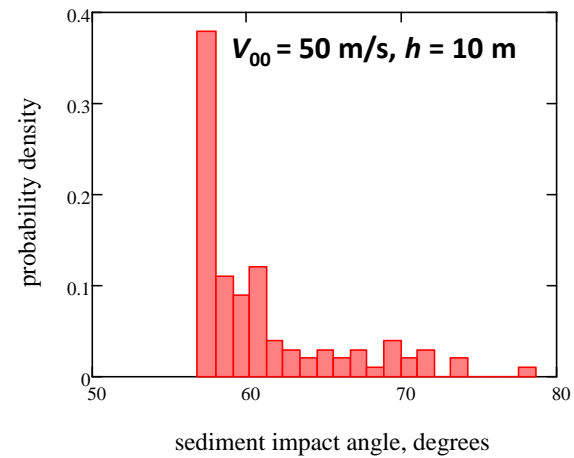
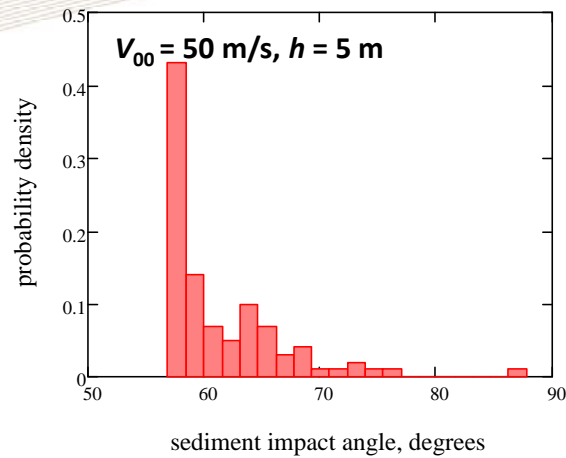
$\psi_{00}$  is normally distributed with mean  $45^\circ$  and standard deviation  $15^\circ$



Shown on the facing page are selected examples of the distributions of the munition's impact velocity at the sediment when the munition's impact angle at the waterline is normally distributed with mean 45 degrees and standard deviation 15 degrees, for several impact conditions.

## **IDA** | Estimating Impact Angle Errors in Munition's Initial Conditions at Mudline

$\psi_{00}$  is normally distributed with mean  $45^\circ$  and standard deviation  $15^\circ$



Shown on the facing page are selected examples of distributions of the munition's impact angle at the sediment when the munition's impact angle at the waterline is normally distributed with mean 45 degrees and standard deviation 15 degrees, for several impact conditions.





## References

---

- Aubeny, C., and H. Shi. 2007. "Effect of Rate-Dependent Soil Strength on Cylinders Penetrating Into Soft Clay." *IEEE J. Oceanic Eng.* 32 (1) (January).
- Chu, P. C., and G. Ray. 2006. "Prediction of High Speed Rigid Body Maneuvering in Air-Water-Sediment Columns. *Advances in Fluid Mechanics* 6:123–32.
- Chu, P. et al. 2001. "Modeling of Underwater Bomb Trajectory for Mine Clearance." *Journal of Defense Modeling and Simulation: Applications, Methodology, Technology* 8 (1): 25–36.
- Chu, Peter C., and Chenwu Fan. 2007. "Mine-Impact Burial Model (IMPACT35) Verification and Improvement Using Sediment Bearing Factor Method." *IEEE Journal of Oceanic Engineering* 32, no. 1 (January).
- Holland, K. Todd. 2015. "A Wide Area Risk Assessment Framework for Underwater Military Munitions Response." MR 2411. Naval Research Laboratory – Stennis Space Center In-Progress Review Meeting, May 20.
- Rennie, Sarah, and Alan Brandt. 2015. "Interim Report: Underwater Munitions Expert System to Predict Mobility and Burial, SERDP Project MR-2227." Laurel, MD: Johns Hopkins University, Applied Physics Laboratory. <https://www.serdpestcp.org/content/download/36174/345934/file/MR-2227-IR.pdf>.
- Wilson, Jeffrey V., and Alexandra DeVisser. 2009. *Final Report: Predicting the Mobility and Burial of Underwater Unexploded Ordnance (UXO) Using the UXO Mobility Model*. Contract Report CR-10-012-ENV. ESTCP. November. <http://www.dtic.mil/dtic/tr/fulltext/u2/a532814.pdf>.



REPORT DOCUMENTATION PAGE				Form Approved OMB No. 0704-0188	
<p>The public reporting burden for this collection of information is estimated to average 1 hour per response, including the time for reviewing instructions, searching existing data sources, gathering and maintaining the data needed, and completing and reviewing the collection of information. Send comments regarding this burden estimate or any other aspect of this collection of information, including suggestions for reducing the burden, to Department of Defense, Washington Headquarters Services, Directorate for Information Operations and Reports (0704-0188), 1215 Jefferson Davis Highway, Suite 1204, Arlington, VA 22202-4302. Respondents should be aware that notwithstanding any other provision of law, no person shall be subject to any penalty for failing to comply with a collection of information if it does not display a currently valid OMB control number.</p> <p><b>PLEASE DO NOT RETURN YOUR FORM TO THE ABOVE ADDRESS.</b></p>					
1. REPORT DATE July 2017		2. REPORT TYPE Final		3. DATES COVERED (From-To) Jun 2017 – Jul 2017	
4. TITLE AND SUBTITLE  UXO Burial Prediction Fidelity				5a. CONTRACT NUMBER HQ0034-14-D-0001	
				5b. GRANT NUMBER	
				5c. PROGRAM ELEMENT NUMBER	
6. AUTHOR(S)  Teichman, Jeremy A. Macheret, Yevgeny Cazares, Shelley M.				5d. PROJECT NUMBER AM-2-1528	
				5e. TASK NUMBER	
				5f. WORK UNIT NUMBER	
7. PERFORMING ORGANIZATION NAME(S) AND ADDRESS(ES)  Institute for Defense Analyses 4850 Mark Center Drive Alexandria, VA 22311-1882				8. PERFORMING ORGANIZATION REPORT NUMBER  IDA Document NS D-8616	
9. SPONSORING / MONITORING AGENCY NAME(S) AND ADDRESS(ES)  Director and Program Manager for Munitions SERDP/ESTCP 4800 Mark Center Drive Suite 17D08 Alexandria, VA 22350-3605				10. SPONSOR/MONITOR'S ACRONYM(S)  SERDP/ESTCP	
				11. SPONSOR/MONITOR'S REPORT NUMBER(S)	
12. DISTRIBUTION/AVAILABILITY STATEMENT  Approved for public release; distribution is unlimited (20 November 2017).					
13. SUPPLEMENTARY NOTES					
14. ABSTRACT The Institute for Defense Analyses (IDA) is a not-for-profit company that operates three Federally Funded Research and Development Centers (FFRDCs). We perform scientific and technical analyses for the U.S. government on issues related to national security. Recently, we performed a numerical analysis for the Strategic Environmental Research and Development Program (SERDP) to explore the fidelity of computational models for predicting the initial penetration depth of Unexploded Ordnance (UXO) in underwater sites. This briefing discusses the details of our analysis. A separate briefing provides a shorter summary.					
15. SUBJECT TERMS  accretion, erosion, IMPACT25, IMPACT28, IMPACT35, MINE6-D, scour, sensitivity analysis, STRIKE35, Unexploded Ordnance, UXO					
16. SECURITY CLASSIFICATION OF:			17. LIMITATION OF ABSTRACT  UU	18. NUMBER OF PAGES  171	19a. NAME OF RESPONSIBLE PERSON Nelson, Herbert
a. REPORT Uncl.	b. ABSTRACT Uncl.	c. THIS PAGE Uncl.			19b. TELEPHONE NUMBER (include area code) 571-372-6400